Protection and Fusing in Advanced

Automotive Electrical Environment

by

Ilija Jergović

Submitted to the Department of Electrical Engineering and Computer Science and Department of Physics in partial fulfillment of the requirements for the degrees of

Bachelor of Science in Physics

and Bachelor of Science in Electrical Science and Engineering

and Master of Engineering in Electrical Engineering and Computer Science

at the MASSACHUSETTS INSTITUTE OF TECHNOLOGY

September 1999

Signature of Author _____
Department of Electrical Engineering and Computer Science
September 9,1999

Certified by _____
Professor John G. Kassakian
Thesis Supervisor

Accepted by _____
Professor Arthur C. Smith
Chair, Department Committee on Graduate Thesis
Department of Electrical Engineering and Computer Science

Accepted by _____
Professor David E. Pritchard
Senior Thesis Coordinator, Department of Physics

Protection and Fusing in Advanced Automotive Electrical Environment

by

Ilija Jergović

Submitted to the Department of Electrical Engineering and Computer Science and Department of Physics in partial fulfillment of the requirements for the degrees of

Bachelor of Science in Physics

and Bachelor of Science in Electrical Science and Engineering

and Master of Engineering in Electrical Engineering and Computer Science.

Abstract

Protection and fusing is a highly important subsystem in an automotive electrical distribution system (EDS). As a result of increased power demand a new 42 V EDS is introduced in the automotive industry. This thesis investigates the impact of voltage change on various types of protection devices such as conventional fuses (CF's), smart power switches (SPS's) and polymeric positive temperature coefficient devices (PPTC's).

In Chapter 2 an overview of the theory of operation of these devices is presented and is then followed by the different means of characterizations and comparison which is given in Chapter 3. Many of these means of characterization are in widespread use for CF in the industry today and their applicability on other device types is discussed. Furthermore, some new means of characterization are presented as a result of added functionality of PPTC's and SPS's. Chapter 4 presents the comparison of the three device types on the basis of theory presented in Chapter 2 and means of characterization presented in Chapter 3. Where possible the performance changes due to source voltage increase are evaluated and compared among different devices. Chapter 5 deals with elements of circuit and system protection closely related to the automotive EDS. Examples of analysis include cable protection and protection coordination.

These analyses reveal that, excluding economic issues, the best performing protection device in many cases is the SPS. However, when inductance is present in the faults the fuses can 'handle' higher inductance values during fault interruption.

Thesis Supervisor: John G. Kassakian
Supervisor's Title: Professor of Electrical Engineering

Acknowledgments

During the course of my academic study at MIT I have never crossed the 30 page boundary of the academic term paper. As I began to write this thesis I never believed that it would be so much different to produce a 100 page document. Fortunately, the help of many people around me made the process substantially easier.

The precious guidance of Dr. Tom Keim has earned him my highest gratitude and respect. Both during the research and the writing of this thesis he evaluated and guided my work in the most professional way. Even at moments when I lost track of my thoughts he was there to help me determine the right direction for this thesis. My Advisor, Prof. John Kassakian, has always found time to help me with my research in spite of his numerous other obligations. During the early stages of the research he helped me define the research unit and the scope of the research. While it seemed initially impossible to find the appropriate direction the advice and conversations between Prof. Kassakian and me defined the research presented in this thesis.

Since this research was done under the sponsorship of the Automotive Consortium, numerous persons in the industry have helped me define the current status of the protection and fusing and identify the elements interesting to my research. Most of the subcommittee members have in some way supported my research effort. Alfons Graf and Tom Tobin from Infineon Technologies have given me both the resources and the technical help necessary to better understand their technology. Furthermore, although Raychem is not a member of the Consortium I would like to thank all the application engineers at Raychem for their help in trying to characterize polymeric positive temperature coefficient protection devices.

Finally I would like to thank my friends Milos Komarcevic, Edo Macan Katja Djepina for many hours of support they have given me throughout the last year. While the morning coffee was one of the most important elements of support, many hours of phone conversations with Mi have proven to be an excellent source of inspiration. Furthermore, I would like to thank the last elements of public sanity in Croatia, Radio 101 and Feral Tribune. Knowing that they still exist gives me hope that some day I might return.

Table of Contents

List of Figures

page

List of Commonly used Symbols

α	Linear temperature resistance coefficient.
c_p	Isobaric specific heat capacity.
E_{max}	Maximum energy allowed to be dissipated in the smart power switch during turnoff.
F	Minimum fusing factor, ratio of I_{mfc} and I_{nom}.
I_{mfc}	Minimum fusing current. Smallest current necessary for the device to begin turnoff.
I^2t	Integral of the square of the current up to some time t. For example, melting I^2t would be integrated up to onset of melting from the beginning of a fault.
I_p	Prospective current.
I_{limit}	Current limit of the current limited power supply.
I_{SCP}	Maximum actual current that can exist in an SPS during a fault. Current limit of the associated MOSFET.
I_0	Magnitude of current at the onset of turnoff.
I_{trip}	Largest value of I_{mfc}.
I_{hold}	Smallest value of I_{mfc}.
I_{nom}	Nominal current.
I_{load}	Current supplied to a load or a group of loads in normal conditions.
I_{post}	Post trip current for resetable devices.
I-t	Usually designating a plot of prospective current vs. virtual time.
L_c	Inductance present in the circuit.
P_d	Power dissipation.
R_{th}	Thermal resistance of the SPS.
R_{ESR}	Equivalent series resistance of the source
R_0	Nominal resistance of a protection device at ambient temperature.
R_f	Resistance of the fuse.
R_c	Resistance present in the circuit excluding the resistance of the protection device.
T_{melt}	Melting temperature.
T_{amb}	Ambient Temperature.
T_{jmax}	Maximum temperature of the silicon junction of the SPS. When this temperature is reached turnoff is initiated.
T_j	Temperature of the SPS junction.
t_{melt}	Time to melt.
τ	Circuit time constant (L_c / R_c).
U	Heat loss coefficient (to the environment).
V_s	Voltage of the source.
V_{DS}	Drain to source voltage of the SPS.
V_{cl}	Voltage at which SPS starts conducting to protect it self from overvoltage.
V_L	$V_{cl} - V_s$
V_{max}	Maximum allowed operating voltage for a protection device

Chapter 1.

Introduction

1.1. History and Description of the Problem

The history of the automotive electrical system clearly reveals the increasing power demand presented to the electrical distribution system. Since power is the product of current and voltage the magnitude of the current present throughout the system is always increasing. Historically, one of the solutions to these increasing power needs was the industry's switch from the old 6V automotive electrical system to the new 12V automotive electrical system. The short term effect of this switch was the reduction in system current by a factor of two. The long term effect were the thirty years in which the 12V electrical system managed to meet the power demands of the automotive environment in an economically feasible way . However, due to the ever increasing power demand in the modern luxury vehicle, the automotive manufacturers have come to the conclusion that the current 12V volt system will need to be changed in order to meet the power demands of the future in the most feasible economical way. The need for a new electrical distribution system (EDS) is visible in the increasing

size of the alternators and batteries. Some luxury cars today even have two alternators and two batteries in order to meet their power demands

One of the initial steps in the specification of the new electrical system was the formation of the MIT/Industry Consortium on Advanced Automotive Electrical/Electronic Components and Systems (1). One of the tasks of the consortium was to determine the appropriate new voltage for the automotive electrical distribution system. The principal tradeoffs were a desire for increased power capability, driving towards higher voltages, and retaining touch safety, which posed an upper limit. These matters were considered by consortium member companies, both in the context of the consortium, and along with other interested parties, in a German-based ad hoc organization called Forum Bordnetz. The voltage chosen was 42V. This represents a three-fold increase in the system voltage. Today 42V volts is an agreed standard by the industry for the nominal voltage of the future automotive EDS.

Unfortunately, economic and technical considerations do not allow an easy transition to a new 42 V system and the abandonment of the old 12V system. Thus came the idea of a hybrid 12V-42V dual voltage system. The development of this dual voltage system is at a stage where the architecture of the final electrical distribution system is not yet clearly defined but the candidate architectures are being examined within the work of the consortium.

One of the issues in the development of this new dual voltage system is the fusing and protection issue. In order to protect the electrical distribution system from various types of failures car manufacturers use electric fuses and other protection devices (2,3). Today's automotive fuses are not capable of operating at 42V. The nonexistence of such a fuse does not imply that it is not being developed. In fact its development is underway. Since there was no need for the automotive fuses rated to safely operate in the new 42V system they did not exist. As the need is becoming more and more apparent the fuses are starting to appear in the market.

However, new advanced technologies have been developed that have the potential to replace the conventional fuse because of the increased functionality

that they can offer. The transitory period now existing in the automotive industry is one of the most convenient times for introduction of these new technologies and the reevaluation of the currently used technologies and protection strategies.

1.2. Objective

The purpose of this thesis is to evaluate conventional fuses and new technologies and compare them on both theoretical and experimental basis. Furthermore, identification and exploration of the circuit and system issues of the current and probable future fusing and protection strategies are important for the transition period since they will uncover existing problems and predict future problems. With respect to the future automotive electrical distribution system this thesis is set out to compare the impact of the future candidate architecture on the protection and fusing issues and strategies. The new fusing and protection devices need to be characterized effectively in the view of the current fusing and protection standards of operation and characterization.

1.3. Organization of the thesis

Chapter 2 presents the theory of operation for conventional fuses (CF), smart power switches (SPS), and polymeric positive temperature coefficient devices (PPTC).

In Chapter 3 different means of device characterization are established and then used to evaluate the performance of different device types on theoretical and experimental basis in Chapter 4.

Chapter 5 investigates various applications of three protection device types and makes a comparison of their performance. The applications include the protection of cables, use of devices in parallel connection, use of devices on a current limited power supply system and their use in a protection coordinated environment.

Finally Chapter 6 contains the conclusions and recommendations for future studies.

Chapter 2.

Theory of Device Operation

2.1. Introduction

In order to evaluate the feasibility of devices for use as protection devices in current automotive electrical distribution system and future dual voltage electrical distribution systems it is necessary to have a comprehensive understanding of the principles of device operation and the underlying physical laws that govern the operation.

The theory of device operation gives the first basis for comparing different device types. It also enables the prediction of behavior of the device only on theoretical basis and is a starting point in the development of simulation models used during the design of the systems. This predictive power of the theory proves to be a major contribution to assessing the usability of different device types in current and future automotive electrical environments.

Furthermore, if we choose to neglect the underlying principles of operation we could easily neglect some factor and thus degrade the reliability of the overall system (e.g. nuisance fuse blowing – a fuse that operates even though its

minimum fusing current is never exceeded). Thus, oversimplification of the theory of device operation is both detrimental and dangerous.

The theory that follows does not only give the underlying physical principles but also facilitates the optimization of protection for systems to be performed to the best of one's ability and provides the system with protection that best suits the needs of that particular system. The theory of conventional fuse operation will be presented first. Although well known, CF theory of operation offers significant advantage to understanding the theory of operation of both SPS and PPTC devices. Furthermore, some of the aspects of the theory of CF operation are often given little attention during the system design today as they have not caused any problems yet (e.g. Inductance limitations). However, some of these aspects might become more and more important as the new 42 V electrical distribution system is introduced. The smart power switch (SPS) and polymeric positive temperature coefficient device (PPTC) theory of operation follows.

2.2. Conventional Fuses

All conventional fuses operate on the same underlying principle. They pass electrical current through a fusible link. When the current exceeds a certain value the energy dissipated in the fusible link is large enough to cause the vaporization and melting of the link. The physical behavior of the CF while the current passes through the material from which the fusible link is composed is termed pre-arcing behavior. After the fusible link has melted and the passage of current is not through any phase of the link material arcing will begin. The physical principles of arcing are termed arcing behavior.

Under normal operating conditions the CF operates in the pre-arcing regime. During the interruption of excessive currents both the pre-arcing and the arcing regime are present. Only in an idealized, inductance-free environment there would be no arcing present. Due to the presence of parasitic inductances the arcing regime is always present. Behavior of the fuse in the arcing regime defines many of the characteristics of the fuse.

2.2.1. Pre-arcing behavior of CF's

The pre-arcing behavior of the conventional fuse can further be divided into three distinct regimes of operation. These three regimes are governed by the amount of current that is passing through a fuse. The behavior of the fuse link in all three regimes can be simply described by a following differential equation:

$$mc_p\left(\frac{dT}{dt}\right) = I^2R - U(T - T_{amb}) \tag{2.1}$$

where m is the total mass of the fuse link, c_p is the specific heat capacity of the material that the fuse link is composed of, T is the temperature of the fuse link in °C, T_{amb} is the ambient temperature in °C, I is the current passing through the fuse link, R is the resistance of the fuse link, and U is the heat loss (to the surrounding) coefficient. The resistance has additional temperature dependence given by:

$$R = R_{amb}[1 + \alpha(T - T_{amb})] \tag{2.2}$$

where R_{amb} is the resistance at T_{amb}=25°C and α is the linear resistance temperature coefficient. In order to separate various regions of operation, the melting temperature for the fusible link material T_{melt} needs to be known. Just looking at Equation 2.1 it can be seen that the left hand side is zero under the steady state condition. In this situation the following equation holds:

$$I^2R = U(T - T_{amb}) \tag{2.3}$$

meaning that for a given current I the fuse link will reach some temperature T. The electrical energy dissipated in the fuse link is lost to the environment. A simple reasoning deduces that if the T reached is above the melting temperature of the fusible link T_{melt} the situation is not physically acceptable since the fusible link has already melted. Thus the first region of operation is the operation under which the steady state current does not cause the melting of the fusible link. This

is the normal operating regime of the system. The fuse can pass some maximum current called minimum fusing current I_{mfc} for an infinite duration without beginning to melt.

On the other hand, if the fuse is passing a current greater than I_{mfc} the fuse link will begin to melt. The time it takes the fuse link to begin melting is determined by integrating Equation 2.1 until T reaches T_{melt}. This defines the second regime of operation.

As the current is further increased the times required for melting to begin become shorter and shorter. At some point the times are so short that all of the electrical energy dissipated in the fuse link is used to heat the fuse link and none is lost to the environment. For this regime of operation, the environment loss coefficient is set to zero reducing the differential equation to:

$$mc_p\left(\frac{dT}{dt}\right) = I^2R \tag{2.4}$$

This regime of operation is called the constant I^2t regime or, somewhat ambiguously, adiabatic regime, to indicate that the energy supplied to the fusible link is entirely used to heat the fuse link and there is no exchange of heat with the environment (however energy is supplied to the fusible link). This is the third regime of operation of the CF during the pre-arcing period of the fuse operation.

In order to obtain theoretical results from the above mentioned equations, it is necessary to define all the constants appearing in Equation 2.1 and 2.2. The results examined in this chapter were created by using a square geometry of the fusible link composed of Zinc (Zn). The exact dimensions and values of all the constants related to this hypothetical fuse are not important for our discussion and can be found in the Appendix A along with the more detailed treatment of Equation 2.1.

Two different kinds of results were obtained using the above mentioned model for the hypothetical fuse given in Appendix A. For the normal regime of operation (regime N - for normal) the temperature of the fuse link for a given amount of current was be determined. This is visible in the Figure 2.1.

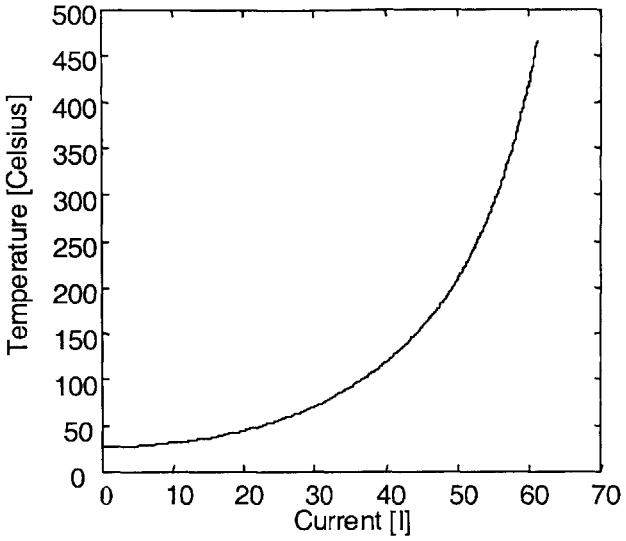

Figure 2.1 Steady state fuse link temperature as a function of current for a hypothetical fuse composed of Zn

If the current exceeds the minimum fusing current the time to melt as a function of current can be calculated. Figure 2.2 depicts this time to melt and the other two regimes of operation. The boundary between normal regime of operation and the regime in which heat exchange with the environment still happens (regime E- exchange regime) is clearly defined as the minimum fusing current I_{mfc}. However, the boundary between the regime E and the adiabatic

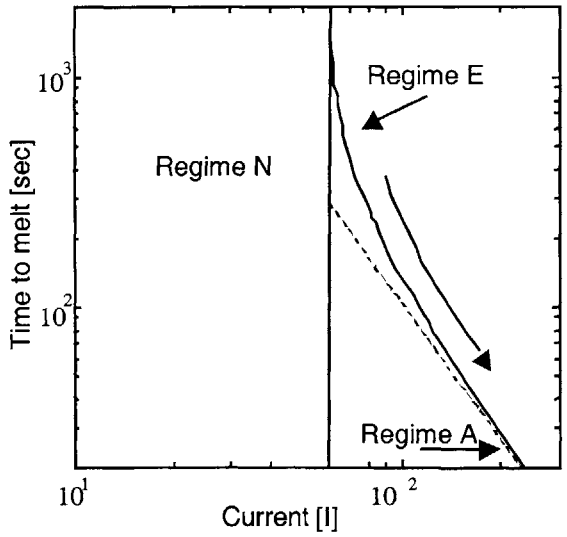

Figure 2.2 A plot of time to melt as a result of applied current for a hypothetical fuse composed of Zn.

regime (regime A) is not sharp. As the current levels are increased regime E slowly transits into regime A. Operation in regime N is shown in Figure 2.1. Figure 2.2 shows the three regimes of operation.

The I^2t line (dashed line) is the line for which U was set to zero and one can see that the fuse characteristic approaches this line asymptotically as I gets large. Thus the transition from regime E to regime A is not sharp, but a slow function of increasing fault current.

However, in this model some simplifying assumptions were made. It was assumed that the current density in the fusible link is constant. It was also assumed that the temperature is the same throughout the fusible link. Furthermore, it was assumed that the fusible link is composed of only one type of metal.

These assumptions do create a certain amount of errors in our model. The first two assumptions are very important because they apply to any type of fusible link. In order to investigate the effect of these assumptions the fusible link has to be divided into a large number of pieces and Equation 2.1 needs to be applied for each individual piece. Furthermore, the exchange of heat between pieces has to be accounted for in U. Further investigation of these refinements can be found in literature (4,5).

The third assumption directly influences the operation in the normal operating regime and deserves discussion. A. W. Metcalf discovered an effect first called 'M' effect (4) and now called diffusion pill technology (6). If the fusible link is coated with solder the interruption of the fuse happens faster since the fusible link acts at lower temperatures than the melting temperature of the fusible link material. The melting temperature of solder is lower than that of the fusible link material and thus it melts before the fuse link does. After the solder is in the liquid state the fuse link material (e.g. Zn) starts to dissolve into the solder and causes the fusible link to break faster due to the formation of solder-zinc alloy which has a lower melting point than zinc.

Unfortunately, if the system design engineer is not aware of the existence of this type of technology in the fuse link he could cause the diffusion process to

begin even at some current in the normal operating regime thus causing the fuse to nuisance blow. Therefore there is a current for which the fuse performance begins to deteriorate. In our theoretical fuse this would be 48.2 A if a solder globule composed of material conforming to the DIN standard L-Sn60Pb was used. The melting temperature of this type of solder is 185°C . This is visible in the Figure 2.1 in which one sees that for 48.2 A passing through the fuse the temperature of the fusible link reaches 185°C. Therefore, although the fuse might continue to operate after its temperature exceeds 185°C the diffusion process has begun and is irreversible. Reducing the current below 48.2 A before the fuse blows leaves one with a faster acting fuse in case of a subsequent fault current appearance. Furthermore, after such an irreversible heating event, the minimum fusing current I_{mfc} of the fuse might be altered, and typically it is reduced.

To summarize, pre-arcing behavior of the fuse link is divided into three different regimes of operation. In the normal region the fuse never blows because the fuse link never melts. However, its performance can deteriorate if its temperature exceeds some specified value (temperature at which the diffusion pill begins to melt). If $I_{mfc}(T_{amb})$ is exceeded the fuse will melt and the only question is how fast. Under a high fault current regime, I^2t is constant which enables determination of this time. At lower fault currents energy exchange with the environment is present and must be accounted for resulting in higher times than a constant I^2t would predict. The minimum fusing current I_{mfc} is defined as the current for which this melting time approaches infinity. All aspects of the pre-arcing behavior are strictly current dependent and are not influenced by the system voltage. The system voltage becomes important in considerations of the arcing behavior.

2.2.2. Arcing behavior of CF's

As the fuse begins to melt some of the fusible link material is present in the liquid phase. If the liquid phase is electrically in parallel with the solid phase the heating is concentrated in the solid phase as a result of its lower resistance. Due to this higher power dissipation, all of the electrically parallel solid phase

eventually transitions into liquid phase. Now, the liquid phase is in series with the lower resistance solid phase resulting in higher heat dissipation in the liquid phase and subsequent vaporization of some percentage of the liquid phase.

Both the vapor and the melted phase are free to move resulting in formation of gaps. These gaps initially act as capacitors. If the inductance of the circuit could be zero the current would be interrupted. However due to presence of inductance in the circuit the current can not go to zero instantaneously. Due to the low initial capacitance of the gaps they charge rapidly till the breakdown electric field of the gap is reached. At this time the arcs are formed.

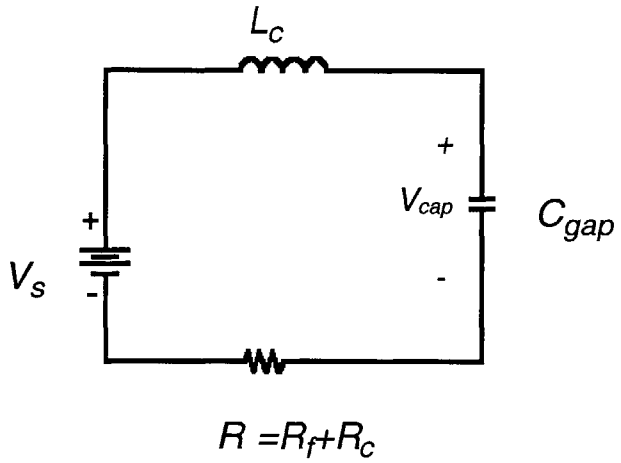

Figure 2.3 Equivalent circuit for a fault at the formation of gaps

Figure 2.3 is the equivalent circuit that represents the above situation. Here L_c is the inductance of the circuit, and V_s is the source voltage. R is the total resistance of the circuit composed of the resistance of the fuse element R_f and any additional resistance R_c present in the circuit. As the fuse begins to melt R_f increases even further since the liquid phase has higher resistivity and the linear dependence (Equation 2.2) does not hold any more. During the pre-arcing period C_{gap} can be taken to be infinity. At the moment the gaps are formed C_{gap} reduces to a rather low value. This causes a fast increase of the voltage drop across the fuse. When V_{cap} exceeds the breakdown voltage, arcing commences and persists until the current goes to zero.

The discussion of arc behavior in the next several paragraphs is drawn from Wright and Newbery (4). It is provided here as a convenience to the reader.

The arc is separated into three distinct regions. The first region is the anode fall region, the second region is the cathode fall region, and the connecting region is the positive column. Vaporized fuse link material ionizes and acts as a conductor in the arc (4).

The anode fall region is 10^{-3}mm long. Voltage drop across the region is taken to be roughly the ionization potential of fuse link material V_{af}. On the other hand, voltage fall across the cathode fall region is more or less constant at 10V. It's length is comparable to the anode fall region. The increase of the arc length is caused by the burn-back of both the anode and the cathode. The anode and the cathode are receiving power from the current passing through them and the bombardment by the ions and electrons. The power supplied to them is readily available to the melting and vaporization of the fuse link. Empirical data shows that the burn-back is the same for both electrodes thus allowing determination of the following energy balance given in Reference (4):

$$m_v\lambda_v + m_t\lambda_t + m_t c_p(T_m - T_{bulk}) = 2(V_{af} + V_{wf} + V_T)\int_0^t i\,dt \qquad (2.5)$$

where m_t is the mass of material melted, m_v is mass vaporized (roughly 40% of m_t), T_{bulk} is the temperature of the bulk of the fuse link at commencement of arcing (the assumption of constant T over the fuse link is not valid), λ_v and λ_t are latent heats of vaporization and melting respectively. The right hand side represents two times the power delivered to the anode where V_{wf} is the work function of the fusible link and V_T is the representation of energy electrons had on entering the anode fall region (roughly 1V). The energy available for the burnback of electrodes is twice the energy dissipated in the anode fall region (4).

The positive column consists of the quasineutral plasma and conducts current through both electrons and ions. A model of the conductivity as a function of temperature and electron density in the positive column is fully explained in Reference (4). That particular model is too advanced and a good approximation

of it is enough for this thesis. For the scope of this thesis it is enough to assume constant resistance equal to the resistance at the onset of arcing. In reality, as melting and vaporization progress, the length and resistance of the positive column will increase with time. Therefore this assumption gives a worst case approximation. Under this assumption the current through the fuse during arcing exponentially decreases. This is shown in Figure 2.4.

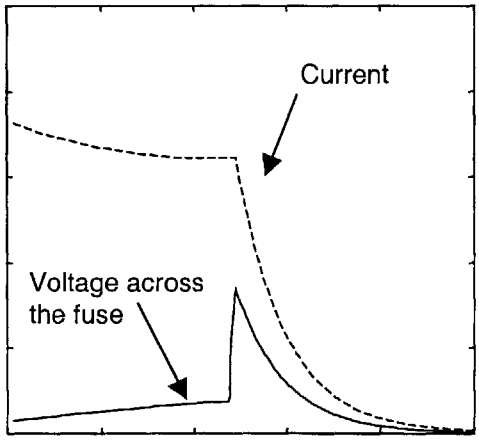

Figure 2.4 Current through a fuse and voltage across the fuse during arcing

Therefore, a conventional fuse operates by melting and then reducing the current to zero during arcing. The time to interrupt the current is highly dependent on the amount of inductance present in the circuit. As the supply voltage is increased by three in the new automotive electrical environments, average prospective fault currents may stay the same under certain assumptions which are further discussed in Chapter 4. Because of the nature of the fuse design and increased source voltage the rate of current reduction during the arcing regime of operation will reduced at 42V for a given fuse design as compared to 14 V. This is the result of the voltage that causes the onset of arcing. This voltage is higher than the sum of the voltage across the anode and cathode fall regions and generally is around 20-50 volts (for today's automotive fuses it is typically ~32 V). In a 14V system this always insures a negative voltage to appear across the inductance resulting in a negative di/dt. In a 42 V system the voltage that appears across the inductor may in fact be positive (for purely inductive load) for

the case of today's automotive fuses. Thus, the interruption times for the same values of inductance present in 14 and 42 volt systems will be longer in the 42 V systems as compared to 14 V systems for a given fuse design.

Thus, today's automotive fuses do not have satisfactory performance at 42 V. In fact they are not rated to safely interrupt currents at such high supply voltages. More importantly, their operating times at higher source voltages will be longer for the same current primarily due to the longer arcing periods for the same amount of L in the circuit. A simple solution of this problem is to form multiple arcs of maximum attainable length. Each arc would then reach some preset voltage $V_{arc}(i)$ and the drop across the fuse would be the sum over all arcs. This approach usually causes the normal (non-overcurrent) resistance of the fuse to be increased. To form multiple arcs one must construct multiple restrictions in the fuse and expect them to fuse at the same current. However in order to achieve this the resistance of each restriction has to be the same. Thus a fuse with two arcs will have twice the resistance of the fuse with one arc if their minimum fusing currents (I_{mfc}) are the same.

While multiple arcs are one possible strategy for dealing with inductances at higher voltages it is not the only one. Wickmann's automotive fuses rated at 32 V have roughly half the resistance of Wickmann's automotive fuses rated at 80 V (7). However, Wickmann does not use the strategy of multiple arcs. In particular, Wickmann employs the strategy of using the filler (most likely quartz sand used in line voltage fuses) to dissipate the energy present in the arc and fusible link materials and construction that require more energy to burn the electrodes away.

Automotive fuses rated to safely operate at voltages up to 60 V are slowly making their way out of the design phase and into the market. One of the first manufacturers of automotive blade type fuses rated to operate within the voltage specifications of the proposed 42 V electrical distribution system is Wickmann. So far Wickman has demonstrated that their fuses can safely operate at higher source voltages. It still remains to be seen how the inductance limitations of 42 V automotive fuses compare to 12 V automotive fuses.

While the car manufacturers are starting to evaluate fuses rated for 42 V electrical distribution system (EDS), other technologies have developed that are also capable of performing the fuse function in the 42 V EDS and offer other additional performance benefits.

2.3. Smart Power Switches

Smart power switches (SPS's) where developed by Infineon Technologies. The brand name PROFET® (protection mosfet) is used by Infineon for smart power switches. While other companies are also developing SPS's, the state of development of their product lines is not as advanced as Infineon's devices. These devices are semiconductor power mosfet switches with on-chip diagnostic, current limiting, overcurrent protection, short circuit protection, overvoltage protection, undervoltage protection and/or reverse voltage protection. In many ways they differ considerably form both CF's and PPTC's and it is important to review their operation while stressing important aspects of this operation.

Figure 2.5 shows a block diagram of a SPS chip BTS640 S2. Other devices

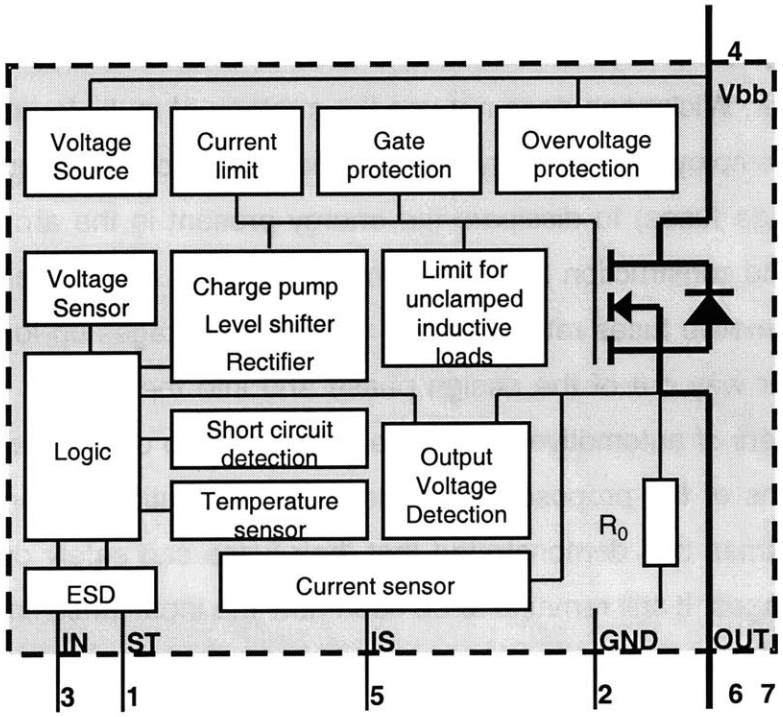

Figure 2.5 Block diagram of the SPS with sense function

differ in their functionality as described in the data sheets provided by Infineon. A thorough description of the device operation can also be obtained from Infineon. The parts important to the fusing and protection behavior will be treated in this chapter.

The main element of the SPS is the power mosfet that acts as switch and carries the load current. The behavior of a power mosfet is known, many theoretical models exist, and is therefore unnecessary to repeat the theory here (9,10). The only interesting behavior of this mosfet relevant to its protection operation is the current saturation of its I-V steady state characteristic.

The I-V characteristic of the power mosfet is shown in Figure 2.6 by thin lines for two gate voltages. However, after the voltage drop between the drain and source $(C) V_{DS}$ of the SPS is increased beyond some value called fold back voltage the device automatically switches to a lower current characteristic by self adjusting the voltage on the gate of the mosfet. The resulting SPS characteristic is visible in Figure 2.6 as a thicker line.

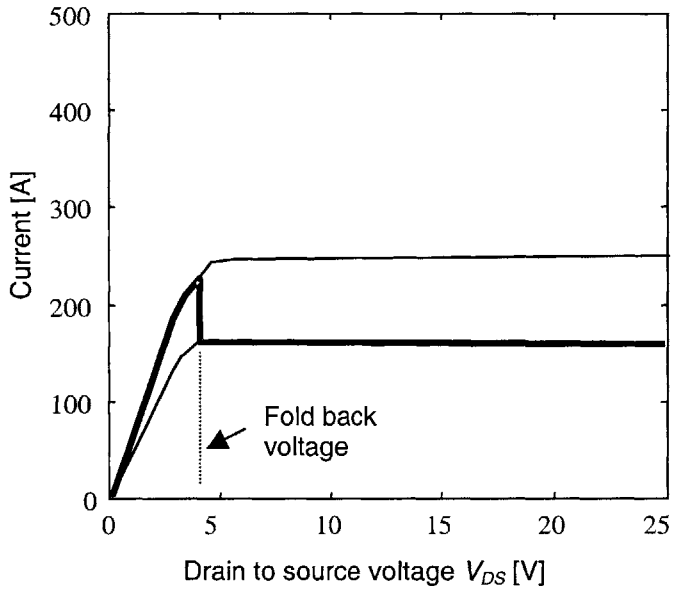

Figure 2.6 I-V characteristic of a power mosfet for two different values of gate voltage and the resulting characteristic of the BTS 660 P type SPS

Due to the thermal nature of the semiconductor the SPS I-V characteristic is dependent on the silicon junction temperature. This relationship is also well

known and its effect on the SPS is shown in Figure 2.7. The curves depicted in Figure 2.7 are I-V characteristics of the Profet when the temperature of the silicon junction is maintained constant. When the device passes high current, the power dissipation of the SPS causes the SPS silicon junction to heat up above ambient temperature and thus the device operates through a range of temperatures depending on the load current level. If the temperature of the junction goes beyond a certain T_{jmax} the SPS will switch off. This protects the device from reaching excessive temperatures and thermally destroying itself. However it presents a behavior quite similar to fuse behavior and is capable of protecting the rest of the circuit as well thus making the SPS capable of doing a fuse function (11,12, 13).

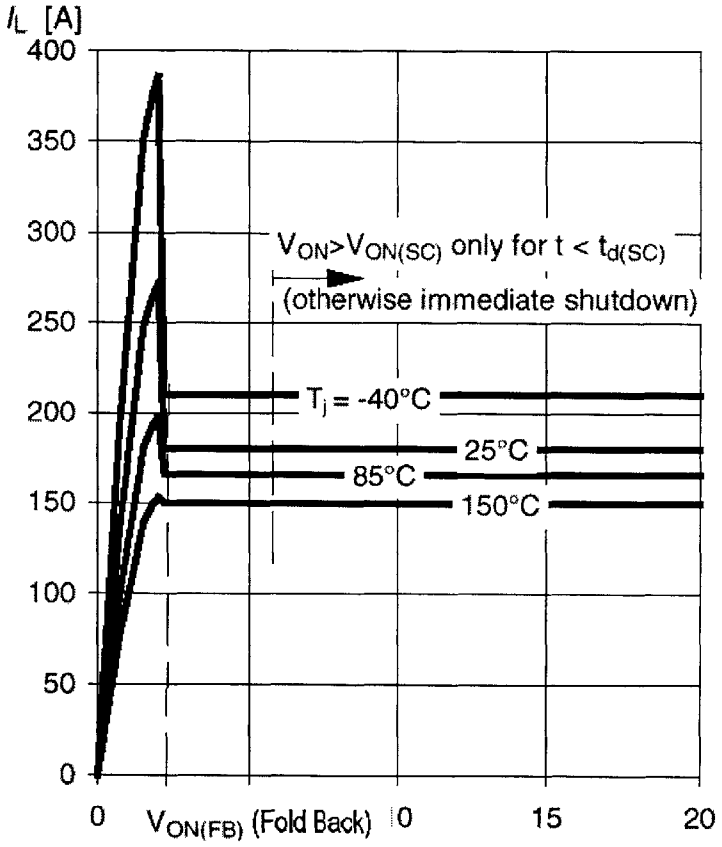

Figure 2.7 I-V characteristic of BTS660P as a function of Temperature (11). Reprinted with permission.

2.3.1. Fuse function of the SPS

To evaluate the usability of SPS as fuses, their behavior needs to be evaluated in a way similar to the way the behavior of fuses is evaluated. There exists a range of currents for a given ambient temperature for which the device will not exceed T_{jmax} (typically 150°C) and will not turn off. This range of currents can be found using Equation 2.3 with obvious changes in the definition of variables. Furthermore the minimum fusing current can be defined by Equation 2.3 by setting $T=T_{jmax}$ and replacing U by $1/R_{th}$ (thermal resistance) of the SPS. Beyond I_{mfc} the behavior is the same as the fuse behavior for small over-currents. As the over-currents increase SPS acts differently. One can plot the time to turnoff (this plot is equivalent to the plot of to time to melt for fuses) for SPS versus the current that would flow if the device had the resistance R_{on} that it has when its junction is at T_{amb}=25°C . This current is called prospective current and

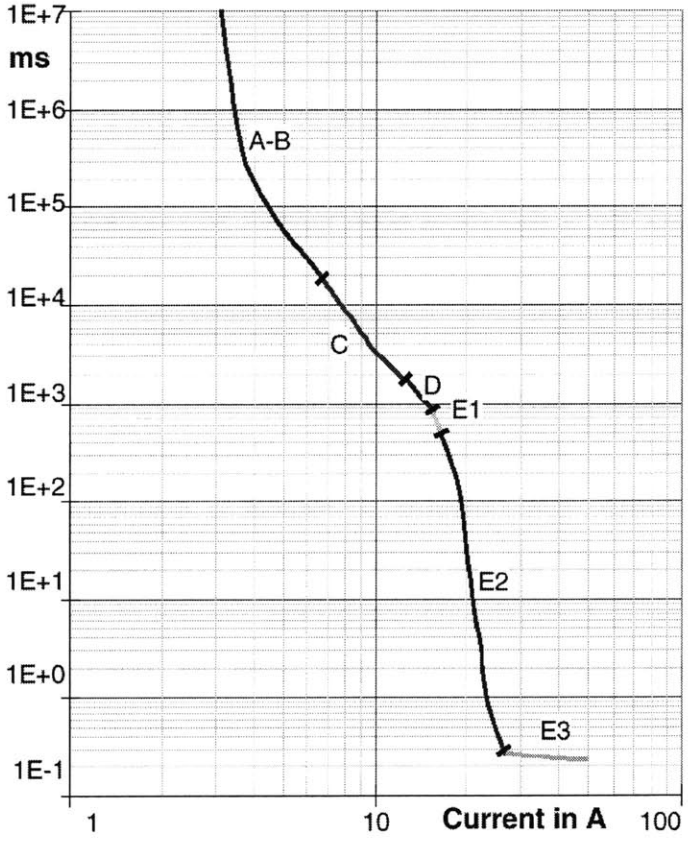

Figure 2.8 Time to switch off for a BTS 410 E2.(Inductive turnoff not included) (11). Reprinted with permission.

the resulting I_p-t is shown in Figure 2.8.

The characteristic is divided into regimes of operation and each one can be discussed separately. In regime A, Equation 2.1 holds and the SPS is acting like a fuse. Regime B is the transition region to I^2t=constant and the I^2t=constant regime. However in region C something interesting happens. When the fault develops the SPS is still in its resistive state. (R is a function of junction temperature T_j only) as it heats up it reaches drain to source voltage V_{DS} where current limiting begins according to Figure 2.6. In regime D the SPS starts in the current limiting regime and the dissipation is now I_{limit}* V_{DS} as opposed to I^2R. I_{limit} is still a function of V_{DS}. In region E1 current is limited and the gate voltage on the mosfet has been reached for which the current is independent of V_{DS}. In these regimes the shutdown is accomplished by reaching a thermal limiting temperature of T_{jmax}. Detailed description of the various regions of operation can be found in References 11 and 14.

Figure 2.8 includes additional regimes that exist for certain SPS devices. They have an additional shutdown based on monitoring of the drain to source voltage V_{DS}. If some fixed value of V_{DS} is exceeded the SPS shuts down in some designated time. Infineon calls this voltage monitoring regime of operation SC protection. Regime E2 is transition from limited V_{DS} regime to SC regime and E3 is the SC regime limited by initial time delay.

It is very important to know that a current higher than the short circuit maximum peak current I_{SCP} as specified in the data sheets can not be exceeded. It can not exist even for transient operation. Thus this leaves only regimes A and B for inrush currents. The currents in region C and onwards are prospective currents only, physically the currents in those regimes cannot exist. If such a current were to be fed into the device by the means of an ideal current source, the device would follow its load line untill its voltage grew beyond the specification given for safe operation. The chip would be destroyed by heat dissipation since it could not shut off the current.

The behavior up to this point could be considered equivalent to the pre-arcing behavior of the fuse with the current limiting added. It is interesting to note

that the fuse also presents some current limiting due to the resistance increase caused by temperature. This fuse limiting is far from being close to the SPS behavior. The fuse limits current by heating up. The SPS limits the current by the nature of the saturation behavior of the mosfet on which it is based.

However, in order to interrupt a current successfully the SPS must deal with the inductive turnoff.

2.3.2. Turnoff of an Inductive load

At the moment the SPS reaches its thermal limit ($T_j > T_{jmax}$) it shuts off the gate. However, to prevent excessive voltages to be induced across SPS, the SPS may turn partially on to limit the voltage across the device to a value V_{cl} (15). This voltage is more or less constant since it is a voltage specified by the zener voltage of the zener diode connected to the gate. For an appropriate choice of source voltage V_s the voltage that appears across the R_c and L_c is some negative voltage $-V_L$. At this point we have:

$$-V_L = V_S - V_{CL}$$

$$L_C \frac{di}{dt} = -iR_C - V_L \tag{2.8}$$

Thus by solving it we can obtain:

$$i(t,R,L) = (I_0 + \frac{V_L}{R_C})e^{-R_C t / L_C} - \frac{V_L}{R_C} \tag{2.9a}$$

$$i(t,R=0,L) = I_0 - \frac{V_L}{L_C}t \tag{2.9b}$$

where I_0 is the current at onset of the inductive turnoff .By using Equation 2.9b we can find the maximum opening time for any given L.

The minimum resistance present in the circuit is the equivalent series resistance of the source in Figure 2.9. Furthermore we can find the energy dissipated in the circuit by integrating the current from $t=0$ to $i_L = 0$ and multiplying it by the average voltage drop across the device. $(V_{clmax}+V_{clmin})/2$. An exact solution involves knowing the $V_{cl}(i_L)$, however because this is a zener voltage it

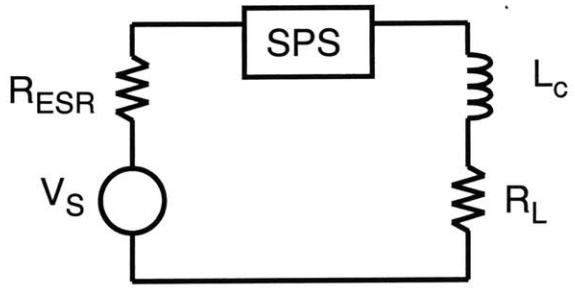

Figure 2.9 Circuit applicable during an inductive load turnoff with an SPS.(R_C=R_L+R_{ESR})

remains relatively constant for all currents not close to zero. Currents close to zero do not pose any trouble since the power dissipation in the device due to these currents is negligible. They cause a collapse of the V_{DS}. Thus the approximation of the V_{cl} as constant is justified. The energy imparted on the device is then given by:

$$E = \frac{\overline{V}_{CL} I_0 L_C}{R_C} - \frac{\overline{V}_{CL}(\overline{V}_{CL} - V_S) L_C}{R_C^2} \ln\left(\frac{\overline{V}_{CL} - V_S + I_0 R_C}{\overline{V}_{CL} - V_S}\right) \tag{2.10a}$$

$$E = \frac{\overline{V}_{CL} I_0^2 L_C}{2(\overline{V}_{CL} - V_S)} \text{ for } R_C = 0 \tag{2.10b}$$

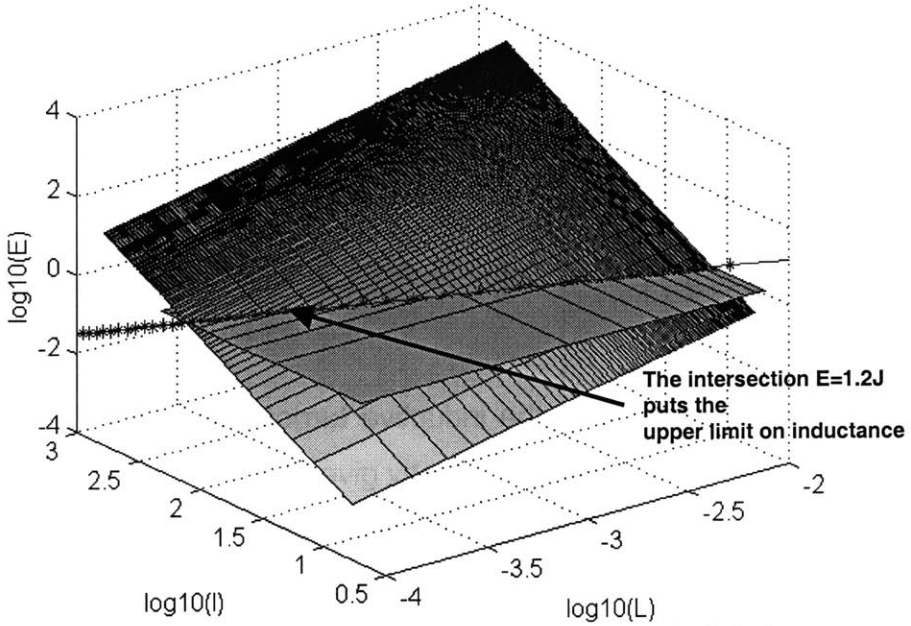

Figure 2.10 Logarithmic plot of energy imparted on the SPS during an inductive load turnoff as a function of initial turnoff current I and inductance present in the circuit. (The horizontal surface is the maximum allowed)

where I_0 is the current at the beginning of inductive turnoff, R_c and L_c are the resistance and the inductance in the circuit excluding the SPS, as shown in the Figure 2.9.

Figure 2.10 is a plot of Equation 2.10b for a BTS 650 P also showing its maximum allowed energy (E_{max}=1.2J) that can be dissipated in the device during inductive turnoff and not cause the device to destroy itself. The knowledge of E_{max} thus gives the necessary restriction on L. One can also see that this is also dependent on the source voltage V_s. As the source voltage is increased the maximum allowed inductance is reduced.

2.3.3. Added functionality

Besides having the fuse protection function SPS's also have substantial added functionality. They are switches, and have to deal with the requirement of turning off the inductive load. SPS's perform this in the same way they clear an inductive fault. Furthermore, SPS's have shutdown if overvoltage occurs, they can block reverse voltage, sense a short circuit to ground and undervoltage and respond by staying off, and two feedback lines, status and current sense. Status feedback tells us the state of the SPS in logic. Current sense tells us the current in the mosfet. Using this feedback one can create a protective device that interrupts current whenever there is a fault current greater than some given amount I_f which has to be less than the I_{mfc} of the SPS. The details of these additional functions are further explained by Infineon datasheets and application notes (16).

By addition of a heat sink the I_{mfc} of the SPS can be changed. This is caused by the change of the thermal resistance of the device R_{th}. Therefore one type of SPS can be used as a fuse with various values of I_{mfc} by choosing the appropriate heat sink.

2.4. Polymeric Positive Temperature Coefficient Devices

The physical behavior of PPTC's has microscopic and macroscopic explanations. While the macroscopic explanation is sufficient to explain their behavior in resistive electrical circuits it is interesting to understand the microscopic behavior as a basis for explaining the macroscopic behavior. The microscopic behavior can be explained by the use of three distinctive processes, percolation, quantum mechanical tunneling and, thermal expansion.

2.4.1. Microscopic behavior

PPTC's are composed of a cross-linked polymer that has carbon particles embedded in it. The packing density of carbon particles is extremely high. These particles have a set conductivity equal to the conductivity of carbon. However, most of the time the carbon particles do not touch each other but are separated by a gap. Electrons traverse this gap by the process of quantum mechanical tunneling or by conducting through the polymer. The transfer of electrons is referred to as a process of percolation.

Percolation is a process responsible for the resistance behavior of the polymer-conductor aggregate. Above some critical length of the gap between carbon particles, material conductivity is primarily due to the conductivity of polymer. However as this gap length is shortened the quantum mechanical tunneling takes over as the defining factor of the gap resistance. Complete description of percolation is given in (17). A model that is sufficient for the scope of this thesis considers the gap between conductive carbon particles as constructed of two resistances connected in parallel. The first resistance is the resistance of the polymer R_{pl} and the second resistance is the effective resistance R_{qt} of the quantum mechanical tunneling. Now we proceed by keeping R_{pl} constant while increasing R_{qt} from a value much smaller than R_{pl} to a value much higher than R_{pl}. We notice that the resistance of the parallel connection for really low values of R_{qt} is primarily R_{qt} and for really high values of R_{qt} the

resistance is given by R_{pl}. The value at which the resistance of the parallel connection changes is termed percolation threshold. An example of this analysis is presented in Figure 2.11.

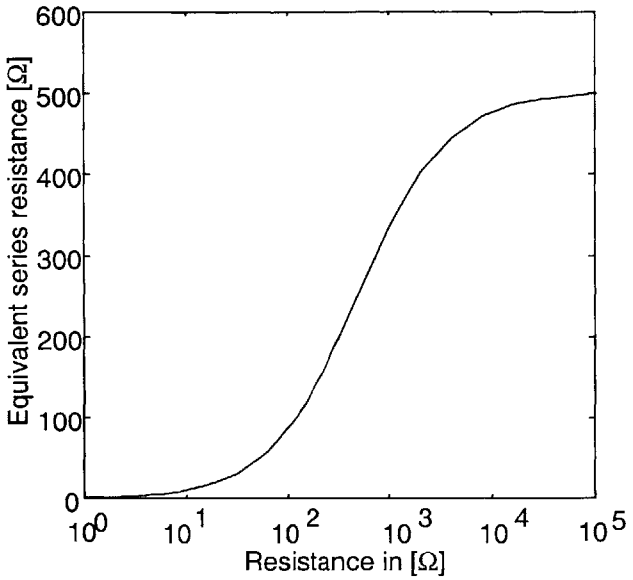

Figure 2.11 The equivalent resistance of two resistors connected in parallel when the resistance of one resistor is kept constant at R=500 Ω and the resistance of the other is varied.

In order to determine the resistance we need to know the effective resistance of the quantum mechanical tunneling. One can use two different solutions for quantum mechanical tunneling. If we choose to ignore the effect of quantum thermal fluctuations we would use the equations for normal quantum tunneling but they would not give us the right results because the thermal contribution at room temperatures can be substantial. These thermal contributions are responsible for Johnson noise in resistors and the theory for the thermally induced voltages can be found in (18). A more general treatment is necessary that includes the quantum thermal fluctuations. This is refereed to as quantum-fluctuations augmented tunneling (17). Average voltage induced due to the quantum thermal fluctuations increases with increasing temperature or increasing voltage applied to the junction (17). This phenomenon is very important because it makes it harder to determine what the true voltage across any gap is. While macroscopic measurements and simulations give one result for

the voltage it should be kept in mind that quantum statistical considerations add additional locally induced voltage on the microscopic level which is macroscopically not apparent.

Thermal expansion of the polymer plays the role of defining the gap length. A properly chosen polymer will expand quite rapidly around some temperature T_{trip}. Figure 2.12 shows the specific volume of the polymer used for automotive PPTC's as a function of temperature. We see that the expansion around 125°C is quite rapid and it is considered that the polymer undergoes a phase change. However, the polymer does not become liquid due to its high degree of cross-linking. The abrupt change in volume of the polymer causes the aggregate to shift from a low resistance state to a high resistance state as described by the percolation theory. While the polymer has the abrupt change in volume as a function of temperature, the carbon particles expand only linearly as

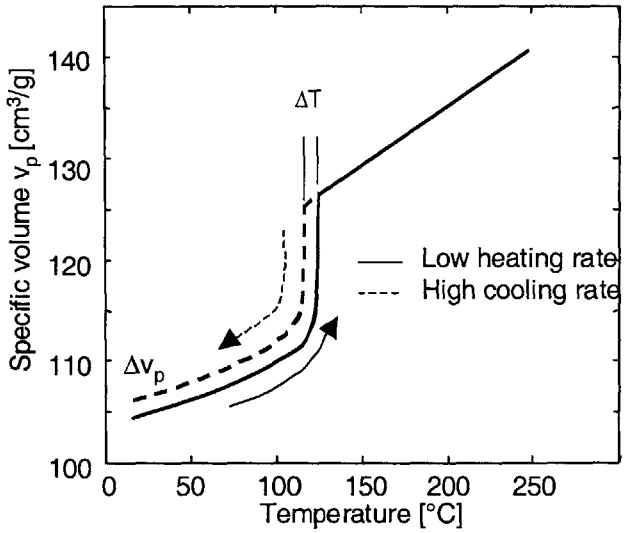

Figure 2.12 Specific volume of HDPE polymer as a function of temperature (17).

a function of temperature. Therefor, the gap between any two carbon particles abruptly changes around the phase transition temperature.

Furthermore, the effective resistance associated with quantum mechanical tunneling increases exponentially as a function of increasing gap length while the resistance of the polymer increases only linearly. This causes the effective resistance of quantum mechanical tunneling to exceed the

resistance of the polymer. According to theory of percolation the resistance of the gap when the polymer has expanded is given by the resistance of the polymer.

Looking at Figure 2.12 one can see that after the polymer has expanded cooling does not return it to its original volume. The hysteresis associated with fast cooling rates is only temporary and goes away with time. However it does leave the PPTC with a higher resistance after the trip event. The effect is not cumulative and repeated trip events will not cause the resistance of the PPTC to keep increasing. However, the post trip resistance is higher than the resistance of the device that never tripped. Implications of this effect will be discussed in later chapters.

2.4.2. Macroscopic behavior

The macroscopic consequence of microscopic behavior is the temperature dependent resistance as visible in Figure 2.13. Thus we can conclude that if we heat up a PPTC its resistance will increase. During the operation as a protective device the PPTC heats up as a result of power dissipation from the current in it

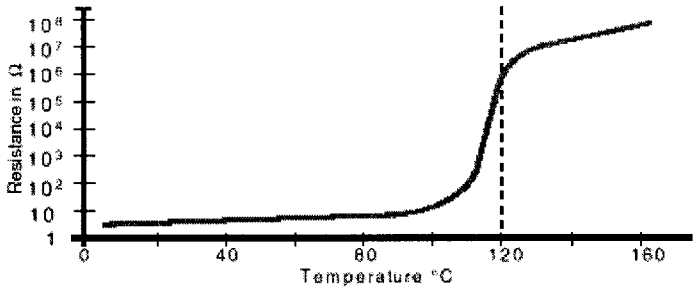

Figure 2.13 Resistance of PPTC as a function of temperature (11). Reprinted with permission.

and has an equivalent behavior as a fuse behavior described in Section 2.2. However now instead of the melting temperature the important temperature is the temperature at which the polymer starts to expand rather abruptly.

In order to model the behavior of the PPTC theoretically on the macroscopic scale we need to solve both the heat diffusion and the magnetic field diffusion equation simultaneously. The heat diffusion equation is given by:

$$\frac{\partial}{\partial x}\left(k\frac{\partial T}{\partial x}\right)+\frac{\partial}{\partial y}\left(k\frac{\partial T}{\partial y}\right)+\frac{\partial}{\partial z}\left(k\frac{\partial T}{\partial z}\right)=\rho c_p\frac{\partial T}{\partial t}-\frac{|\underline{J}|^2}{\sigma} \qquad (2.11)$$

where k is the thermal conductivity of the PPTC, ρ is the density, $\underline{J}$ is the current density and σ is the electrical conductivity. Unfortunately, all the parameters of this equation are temperature dependent. Furthermore, the current density is governed by the magnetic field diffusion equation given by:

$$\frac{1}{\mu}\left[\frac{1}{\sigma}\left(\nabla^2 \underline{B}\right)+\left(\nabla^2 \frac{1}{\sigma}\right)\underline{B}\right]=\frac{\partial \underline{B}}{\partial t} \tag{2.12}$$

which when combined with Maxwell's equations and Ohm's law in its differential form:

$$\underline{J}=\sigma \underline{E} \tag{2.13}$$

gives the current density. Thus having these two equations and knowing the electrical circuit connected to the PPTC gives us the necessary elements to formulate the theoretical problem of the PPTC behavior.

The problem at hand is too complicated to fall within the scope of this thesis but the discussion of the issues related to the solution is presented. In the attempt to simplify the problem it is interesting to investigate various parameters of Equations 2.11 through 2.13. The first simplifying assumption is to set the density, thermal capacity and thermal conductivity to a constant. In reality density reduces with increasing temperature due to increasing volume. However, from experimental data of the thermal capacity we can see that the thermal capacity increases as a function of temperature so to a first order approximation these two effects cancel each other. Thus one can assume that density and thermal capacity are to first order constant.

In order to assume that thermal conductivity is constant we need to know its behavior as a function of temperature. Currently no experimental data exists but preliminary testing by Raychem suggests that thermal conductivity decreases as a function of temperature. In fact, this can be directly postulated from the realization that thermal conductivity is explained by a similar theory as the electrical conductivity (excluding the quantum mechanical tunneling). The initial tests performed by Raychem suggest that thermal conductivity only decreases by 20% as the polymer changes phase. This is theoretically justified by the fact that

heat is not conducted away through the process of quantum mechanical tunneling. Thus as the polymer expands its thermal conductivity decreases as a result of volume change and reduced interaction of particles due to larger particle separation.

Any differential volume within the PPTC that has undergone the phase transition will conduct heat away from itself less rapidly. At the same time more heat will be generated in it due to the nonlinear resistance characteristic.

In trying to guess the behavior of a cubical PPTC with two electrodes on opposite faces of the cube, one can begin with the assumption that the midpoint is going to go through the phase transition first. To continue the analysis, consider the plane that crosses through the midpoint and is parallel to the electrode planes. Because the midpoint is in a high resistance state the current is diverted away from the midpoint. The concentration of the current in the area which has not undergone the transition results in faster transition of the remaining portions of the plane. This causes the whole plane to transit into a high resistance state very rapidly. One is at liberty to justify the reduction of the model into a one-dimensional model provided the time constant representing the transition of the plane into a high resistance state is larger than the magnetic diffusion time constant in the material. As a result, the reduction to a one-dimensional model is justified only up to some magnitude of overcurrent. For higher currents and the resulting faster transition, the magnetic diffusion starts to resist the redistribution of current into low resistance area and the one-dimensional argument cannot be made.

For lower overcurrents the transition and redistribution happens slow enough for the magnetic diffusion to play no factor in the behavior. Because the current chooses the path of least resistance it forces the above-mentioned plane to become an isothermal plane within the PPTC. If the plane is an isothermal plane a one-dimensional approximation can be made.

At this point the heat diffusion equation is given by:

$$k\frac{\partial^2 T}{\partial x^2} = \rho c_p \frac{\partial T}{\partial t} - \frac{I^2}{A^2\sigma} \tag{2.14}$$

where A is the cross-sectional area of the PPTC and I is the current in the PPTC. Here the assumption was made that the density, thermal conductivity and capacity are constant. In order to obtain the resistance of the PPTC the conductivity is integrated over the length of the PPTC at any given time:

$$R = \int \frac{1}{A\sigma}\, dx \tag{2.15}$$

Unfortunately, due to the nonlinear temperature dependence of electrical conductivity even this simplified model is not solvable in a closed-form solution. One way to obtain a solution would be to linearise the problem. However, this would take away the essential behavior under investigation. The second approach is to solve the problem numerically by means of finite difference methods. Because the model has been simplified so much, many of the defining factors of the behavior are being left out. And thus it seems unreasonable that this model can help us simulate the behavior of the device to the extent necessary to predict device failures. The solution of the more general model can be done through the finite difference method, but is beyond the scope of this thesis.

When the PPTC is put into a purely resistive circuit with currents large enough to cause it to trip, its temperature starts to grow. The midpoint of the PPTC transits into a high resistance state and causes the fault current to decrease. Finally the PPTC reaches the steady state temperature distribution in which the electrical power dissipation is equal to the heat dissipation to the environment. Because the resistance strongly varies with temperature (note the log scale of Figure 2.13) the device in the tripped state operates nearly as a constant power device over a substantial range of fault impedance. The heat necessary to keep the device in the tripped state is dependent on the heat dissipation. Heat dissipation is a function of temperature difference between the device and the environment. However, the temperature of the device in the region of rapid change of resistance in nearly constant. Thus, the device that tripped operates as a constant power device.

Furthermore, the minimum current necessary to keep the device in the tripped state is less than the current that causes the device to trip. If the circuit is returned to its pre-fault conditions the device may not reset. The only way to practically reset the device is to turn the current off with a switch and wait for the device to cool down.

2.4.3. Inductive fault interruption

When there is inductance present in the circuit, the PPTC needs to absorb more energy to interrupt the fault current. Here the strong temperature dependence of resistance presents a risk to the device. The transition of the device produces a large resistance. The inductor prevents a rapid decline in current. The result is a large voltage across the inductor and the PPTC. The transient energy absorption of the device during transition is small, because of small device mass and limited temperature change. On the other hand, the rate of electrical energy dissipation is large, because of large voltage and high current. The transition is therefore very rapid. A large voltage appears across the PPTC as soon as the midpoint has undergone the transition. The large voltage is at that instant localized at the midpoint of the device. And the midpoint is pushed to a higher temperature than it would normally experience in a purely resistive circuit.

While the exact mode of failure is not yet identified, it was observed experimentally that some values of inductance do result in device destruction. One can postulate two different modes of failure. If the electric field locally exceeds the punch-through value of the polymer, an arc will form and most likely fracture and/or ignite the polymer. On the other hand, if the thermal decomposition temperature of the polymer is reached the polymer will locally decompose and facilitate the formation of the carbon resistor as a low resistance path. In turn this will cause the polymer to ignite due to majority of the power dissipation being localized in a relatively low impedance carbon resistor as opposed to the polymer.

However, the macroscopic analysis presented above assumes that the material is a continuum and neglects the microscopic effect of quantum thermal fluctuations. If the mode of failure for the device is considered to be electric punch-through through the polymer then the defining factor of this punch-through is going to be both the quantum thermally induced voltage across the gap as well as the macroscopically present voltage due to the voltage across the device and its localized resistivity. Therefore any macroscopic study will have problems in determining the true values of the voltage across any given gap and consequently the electric field strength in the gap. In particular the macroscopic study presented above would underestimate this electric field strength by underestimating the voltage across the gap.

Presently, PPTC's are qualified experimentally for each application. There is no general guidance for what value of inductance is permissible. According to the manufacturer, the PPTC can deal with a wide range of fault inductances in realistic conditions. However, the bound on maximum inductance present in the circuit during a fault should be established by the manufacturer to allow more systematical use of the PPTC as a protection device. In some automotive applications today the load inductance can present problems to the PPTC. In future 42 V EDS the inductance will increase for a given inductive load under the assumptions of constant energy storage and constant power dissipation. Furthermore, the future loads planned for the 42 V EDS are to a great extent inductive (i.e. electromagnetic suspension and electromagnetic valves).

Chapter 3.

Characterization of Devices

3.1. Introduction

Before discussing various results that can be deduced from the theory presented in Chapter 2 and experimental testing of devices, it is important to establish certain means of comparison of device performance. Today many different measures are used to compare the characteristics of fuses. Some of these are defined and explained in this chapter. Furthermore, their applicability to the SPS and PPTC is considered. Because SPS and PPTC have some added functionality, additional means of comparison need to be established in order to characterize the added functionality. These additional means of comparison are described in Section 3.3.

3.2. Means of characterizations currently in use

3.2.1. Definitions

Some definitions need to be made before we can begin this section. Some of the things being defined are means of comparison too.

I_{mfc} is the minimum fusing current for a device at a given ambient temperature. If this current was flowing through a CF it would take infinite time for the CF to fuse. In case of SPS it would take infinite time for it to turn off. The PPTC would take infinite time to develop 90% of the source voltage V_s across itself. At this current the thermal equilibrium is established at temperature T that is critical for the device operation. The electrical power dissipation in the device is equal to the heat loss to the environment. If the current is only increased by a differential amount the CF will melt, the SPS will turn off and PPTC will trip to a high resistance state. However, due to production process variations and device aging under the stress of operation there will exist some range ΔI_{mfc} for any given group of devices with same ratings and part numbers. The extremes of these variations are reflected in the trip current I_{trip} and the hold current $I_{hold.}$

I_{trip} is the trip current. If this current is exceeded all devices in a group with same part number being characterized will fuse or trip. This is the maximum value of I_{mfc} for the devices with same part numbers.

I_{hold} is the hold current. If this current is not exceeded no device in a group with same part number being characterized will fuse or trip. This is the minimum value of I_{mfc} for the devices with same part numbers.

I_{nom} is the nominal current for a given device type. Although devices will not necessarily trip above this current they are guaranteed not to trip or degrade their behavior if this current is not exceeded in a steady state conditions.

A minimum fusing factor f is defined as the ratio of I_{mfo}/I_{nom}. This fusing factor is built in to the specification to ensure the performance degradation does not occur during normal operation and to account for differences in the production of devices and variability across manufacturers conforming to a given standard for rating the devices. Not all devices with same rating have the same performance. The fusing factor is usually between 1 and 2.

Prospective current I_p is the current that would flow in the device if the device was a resistive element and had the same resistance as the resistance it has when its temperature T is equal to ambient temperature T_{amb}. None of the three devices ever carry this current for a long time due to changes arising from

the increase of the device temperature. However, while the PPTC and the CF can carry 100% of the prospective current initially, SPS has a mosfet I-V characteristic and therefore never carries more current than specified in its current saturation region of operation.

Virtual time t_v is an old means of characterization not widely used any more. Knowing the melting I^2t of the fuse we can calculate the time needed for a fuse to begin melting if we know the current that flows in the circuit. Virtual time is the time obtained by dividing the I^2t value of a fault by the square of the prospective current. Since the time is different for each individual fault condition this standard is not widely used any more. However the *I-t* plots still use virtual time since the values of I^2t of a given fault are integrals of the square of instantaneous current and the time is calculated by dividing this integral by the square of prospective current.

3.2.2. I^2t value

As described in Chapter 2, for very high currents in conventional fuses, the product of time to t_{melt} and the square of prospective current I_P becomes a constant. This constant value is called the fuse's melting I^2t capability. For high current this value can be used to calculate the time to melt for a fuse passing a given current. While conventional fuses asymptotically approach constant melting I^2t values for high currents, SPS's do not have this behavior due to their substantially different *I-V* characteristic. PPTC's also do not have constant I^2t for high current values because of their nonlinear resistance characteristic and different behavior at different rates of heating.

Many CF manufacturers calculate melting I^2t values by integrating the square of the instantaneous current during a fault up to onset of melting. The value of this integral is called the melting I^2t and it applies for high currents. Furthermore they also give us a maximum arcing I^2t. This is the integral of the square of the instantaneous current during the arcing period only and it tells us the maximum time permitted for arcing given any current behavior and its initial value at onset of arcing. In a way this value also imposes the upper limit on the

allowed inductance in the circuit. If we make the assumption that the resistance of the fuse is constant during arcing then I^2t is a measure of the energy imparted on the fuse. If too much energy is imparted to the fuse it will not safely interrupt the current.

The SPS have constant drain to source voltage V_{DS} during turnoff of inductive loads and one can calculate the maximum inductive turnoff I^2t for a SPS switch based on the Equation 2.9 by integrating the square of the instantaneous current. Furthermore, the data sheets also provide the maximum energy that the device can dissipate during an inductive turnoff. This energy gives us the limits on L and R thus giving us the maximum 'arcing' I^2t as a function of circuit inductance and circuit resistance.

3.2.3. Current versus time plot

Another name for this is the *I-t* characteristic. For conventional fuses these graphs depict prospective current I_p versus virtual time to melt t_v at a given ambient temperature (usually T_{amb}=25°C) and are referred to as *I-t* melting plots. An example of this graph is given in Figure 2.2 for the hypothetical fuse discussed in Chapter 2. Furthermore, if the inductance in the circuit is known, one can plot in a similar way a virtual time to extinguish the current versus the prospective current. The resulting *I-t* plot would be the arcing *I-t* plot. Since these plots are circuit dependent it is rarely done as a part of the specification. However, one can plot the worst case *I-t* arcing plot assuming the maximum allowed value of inductance present in the circuit.

SPS's *I-t* plots depict virtual time t_v to beginning of turnoff. Again, depending on circuit inductance L_c the time for completion of turnoff could extend by any amount as described in Equation 2.9 to give us the time to clear.

I-t plots for PPTC's are different. They plot the time for the voltage across the PPTC to raise above some percentage of the source voltage V_s. This time will depend on the source voltage and the circuit inductance.

Figure 3.1 shows an example for a SPS with I_{mfc} and I_{nom} plotted as straight line. Figure 3.2 is a family of curves for one product family of PPTC's.

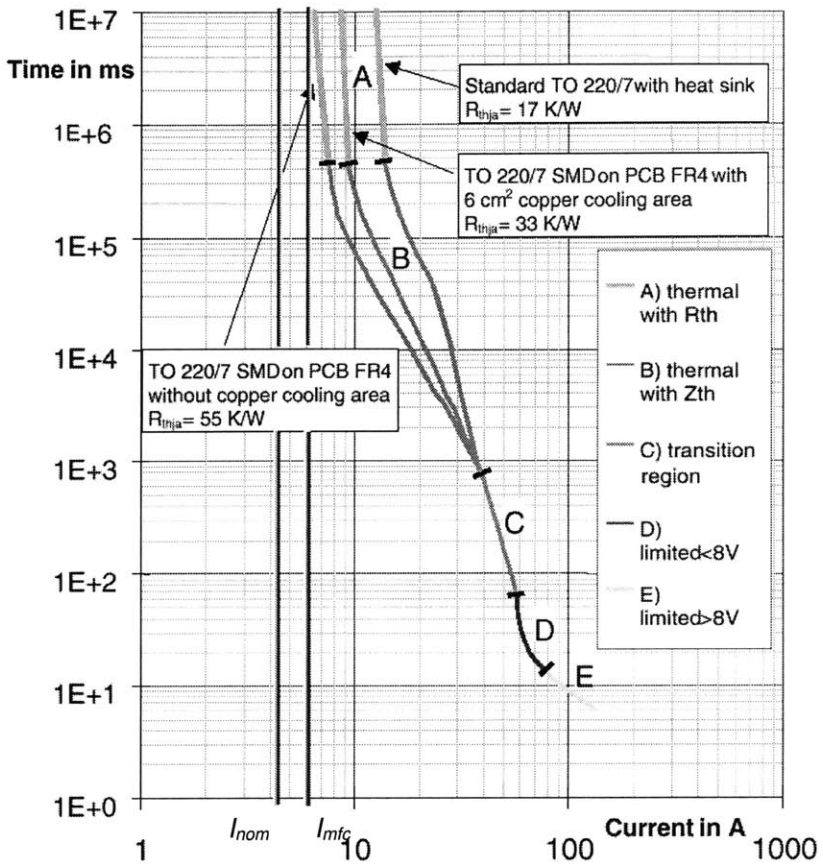

Figure 3.1 I-t plot for a BTS 640 S2 showing I_{mfc} and I_{nom} for a leftmost curve. Variations due to different heat sinking strategy (11). Reprinted with permission.

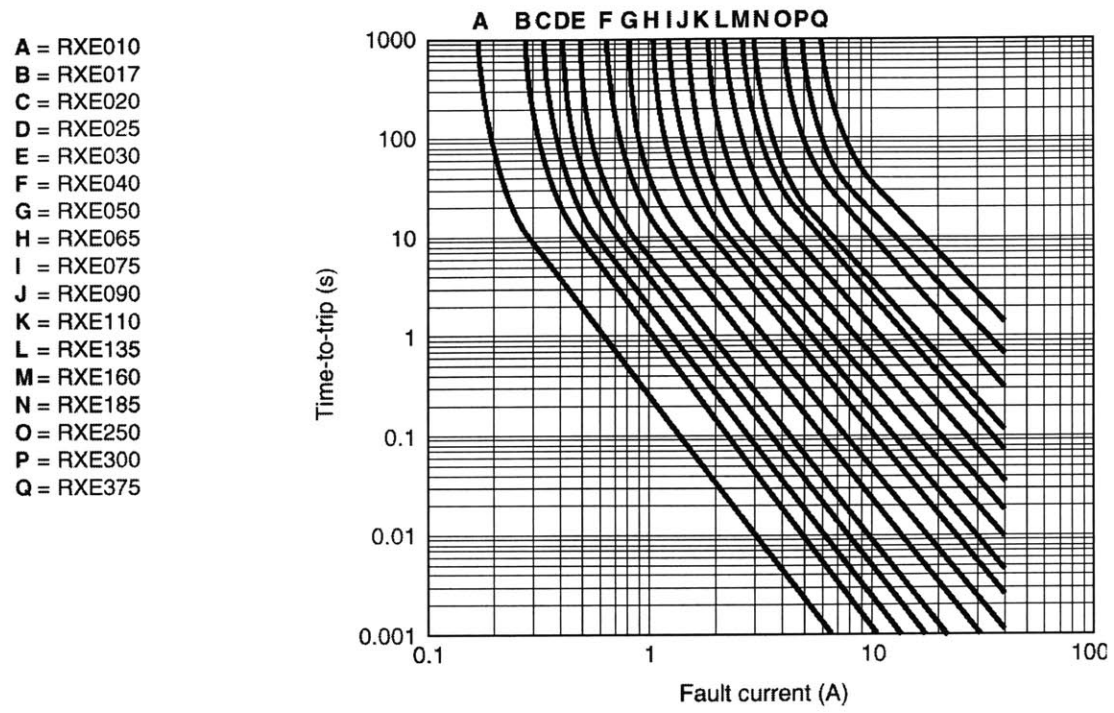

Figure 3.2I-t plots of Raychem's RXE product family of PPTC's (19). Reprinted with permission

3.2.4. Thermal derating coefficient and curves

The rate of heat transfer between a device and the environment is dependent on the temperature difference between the device and the environment. The temperature at which CF's melt, SPS's turn off and PPTC's trip is in each case an absolute temperature of the device. Because their behavior is dependent on both absolute and relative temperatures all these devices exhibit some static thermal derating. Thermal derating causes the minimum fusing current I_{mfc} to be temperature dependent and this temperature dependence is reflected in thermal derating curves.

The resistance of the device R_0 when its temperature T_{dev} is T_{amb} has a certain dependence on T_{amb}. These dependencies are given in the data sheets. As a result of this temperature variation in R_0 and the difference in the heat exchange rate with the environment, the behavior of devices is different at various T_{amb} and can be reflected as a shift in I_{mfc} value. Thermal derating curves are shown in Figure 3.3. These thermal derating curves cause the shift in I_{mfc} and

thus the total shift in the *I-t* characteristic where the interaction with the environment is high.

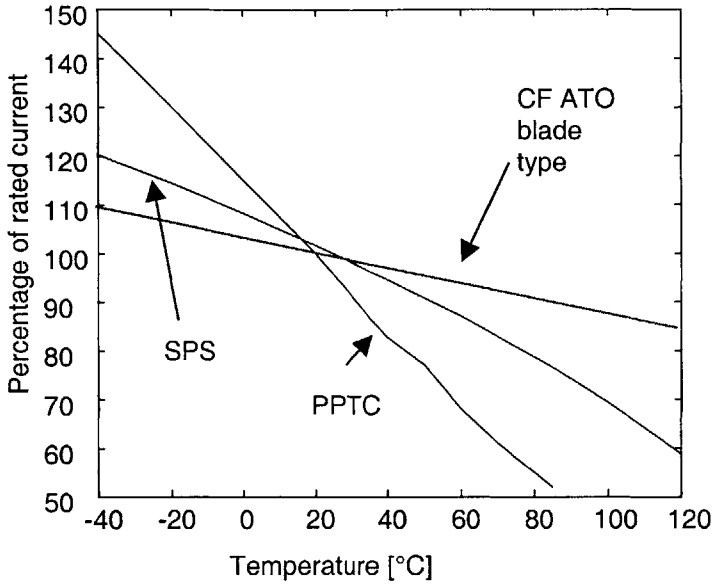

Figure 3.3 Temperature derating factors for three device types

3.2.5. Safe operating voltage (Voltage rating)

The devices are rated to safely operate up to some voltage V_{max}. This is the voltage across the device. After the turnoff of current (end of arcing for CF) and following a fault the voltage across the device is of the order of the source voltage V_s and therefore V_s should not exceed V_{max}. During the transient behavior this voltage can be exceeded by some specified amount.

SPS's have a fixed voltage V_{cl} across them during the turnoff of inductive load and this voltage V_{cl} is the maximum voltage to which the SPS should be subjected. SPS can take transient overvoltages higher than V_{cl} as described in the data sheets. However, safe interruption of faults is not guaranteed under these conditions. Furthermore, Infineon Technologies guarantees the safe interruption of voltages only to some specified voltage V_{max}.

PPTC's also have a maximum voltage rating at which they will safely operate. However, during a fault this voltage can increase to a much higher value as a result of PPTC current being unable to decrease due to presence of

inductance. If there is too much inductance in the circuit the PPTC will not operate safely and might fail to interrupt a current and can potentially damage itself.

3.2.6. Maximum fusing current (Breaking capacity test)

Maximum fusing current is the maximum prospective current that the device can safely interrupt at some specified voltage (usually V_{max}). Any prospective current larger than maximum fusing current cannot be safely interrupted. To an extent this puts a lower limit on the equivalent series resistance of the source and the resistance of the cable.

SPS's have a maximum fusing current defined as the maximum prospective current that can safely exist in an SPS when V_{max} is connected. This is not cited in the data sheets but is visible from their *I-t* graphs. The *I-t* graphs do not extend beyond this point.

3.2.7. Cut-off characteristic

The cut-off characteristic is measured at a given ambient temperature and plots the highest instantaneous current that a fuse will carry during interruption as a function the prospective current.

In circuits where the load is purely resistive the cut-off characteristic of PPTC's and CF's is a line with constant slope (slope is equal to 1). SPS's on the other hand have a rather interesting cut-off characteristic. Depending on how the fault was produced two different cut-off characteristic are produced. Both of them are constant above a certain value of prospective current. If the fault occurs while the device is conducting current, it takes a little bit of time for the internal circuitry to reduce the gate voltage as described in Chapter 2. However, if the device is turned on into a fault the operation begins with the gate voltage already lowered.

The cut-off characteristic is important because it shows the maximum instantaneous current that can be present in the circuit. This current should be used when calculating the mechanical stresses in the devices being protected (motors and wires). Furthermore the instantaneous value of any transient current peak can not exceed the value given in this graph. If such a transient current

peak existed without the protection device present in the circuit it would not be achievable with the protection device present in the circuit. An example of a cut-off characteristic is shown in Figure 3.4 for an SPS.

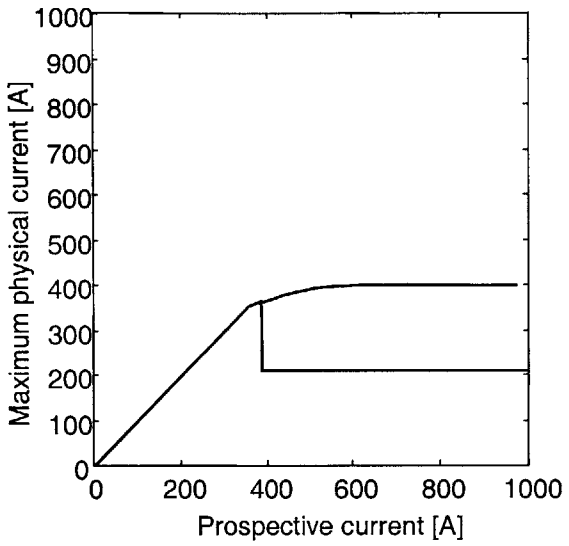

Figure 3.4 Cutoff characteristic of the BTS 650 P type SPS. The higher curve obtains for the device turned on at the moment the fault occurs

3.3. New means of characterization

In order to better characterize the new devices it might be suitable to create some new means of evaluating their performance in short circuits. Because the CF do not have all the characteristics of the new protective devices they do not exhibit some of the behavior that PPTC's and SPS's do. Thus, in order take opportunity of the new functionality we need to characterize the devices with respect to this new functionality.

3.3.1. Resetability

CF's are not resetable. Their design insures that after they have operated under fault conditions no current will flow in the circuit till the fuse is replaced. Thus a fuse that operated needs to be replaced. SPS and PPTC are resetable devices. The devices can be better than fuses since they do not have to be

physically replaced after they interrupt a fault. If an average of 10 faults can be expected during the life of the circuit than one would need 10 fuses for this circuit to operate throughout its lifetime. However we would only need one SPS or one PPTC.

The degree of resetability varies among the devices. SPS's come in two flavors. The first kind has an automatic reset built in. When a fault occurs the SPS will turn the circuit back on after the device temperature goes down by some specified amount (typically 10°C). The second kind has a latch function. The device will not reset until its control input has been cycled off (on->>off->>on). The SPS will then turn back on only if its temperature has gone down by the above mentioned specified amount.

Only cooling can reset PPTC's. If the circuit is returned to nominal conditions it will remain in the tripped state since the power dissipation in the normal conditions is enough to keep the device tripped. Thus a manual shut off of the current is needed. At this time the device cools and resets to its nominal resistance. If the fault is removed the PPTC will again operate normally. Thus a PPTC protected circuit must have a switch associated with it in order to utilize the resetability of these devices

3.3.2. Modes of Failure

Under certain conditions the device might stop to operate according to its specifications. This can occur either as a result of exceeding some specification (such as V_{max}) or because of the device reaching the end of its lifetime. At such a time several modes of failure exist. The device can fail as a short or as an open circuit.

A device that fails as an open circuit still protects the remaining circuit from any fault current but it needs to be replaced. Thus this mode of failure does not cause the destruction of the remaining elements in the circuit and resembles the operation of the fuse. In fact, for a fuse this is the mode of operation under fault conditions with the restriction that the fuse opens the circuit safely. Thus if

we exceed the voltage specified for a fuse it might fail to operate safely but will always fail as an open circuit.

On the other hand, SPS and PPTC can fail both as open and as short circuits staying permanently on or permanently off. This brings to question their applicability as protection devices. If there can be found a set of conditions within which an SPS and a PPTC will always fail as an open circuit, the boundaries of this set should not be exceeded.

If the voltage is increased substantially across the SPS it will not be capable of blocking the current for a long time. Once this time is exceeded it might fail as a short or it might eventually burn itself and become and remain an open circuit. If it remains a short this is unacceptable. Since these conditions exist for the operation beyond the specified range of operation the safety of current interruption is not guaranteed and can result in a fire. Thus the SPS should never be subjected to these conditions. Similarly a fuse will interrupt a current at V greater than V_{max} but it might do it with arcs coming out of it and setting its housing on fire or melting the contacts.

PPTC have rather strict current limitations and if this limitation is exceeded the PPTC might fail as a short.

3.3.3. Maximum load inductance during operation and fault conditions

While the maximum load inductance is not important for PPTC's and CF's during normal operation it is important for SPS because the SPS is the switch that turns off the nominal current. Thus for an SPS there is a maximum load inductance that can be present in the normal mode of operation, since the SPS must be capable of switching it off and not destroying itself. The maximum value of inductance for a inductance only circuit is given in the data sheets. This value causes the highest possible power dissipation allowed in the SPS. Furthermore the data sheets provide the value of maximum energy allowed to be imparted to the SPS during its turnoff. Since the Voltage across the SPS during inductive turnoff is known we can determine the turnoff I^2t as a function of load inductance.

The maximum arcing I^2t allowed for conventional fuses is measured at a maximum value of the time constant (L/R). The maximum time constant allowed in the circuit during a fault is given in the data sheet. If this value of time constant is exceeded the safe interruption of faults is not guaranteed (i.e. the result might be a fire). The reason for this limitation is explained in later chapters but the failure mechanism is excess power dissipation in the fuse during interruption of faults with large values of circuit time constant and consequently large inductances.

Limitations of inductance for PPTC's are not established yet.

3.3.4. Post-trip current

SPS's with automatic reset (thermal reset) and PPTC's have some current going through them after they interrupt a fault. The RMS value of this current is important since it can be used to calculate the energy delivered into a faulty circuit. The actual current for the PPTC and its RMS value are the same. For the SPS there is a shut off followed by turn on into the fault. This can result in quite a substantial current going into the fault. The steady state post-trip RMS current magnitude is explored and determined in the later chapters.

It is interesting to note that even fuses often pass some current after they have blown (although the magnitude of this current proves to be insignificant). This is a result of the vapor deposits on the fuse housing that extend between two electrodes after the arc is extinguished. The resistance of these paths is rather high and is therefore almost always neglected. But Littelfuse mentions that these currents can be in excess of several mA.

Chapter 4.

Theoretical and experimental comparison of protection devices

4.1. Introduction

Using the theory developed in Chapter 2 and the characterizations developed in Chapter 3 the performance of previously mentioned protection devices under various changing parameters can be investigated. The changes in the *I-t* characteristic due to T_{amb}, V_s, L_c and the production process itself can be determined. This analysis gives one the power to establish the limits of use by plotting the worst case *I-t* curves. For example, the earliest time to melt t_{melt} of the given fuse as a function of prospective current I_p and influenced by T_{amb} can be plotted.

Before doing this it is worthwhile to investigate what happens with several parameters in the automotive electrical distribution system as the system voltage is increased from 14 V to 42 V.

4.2. 42 V faults compared to 14 V faults

Changes in the system as the voltage is increased from 14 V to 42 V can be investigated theoretically. By considering the power of the load as a constant and the energy stored in the load as a constant certain predictions can be made. Nominal steady state current reduces by a factor of 3. This allows the system engineer to use a protective device with a 1/3 rating of the protection device used in 14 V system. If the wiring is reduced so that it has the same end to end voltage drop its resistance would increase by a factor of 3. Furthermore, one can assume that the equivalent series resistance R_{ESR} of the 42 V source is 3 times the R_{ESR} of the 14 V source (if the 42 V source was obtained by connecting three 14 V sources in series). If on the other hand one assumes that the 42 V source has the same internal power loss as a 14 V source, at a given power delivered to the load, then the R_{ESR} and the wiring resistance both increase by a factor of 9.

Under these assumptions short circuit current on the average remains the same (for R_{ESR} increase by a factor of 3) or is reduced by a factor of 3 (for R_{ESR} increase by a factor of 9). Constant energy storage assumption causes the inductance in the circuit to increase by a factor of 9. However, it is important to note that during short circuits the load inductance is often not the important inductance since it is shorted. Thus the inductance present in a circuit during a short circuit is primarily due to the stray inductance of the connecting cables and to first order this remains the same as source voltage changes (detailed analysis of cable self inductance is presented in Chapter 5).

4.3. Variations in I-t plots of protection devices due to various effects at constant ambient temperature

The purpose of this section is to investigate the variability of melting and initial turnoff *I-t* plots for CF's, SPS's and PPTC's at constant ambient temperature. These *I-t* plots do not include the turnoff of inductive faults. Since the governing factor for this part of the operation is current and its magnitude, the introduction of a higher source voltage causes no changes in operation of

protection devices. Therefore, the analysis is done at 12 V and any change in source voltage to 42 V will not cause a change in the results here obtained if the prospective currents under consideration are the same.

Since it would be impossible to investigate each fuse separately one fuse type and rating is considered. Generalizing the obtained results is trivial. The fuse chosen as a test case is the ATO type automotive blade fuse with I_{nom}=10A. The particular fuse under considerations is manufactured by Littelfuse (6). The

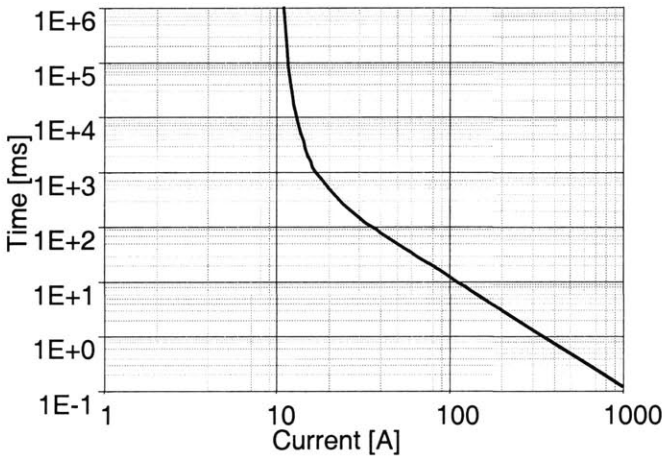

Figure 4.1 *I-t* plot for a ATO blade fuse with I_{nom}=10A

published average melting *I-t* graph of this fuse is shown in Figure 4.1 Data for the Figure 4.1 comes from Reference (6). Using the data sheet one also finds that minimum value of I_{mfc} is 11 A (6). Thus, the hold current I_{hold} is 11 A and this corresponds to a minimum fusing factor of 1.1.

The purpose of this investigation is to determine the fuse performance variations due to production process but at constant ambient temperature T_{amb}=25°C. The minimal melting I^2t for this fuse is 115 A^2s (6). However the published average melting *I-t* curve reveals an average melting I^2t (in high current region of operation) to be 122 A^2s. In order to obtain a minimum melting *I-t* graph (hold characteristics) at T_{amb}=25°C the values of current for any given time should be multiplied by the square root of the ratio of melting I^2t's. Thus a following relationship obtains for shifting any given point (I_p, t_v) from the average melting *I-t* curve to a minimum melting *I-t* curve:

$(I_p, t_v)@(T_{amb}=25°C$, average melting $I^2t) \rightarrow$

$\rightarrow (I_p*[(\text{minimum melting } I^2t)/(\text{average melting } I^2t)]^{0.5}, t_v)@$

$@(T_{amb}=25°C, \text{minimum melting } I^2t)$ (4.1)

This shifting procedure works in the high current regime of operation because the melting I^2t value for a given fuse is constant at high currents. The I^2t in this regime of operation is proportional to the energy necessary to melt the fuse. Therefore, a fuse with lower melting I^2t needs less energy to melt in a given constant amount of time. Since energy delivery is proportional to current, a fuse with lower melting I^2t needs less current to melt in a given constant amount of time.

While it is inherently obvious why the above-explained shifting procedure works in the region where I^2t is constant (high current faults), further explanation is necessary for the region where the interaction with the environment takes place. When the heat loss to the environment is present, the values of I^2t associated with any given I_p represent both the energy required to melt the fusible link and the energy exchanged with the environment. Examnination of Equation 2.1 shows that production variations cause a change in the energy necessary to melt the fuse and energy exchanged with the environment by the same relative amount (for detailed analysis refer to Appendix A). For example, let's investigate the case where (melting I^2t)=10*(average melting I^2t). The energy exchanged with the environment is proportional to 9 times the average melting I^2t. For a given time t_v and temperature T_{amb} the 9:1 ratio between the energy exchanged with the environment and energy used to melt the fuse remains constant under the theory explained in Appendix A. Manufacturing variations change the amount of power dissipated in the fuse for a given amount of current. Energy is proportional to I^2t values. Thus, the current necessary to melt the fuse in a given constant amount of time changes. I^2t values differ both for the melting energy and the energy exchanged to the environment. However, The ratio is the same if constant time is assumed.

Furthermore, the distribution in melting I^2t values $\Delta(I^2t)$ can be determined by subtracting the minimum melting I^2t from the average melting I^2t. Now if we assume that the distribution of melting I^2t is symetric and finitely bounded by the production process we can determine the maximum melting I^2t by adding the $\Delta(I^2t)$ to average melting I^2t. Now we repeat the shifting process of Equation 4.1 with obvious changes to the I^2t values to obtain the upper limit for the fuse *I-t* plot at T_{amb}=25°C. This gives us the trip characteristic. The trip characteristic depicts the minimum *I-t* plot for which all the devices with the same part number will trip. The variations are due to production process variation. The average melting *I-t* plot together with trip and hold *I-t* plots is shown in Figure 4.2. Figure 4.2 shows that it is it is almost impossible to distingush between the trip and hold characteristics of a fuse. This is a result of extremely tight tolerances in the fuse production process.

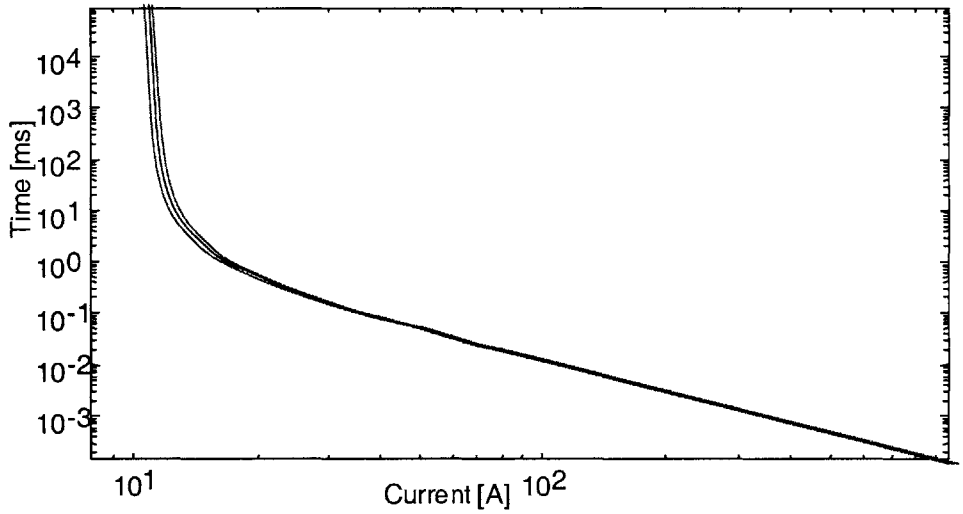

Figure 4.2 Variations in *I-t* plots as a result of variations in fuse production process for an ATO 10A fuse

The production process of an SPS causes a variation in several different parameters affecting the performance of an SPS. The manufacturing process creates a range of different cold resistances R_{cold} and current limits I_{scp} at a given ambient temperature. After these variations are all accounted for a hold and a trip *I-t* curves can be created for a given T_{amb}. A hold characteristics insures that any device with a given part number will not trip before reaching this current. The trip characteristic ensures that all given devices will trip at least according to this

curve or before. Alfons Graf examined these variations and their influence on the *I-t* curves (11). It would be pointless to repeat the procedure and replicate the results. However, for the reasons of comparison some examples of the results are replicated here.

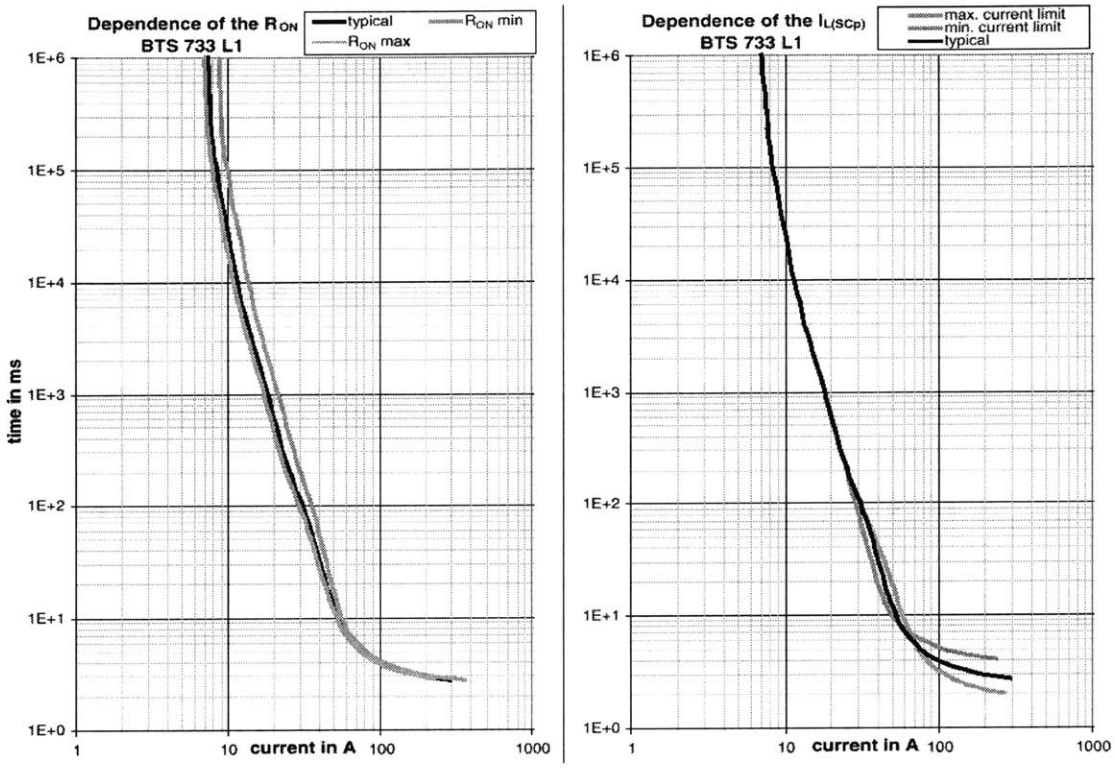

Figure 4.3 Dependence of production parameters such as R_{on} and I_{scp} on SPS *I-t* curve (11). Reprinted with permission

Figure 4.3 shows the variations due to the differences among devices of the same type caused by the production process parameters such as I_{scp} and R_{cold} for all devices at the same ambient temperature. R_{cold} has the strongest influence in the regimes of operation where the SPS is operating in the linear region of its mosfet characteristics. The I_{scp} has the strongest influence on the regimes of operation where the SPS is operating in saturation region of its mosfet characteristics. These two plots combined give the hold and trip characteristic of the SPS as a result of production process variations.

In comparison to the conventional fuse of similar current rating the performance variations due to production process in the high current region of operation are much more substantial for the SPS. The variations in the region

where the exchange of energy with the environment is substantial are comparable to the conventional fuse but slightly larger in magnitude.

The production process also affects the performance of PPTC's. Many things can vary in the production process of a PPTC. For example, the amount of conductive particles relative to the amount of the polymer and the dimensions of the PPTC can be altered during the production process.

Furthermore, increased post trip resistance of the PPTC as compared to the resistance prior to tripping will also influence the performance of any given PPTC. After the PPTC trips it has higher resistance that the PPTC that never tripped. Higher resistance causes higher power dissipation for the same amount of current and results in faster tripping times. While this is not an effect caused by variations in the production process, it is an effect that affects performance at constant temperature and causes the performance variation between a group of PPTC's of the same part number.

A hold and a trip characteristics that account for all possible variations in performance at T_{amb}=20°C for devices with the same part number can be determined. These two characteristics are a result of both the variability of the production process and the difference in post trip resistance compared to minimum resistance. To obtain the hold and trip characteristics a shifting procedure similar to the shifting in the fuse case needs to be performed. The data sheets give an average *I-t* characteristic. By shifting the average *I-t* characteristic to the location of the hold current I_{hold}, the hold characteristic obtains. Similarly, the trip characteristic is obtained by shifting the average *I-t* characteristic to the location of the trip current I_{trip}. Again, as in the SPS and CF case, any given device is guaranteed to trip above I_{trip} and no device will trip below I_{hold}. Data sheets for PPTC's contain the values of average turnoff *I-t* plots as well as the I_{trip} and I_{hold} (19)

Thus at T_{amb}=20°C we can right away notice from the data sheets that the fusing factor for a PPTC from a group of PPTC's with the same part number can vary from 1 to as high as 2. This follows from the fact that a device could be used with nominal current I_{nom} as high as the hold current I_{hold} and still in the worst

case the resulting fusing factor would be the ratio between I_{trip} and I_{hold}. Thus, the performance variations produced due to the post trip resistance behavior of PPTC's and the production process variations, show that the PPTC's have the biggest gap between the hold and trip characteristic of all three protection device types. All the performance variations examined in this section were performed at constant temperature. An example of PPTC's trip, hold and average *I-t* characteristics is shown in Figure 4.4.

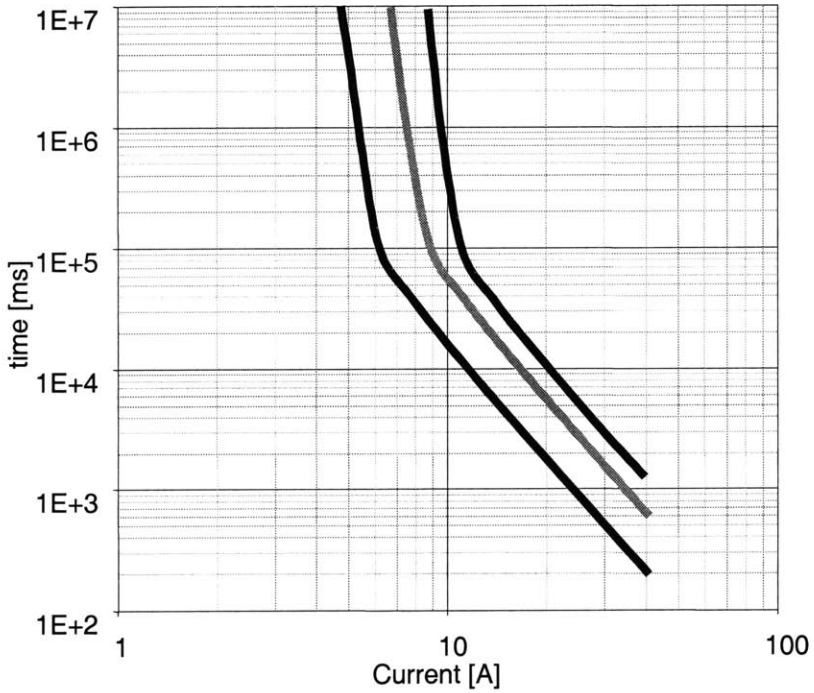

Figure 4.4 Hold and Trip characteristic for the RUE 400 PPTC device at T_{amb}=25°C.

In conclusion, the CF exhibits the smallest performance variation at a given constant ambient temperature. Due to the simplicity of CF construction many of the parameters influencing the pre-arcing performance of conventional fuses can be tightly controlled.

4.4. Variations in I-t plots due to changes in ambient temperature

Up to now, the variations in protection device performance due to various effects were calculated and compared at constant ambient temperature. In the

automotive electrical environment the protection devices are required to operate over a wide range of ambient temperatures. In the passenger compartment the ambient temperatures vary from –40°C to 85°C. In the engine compartment the ambient temperature can vary from –40°C to 125°C. In order to use the devices in such extreme temperature ranges melting *I-t* plots for CF's and initial turnoff *I-t* plots for SPS's and PPTC's at various temperatures need to be determined. Furthermore, hold and trip characteristics at the extremes of these temperature ranges also need to be established.

In order to calculate the *I-t* plot for a fuse at any ambient temperature the shiffting procedure of Section 2.3 must be done. To use the shifting procedure the ratio of I^2t's at different temperatures has to be determined. The I^2t at T_{amb}=25°C is given in the data sheets. To obtain the I^2t value at any other temperature Equation 2.4 has to be solved. This can be done through the use of numerical methods and various computer programs. In this research Matlab was used to solve the Equation 2.4. The assumption of constant temperature distribution across the fusible link is justified by the fact that pre-arcing times are short in the high current regime of operation (4).

Performance variations described in Section 4.3 are again present at any

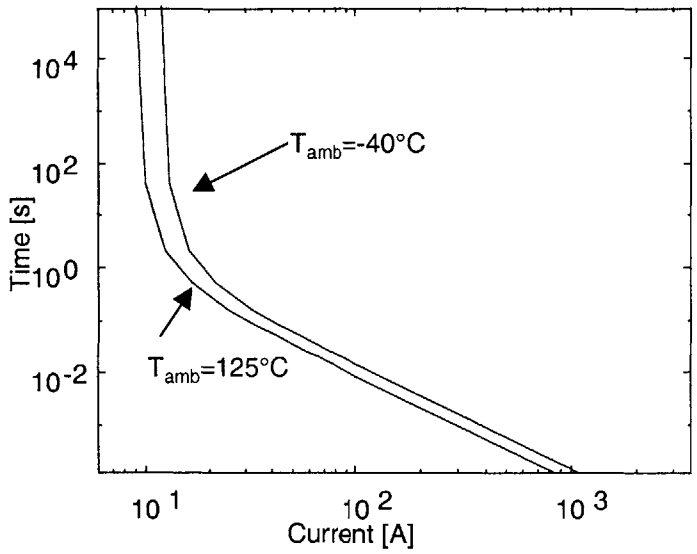

Figure 4.5 Temperature variations in the *I-t* characteristics for an ATO 10A fuse

given ambient temperature. This results in separate average, hold and trip *I-t* plots for any given temperature.

Thus by using this method the *I-t* plot variations across any temperature range can be determined. The 'fastest' curve is the hold characteristic at highest ambient temperature. On the other hand, the slowest curve is the trip characteristic at lowest ambient temperatures. The results of applying this analysis method is shown in Figure 4.5 for the temperature range applicable to the automotive engine compartment ambient temperature range specifications.

However, if a fuse utilizes diffusion pill technology then it needs to be examined differently. In the region of operation where I^2t is constant, the critical temperature is the melting temperature of the fusible link material (typically Zn or Cu). As fault currents approach the minimum fusing current I_{mfc}, the critical temperature to be used for calculations is the melting temperature of the diffusion pill material (typically solder). Thus when determining the shifts in *I-t* plots caused by the change in T_{amb} two critical melting temperatures must be utilised, melting temperature of the fusible link material and melting temperature of the diffusion pill material. This produces two new values of I^2t and two ratios with the unshifted I^2t. The ratio produced with the melting temperature of fusible link is

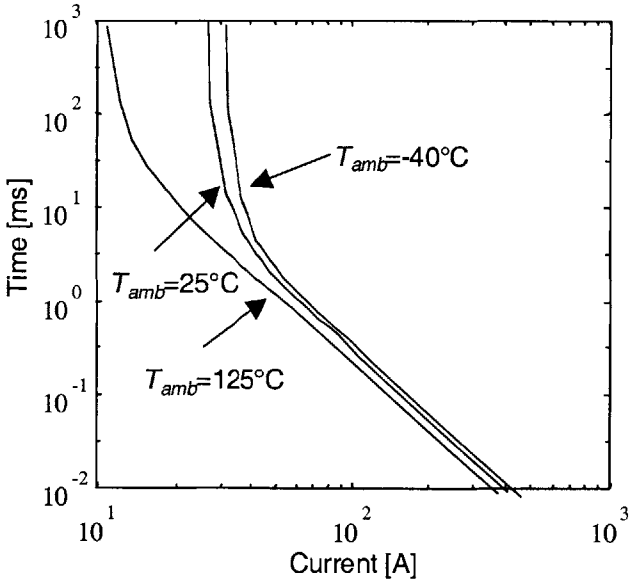

Figure 4.6 Effect of the ambient temperature change on the I-t characteristic of a 20A MAXI fuse

used in regime where I^2t is constant. The other ratio is used in regime where the interaction with the environment is high (for fault currents just above I_{mfc}). This procedure applies for the slow blow fuses such as the MAXI fuses. The results for a 20 A MAXI fuse are shown in Figure 4.6.

The performance of SPS's is also influenced by changes in ambient temperature. These changes are a result of the thermal properties of silicon. This was shown in Chapter 2 where the effect of temperature on the SPS I-V characteristics was presented. Alfons Graf from Infineon Technologies investigated the effect of ambient temperature influence on the performance of SPS's. His results are in the form of *I-t* plots with hold and trip characteristics at two extreme temperatures in the passenger compartment automotive electrical environment. The procedure for generating ambient temperature performance variation data will not be repeated since it can be found in References (11,14). An example will be presented for the sake of completeness of this section.

Figure 4.7 shows the temperature dependence of *I-t* plots as a function of

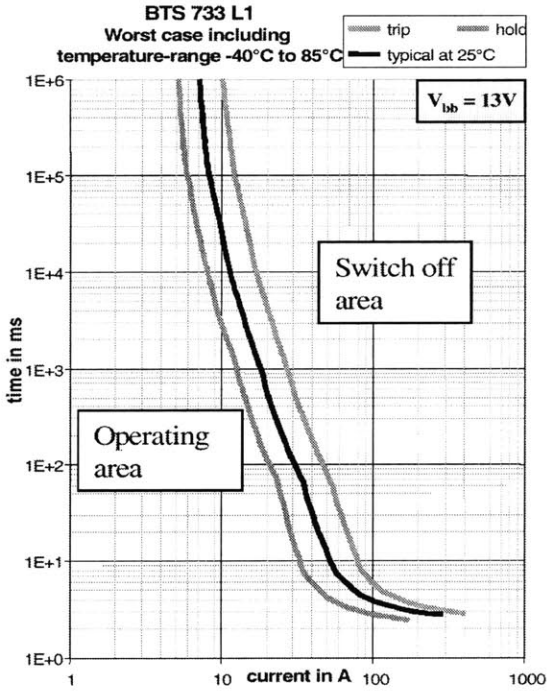

Figure 4.7 Worst case dependence of *I-t* plot for the SPS accounting for all parameter variations and temperature operating range (11). Reprinted with permission

temperature. Again, as in the CF case the fastest acting curve is the hold characteristic at highest ambient temperature. The slowest acting curve is the trip characteristic at lowest ambient temperature.

It is interesting to note that the operating ambient temperature range in this plot is the operating ambient temperature range of the passenger compartment. Thus by comparing Figure 4.7 with Figure 4.5 it is obvious that the performance variation for a CF is much smaller than for the SPS as a function of ambient temperature. This is a result of much smaller critical temperature for the device operation. The critical temperature for conventional fuses is the melting temperature of the fusible link (greater that 400°C for Zn). On the other hand the critical temperature of the SPS is the junction temperature T_{jmax} at which turnoff begins (T_{jmax}~150°C). Consequently, the CF's have less performance variation due to changes in operating ambient temperature. If the conventional fuse utilizes the diffusion pill technology, then the critical temperature for fault currents close to I_{mfc} is comparable to the critical temperature of the SPS. The performance variations in this regime of operation of the two devices are in that case comparable.

Because PPTC's have nonlinear temperature dependence they do not thermally derate in the same manner as CF's do. Their static thermal derating curve tends to be constant but having a much higher slope (Figure 3.3). This thermal derating can be directly applied to the regime in which there is a lot of interaction with the environment. In this regime we know that for a given current I_p it takes time t_{trip} for the device to trip at a given ambient temperature T_{amb}=25°C. If the temperature changes the current also changes by the thermal derating factor while the time remains the same.

However, for high current faults PPTC do not have a constant I^2t and calculating the appropriate I^2t for the device at a different temperature and current becomes hard due to nonexistence of a simple theoretical model for the behavior of PPTC's. Experimental results exist for typical devices and they can be used to guide us in determining the worst case I-t plots for a PPTC in some operating temperature range. The experimental results exist showing best and

worst performance for three different temperatures, 85°C, -40°C and 20°C. These experimental results are depicted in Figure 4.8.

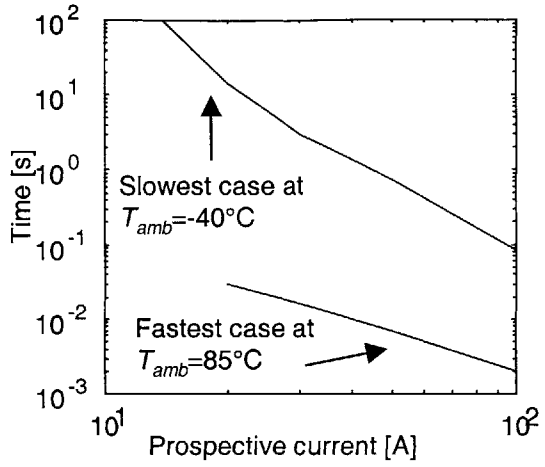

Figure 4.8 *I-t* characteristic of a RGE500 type PPTC for high currents, obtained by experiment at Raychem

To obtain the *I-t* plot at any other temperature the existing ambient temperature performance variation data can be interpolated. The interpolation procedure does create certain errors but they stay within bounds. When virtual time is plotted as a function of temperature for some given prospective current, a monotonically decreasing curve results. This is always the case since higher

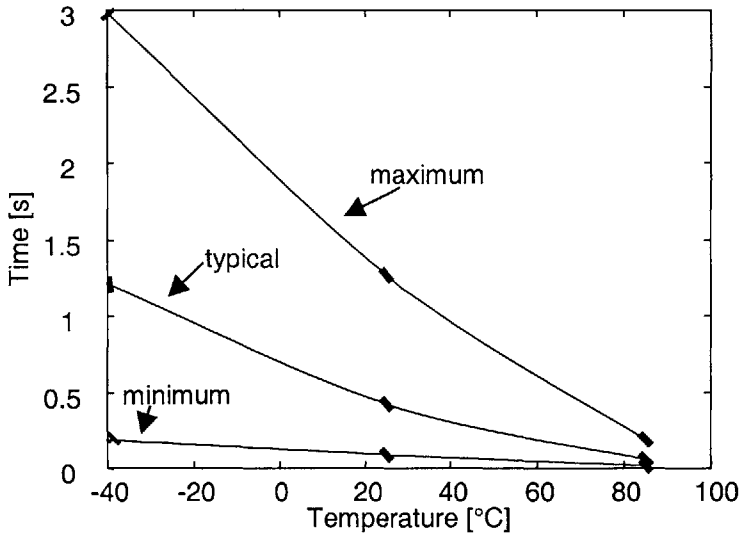

Figure 4.9 Interpolated time to trip as a function of ambient temperature at I_p=30A for a RGE500 type PPTC. Shown are the maximum minimum and typical times

temperature always results in shorter tripping time for a given device and prospective current. Thus our interpolation procedure creates minimal error as long as the resulting time versus temperature plot is monotonically decreasing. Figure 4.9 shows interpolated times as a function of T_{amb} for a given prospective current. The curve labeled as maximum time curve, represents a data point of the trip *I-t* characteristics as a function of temperature. Correspondingly, the minimum curve represents the data point of the hold *I-t* characteristic as a function of temperature.

Performance variations caused by the changes in operating ambient temperature of the PPTC are the largest of all three protection device types. This is a result of the PPTC having the lowest critical temperature (T_{trip} ~125°C). As a result of this low critical temperature the PPTC may not even be capable of working in the automotive engine compartment. By some automotive standards the highest operating ambient temperature in the engine compartment is 125°C. If we placed the PPTC in this environment at this highest temperature it would trip without having any current present in it.

Considering both the impact of ambient temperature changes and other effects (which are present from sample to sample at any given temperature), the conventional fuse has the smallest performance variation. SPS's have comparable performance to slow blow fuses utilizing diffusion pill technology. PPTC's have the largest performance variations of all three protection device types and the largest gap between the hold and trip *I-t* characteristics.

4.5. Comparison of performance during turnoff of fault currents in circuits with inductive loads

If there is inductance present during fault conditions, the current cannot be turned off until the energy stored in the inductance has been dissipated. The rate at which the current is turned off is a function of the voltage across the inductor. In a purely inductive fault the voltage across the inductor is the difference between the source voltage and the voltage across the protection device. Thus

the performance in inductive circuits will change when the system voltage goes from 14 V to 42 V.

For conventional fuses the introduction of inductance changes both the pre-arcing and the arcing behavior. Due to the fact that *I-t* plots show virtual time, the pre-arcing period remains the same for a given ambient temperature. The arcing time is determined from the maximum allowable arcing I^2t measured at maximum allowable circuit time constant L_C/R_C. This limit is specified by the manufacturer (6). Arcing I^2t only adds to the characteristic by adding time at a given I_p. It is

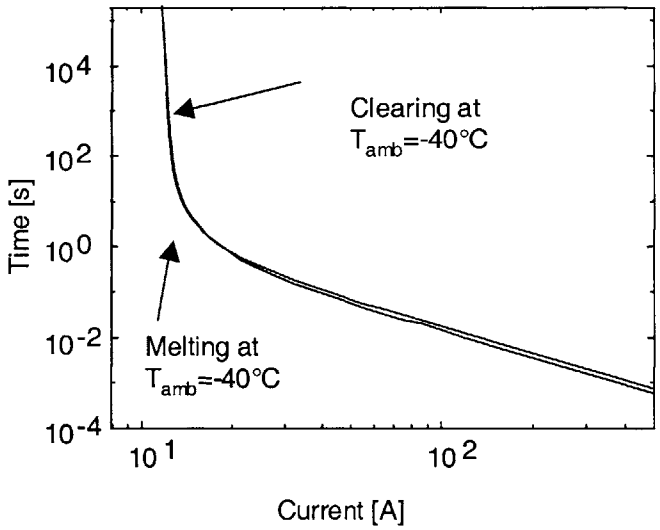

Figure 4.10 Effect of Arcing I^2t on the ATO 10A fuse performance

important to realise that the *I-t* plot is shifted vertically for adding the arcing I^2t. The reasoning for this comes as a result of the realization that I_{mfc} remains the same since arcing never comences if the current in the fuse is exactly the minimum fusing current. The time added is thus virtual time obtained by dividing the maximum arcing I^2t by the square of I_p. Difference between clearing (melting+ arcing) and melting *I-t* plots is shown in Figure 4.10. Since arcing times are extremely short for the fuse under consideration, it seems that arcing time is insignificant and can be neglected. However, other automotive fuse types, such as the MAXI and MEGA fuses by Littelfuse, have longer arcing times that should not be neglected when the performance is evaluated.

However, arcing I^2t is also a measure of energy imparted on the fuse and thus the maximum arcing I^2t should not be exceeded. We can calculate the I^2t_{arcing} by making certain assumptions about the behavior of fuses during arcing previously described in Chapter 2. Then, the I^2t of an exponentially decaying current is equal to the initial current squared multiplied by the time constant of decay. Note that the time constant for decay of I^2 is ½ the time constant for decay of I . Under these assumptions and using the previously introduced terminology the following equation holds:

$$I^2 t_{arcing} = K I_0^2 \tau \left(\frac{V_S - \theta R_{cold} I_0}{V_0 - \theta R_{cold} I_0} \right) \tag{4.2}$$

where K and θ are constants used to achieve better fit with experimental data, I_0 is the current at the beginning of arcing, R_{cold} is the cold resistance of the fuse, V_S is the source voltage V_0 is the initial voltage across the fuse at onset of arcing and τ is the circuit time constant.

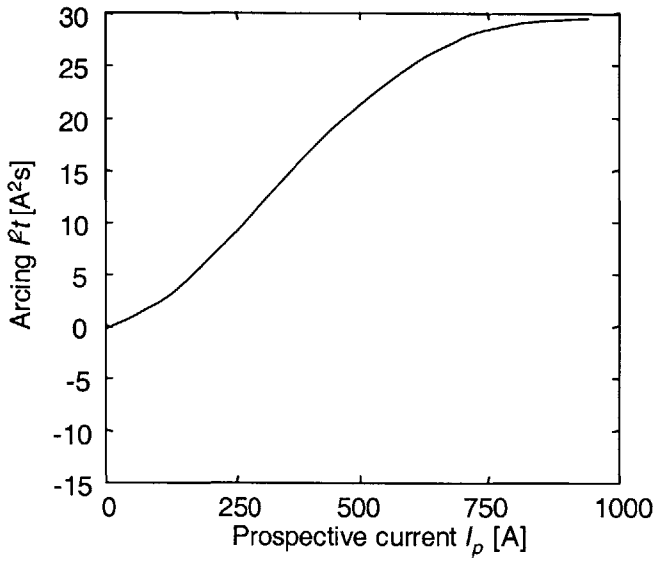

Figure 4.11 Arcing I^2t for an ATO 10A fuse when τ is kept constant

By solving Equation 4.2 for a maximum allowable τ given in data sheets (Figure 4.11) and V_S=13 V we notice that the maximum arcing I^2t occurs for only one value of I_p. Thus keeping the τ below this will insure that the maximum arcing I^2t is as specified in the datasheet. However, one can calculate the value of τ that

results in the maximum allowed arcing I^2t as a function of prospective current. The circuit designer needs to guarantee that any possible fault does not exceed the maximum value of τ allowed at that fault current. This insures that the power dissipation limit of this particular fuse design is not exceeded during arcing in any possible fault condition.

Figure 4.12 shows the relationship between τ and I_p calculated by solving Equation 4.2 for I^2t_{arcing} set to maximum allowed and kept constant.

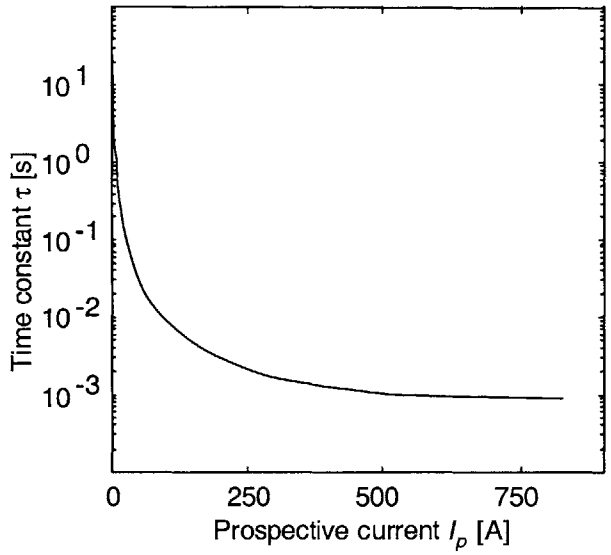

Figure 4.12 Maximum allowable time constant as a function of I_p for an ATO 10A fuse

Based on this theory, if it can be assumed that the prospective current will be limited to a range which does not include the minimum value of τ in Figure 4.12, it would be justified to use the fuse in a circuit with a larger value of τ. The larger value of τ would be the minimum value of τ in the range of prospective currents that can exist in the circuit and could be obtained through Equation 4.2 or from Figure 4.12.

Despite this possibility, suppliers of fuses specify in their application literature a maximum τ, independent of the range of prospective currents. The limitation of τ given by the manufacturer insures that maximum arcing I^2t is never exceeded. Figure 4.13 shows this limitation as the function of load resistance and load inductance during faults. Product design dictates adherence to this

guidance, unless robust empirical evidence, and not just this theory, demonstrates that another practice is safe.

The investigation of effects of higher source voltage have not been performed yet since the first automotive fuses rated to operate in 42 V environments are either in the prototyping phase or have just shown up on the market.

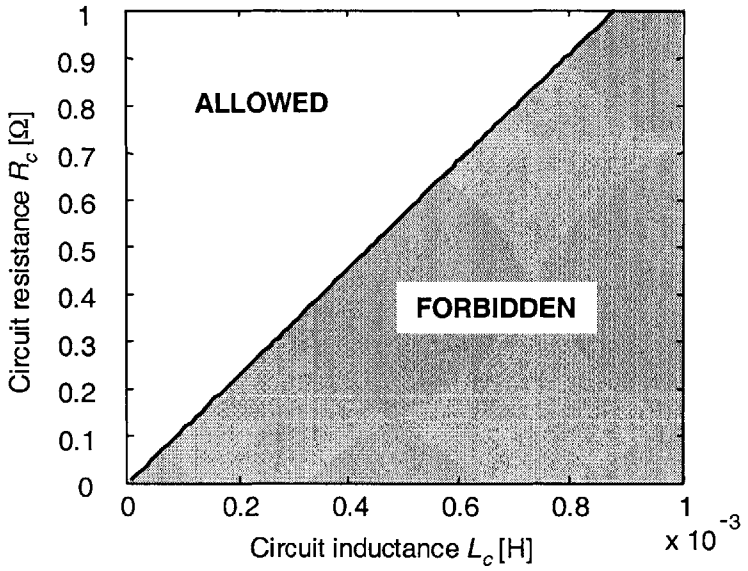

Figure 4.13 Inductance limitation for an ATO 10A fuse under the constant τ limitation given by the manufacturer.

The application notes published by Infineon Technologies do not cover the turnoff of current by the SPS for faults that contain inductance. Thus, it is interesting to investigate this effect further. The inductive turnoff for an SPS was completely described in Chapter 2 and it is therefore straightforward to calculate the I^2t associated with it. By integrating Equations 2.9a and 2.9b we obtain:

$$I^2t = \frac{L_C I_0^3}{V_C - V_S}\left[-\alpha^3 \ln\left(\frac{\alpha}{1+\alpha}\right) + \frac{\alpha}{2} - \alpha^2\right] \quad \text{in general} \tag{4.3a}$$

$$I^2t = \frac{1}{3}\cdot\frac{L_C I_0^3}{V_C - V_S} \quad \text{assuming a purely inductive load} \tag{4.3b}$$

where α is given by:

$$\alpha = \frac{V_C - V_S}{V_S - R_0 I_0} \qquad \alpha > 0 \text{ when operating within specified limits}$$

However, since Equation 4.3a always gives values smaller than Equation 4.3b the worst case is computed by using Equation 4.3b. Combining Equation 4.3b with the Equation for the energy 2.10b and solving by using a given maximum allowed energy we obtain the following simple equation for arcing I^2t:

$$I^2t = \frac{2}{3} \cdot \frac{E_{max} I_0}{V_L} \tag{4.4}$$

And again by the standard procedure we divide this "arcing" I^2t by the square of prospective current and add the resulting virtual time to our *I-t* plot. Figure 4.14 shows *I-t* plot of virtual time during turnoff of an inductive load as a function of prospective current for an SPS.

To put the necessary limits on the maximum value of inductance in any

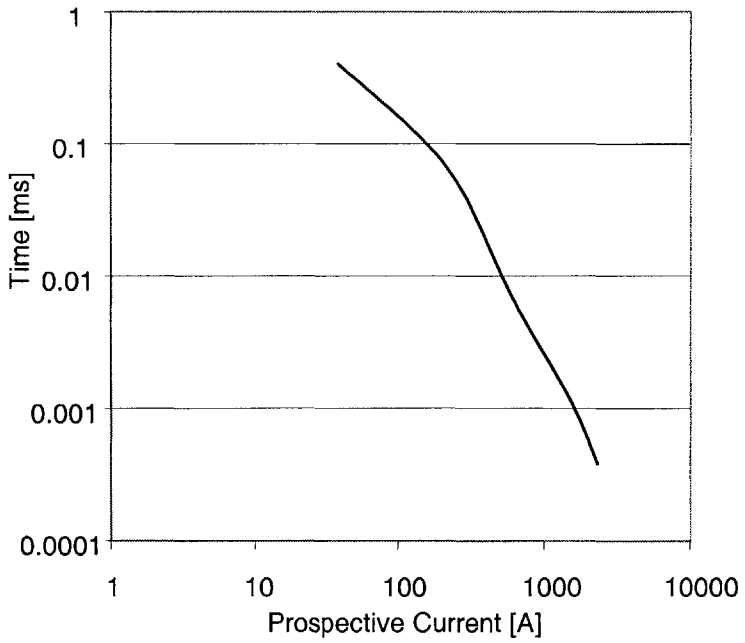

Figure 4.14 Virtual arcing time as a function of prospective current for a BTS 550 P assuming V_s=13V and E_{max}=1.2J

given situation we can plot R_c versus L_c graph (figure 4.15) that shows the energy boundary obtained from Equation 2.10a and tells us the allowed L_c at any given value of R_c. Thus, to use the devices properly it is important that any fault condition that can occur does not fall in the forbidden region since that would result in the destruction of the SPS. Furthermore, unlike a fuse, the SPS must be

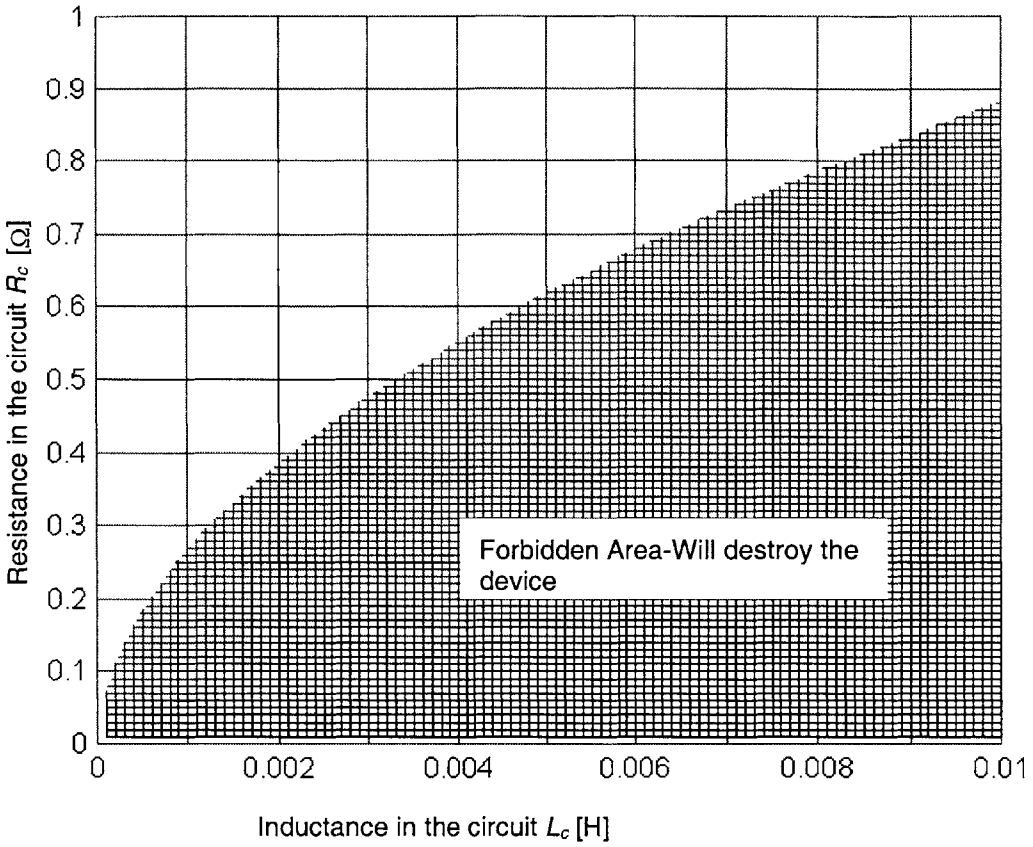

Figure 4.15 Allowed values of resistance R_c and inductance L_c in any mode of operation for a BTS 650P type SPS.

capable of switching off the nominal load R_n and nominal inductance L_n and thus they too should also fall in the allowed region of the plot in Figure 4.15.

In comparing the inductance limitations of the SPS to the inductance limitations of the CF we can compare Figure 4.15 with Figure 4.13 and notice that at source voltage of 14 V SPS can deal with a lot more inductance during fault interruption. As the source voltage is increased, the SPS will be less capable of dealing with fault and normal load inductances. This is a result of the fact that SPS's designed to operate in the new 42 V environment develop a 60V voltage drop across themselves during the turnoff of inductive currents.

In case of the 14 V system the negative voltage that appears across a purely inductive fault load is 46 V. In a 42 V system the negative voltage across the inductor would only be 18 V. Thus one can conclude that it will take longer to dissipate the energy stored in the inductance. However, at the same time the power dissipation in the SPS is proportional to the product of 60 V and the

current in the SPS. The exact equation that gives the limitation on load inductance L_C as a function of voltage across the SPS V_{cl}, the source voltage V_s, energy dissipation limit E and load resistance R_C is given by:

$$L_C = \frac{2 \cdot E \cdot R_C^2 \cdot (V_{CL} - V_S)}{V_{CL} \cdot V_S^2} \tag{4.5}$$

If the value of inductance given by the above equation is exceeded the energy dissipated in the SPS will exceed the safe value and the SPS will fail. Using the above equation a plot of maximum allowed inductance versus resistance in the circuit can be generated. An example of this plot was shown in Figure 4.15. Figure 4.16 shows the maximum inductance versus the load resistance as a function of two source voltages. As the source voltage is increased from 14 V to 42 V the allowed inductance present in the circuit is

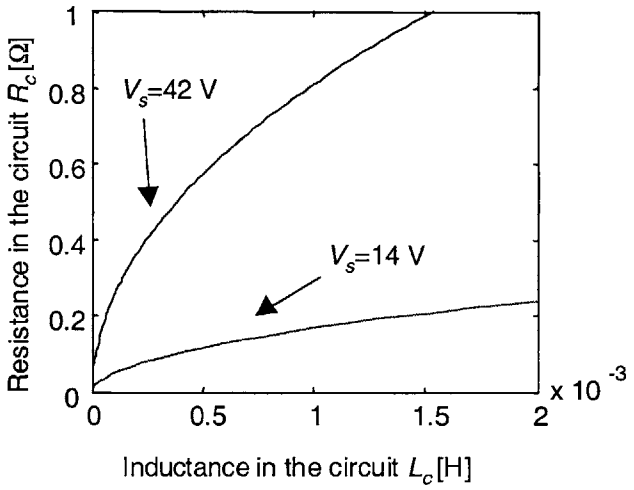

Figure 4.16 Inductance limitation as a function of circuit resistance for BTS 410 E2 type SPS. Results for two source voltages are shown.

reduced by the ratio of voltages appearing across the inductor in the two systems. For the SPS's rated to operate in 42 V EDS the maximum allowed inductance at any given load resistance is reduced by a factor of about 4 compared to operating the same switch in a 14 V EDS.

The limitations of inductance of the new 42 V fuses have not been established yet. Once they are established they will not prove to be better than

the limitations at 14 V case. In order to perform the comparison of performance between fuses and SPS's these limitations need to be established by the fuse manufacturers. Since each fuse manufacturer will have his own strategy for making automotive fuses rated to operate in 42 V systems, it is hard to predict the performance of future automotive fuses during turnoff of currents in circuits with inductance present. According to Section 4.2 the load inductance could increase by a factor of 9. In that case many of the inductive loads that did not create problems during fault conditions could start to pose problems for both conventional fuses and SPS's. Without a standard for performance in inductive faults, future automotive fuses might not be interchangeable among different manufacturers.

The limitations on load inductance during fault conditions have not been established for PPTC's. The complexity of the theory of their operation poses a problem for establishing this limitation. However, one can surely say that the limitations will be lower as the source voltage is increased to 42 V. Since the fault inductance already is a problem in certain 14 V circuits, it can be expected that the problem will be even more apparent in the future 42 V system.

4.6. Comparison of power dissipation of protection devices in normal mode of operation.

The space allocated for the protection devices in the automotive electrical junction boxes is getting smaller and smaller. On the other hand, the number of circuit to be protected is constantly getting bigger. As the result of these trends the protection devices are closely packed together next to each other. If the power dissipation of the protection device is too high the protection device will generate too much heat in its near vicinity. In order to compare the protection devices with respect to heat that they generate an investigation of power dissipation needs to be performed.

All protection devices behave as resistors during the normal mode of operation (no fault is present). Even in normal mode of operation the devices

heat up. Because the devices operate at some temperature higher than the ambient temperature, their resistance changes and affects the power dissipation.

Conventional fuse manufacturers publish typical voltage drop across the fuse when nominal current is present in the fuse. The product of this voltage drop and nominal current is the power dissipation in normal mode of operation. Using data published by Littelfuse a plot of power dissipation as a function of nominal current is generated in Figure 4.17 (16).

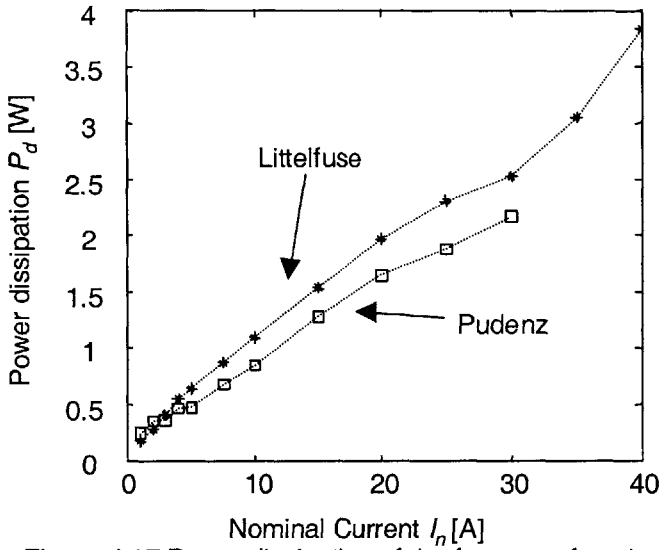

Figure 4.17 Power dissipation of the fuse as a function of nominal rated current. Results shown are for Littelfuse 32 V ATO type standard fuses and Pudenz 58 V FKS type fuses.

Furthermore, preliminary data for Pudenz's 42 V automotive fuses is plotted as well. The new 42 V fuses rated to operate at 58 V have the same power dissipation as the old 14 V fuses. Thus they do not present any new thermal problems that do not already exist in the fuse boxes today. These Pudenz 58 V automotive fuses are different from previously mentioned 80 V Wickmann's blade type fuses (Chapter 2). They have roughly the same cold resistance as Littelfuse's ATO type fuses for a given I_{mfc}.

In the 42 V system the fuse necessary to protect the load of the same power has one third of the rating of the 14 V fuse as discussed in Section 4.2. That implies that the power dissipated in the fuse for a load with given power goes down by a factor of 3 as the source voltage is increased from 14 V to 42 V .

However, one should keep in mind that 42 V automotive blade fuses are not standardized yet. It can be expected that a standard for a blade type fuse for the 42 V EDS will be established among the fuse manufacturers and auto makers. As such a standard is reached the above conclusions might become invalid. Future 42 V automotive fuses could have power dissipation higher or lower than the Pudenz's 58 V fuses presented here.

However, if the standardized 42 V fuses end up having power dissipation higher at 42 V, they will most probably be capable of dealing with higher load inductances. This conclusion is a result of the theory of fuse arcing presented in Chapter 2. If the fuse resistance is higher the constricted portion of the fusible link is longer. This longer constricted portion develops a longer arc. A longer arc implies higher voltage drop across the fuse and consequently faster interruption of current. If the current is interrupted faster, the source can deliver less energy into the fault. Consequently, the fuse is capable of discharging higher energies stored in circuit inductances without exceeding its own power dissipation limit for safe interruption.

There is no standard way to calculate power dissipation of SPS's at their nominal current. The addition of the heat sink to the SPS changes its thermal resistance, which changes both the nominal current and the power dissipation of the SPS.

In order to create some data to compare with conventional fuses device is assumed to be in T_{amb}=25°C. The junction of the device is presumed to be at T_{jmax}=150°C and power dissipation is plotted as a function of current. Because the temperature of the device is considered to be constant as power dissipation changes, different points on such a plot represent different values of thermal resistance R_{thja}. In order to change the thermal resistance of the device, a heat sink needs to be introduced to the casing of the device. Because the operating temperature chosen is the threshold between tripping and normal operation, power dissipation is plotted as a function of minimum fusing current I_{mfc}. Each value of minimum fusing current and power dissipation corresponds to a certain heat sink.

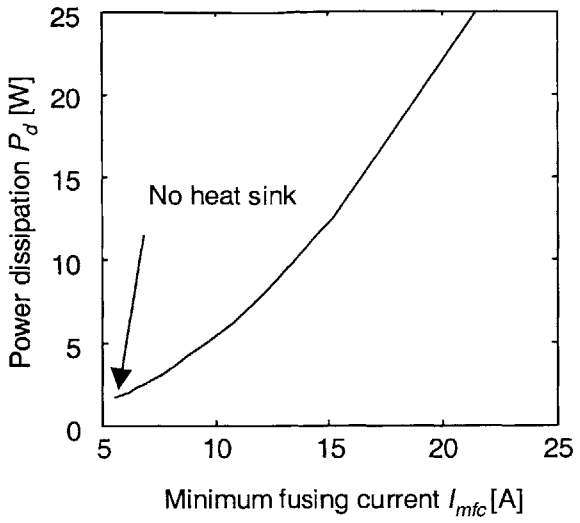

Figure 4.18. Power dissipation as a function of minimum fusing current for BTS 640 S2 type SPS. Minimum fusing current changed by addition of heat sink. Smallest value represents no heat sink.

Figure 4.18 depicts power dissipation of a given SPS as a function of I_{mfc}. Both the power dissipation and the I_{mfc} are altered by addition of a heat sink. As the Figure 4.18 shows, the power dissipation increases as I_{mfc} is increased by addition of the heat sink. As I_{mfc} is increased the thermal resistance is reduced. The minimum value of power dissipation is given at minimum value of I_{mfc}. The minimum value of I_{mfc} results from the device with no heat sink present and therefore highest value of thermal resistance.

However, in order to compare the power dissipation of SPS's with the power dissipation of CF's, power dissipation of each available SPS with no heat sink present can be plotted as a function of I_{mfc}. Figure 4.19 depicts both the power dissipation of SPS's (without heat sinks) and power dissipation of CF sorted out by type of device (SPS or CF) and the voltage rating (rated for 42 V EDS or for 14 V EDS).

Figure 4.19 shows that the power dissipation of currently available SPS's is larger than the power dissipation of CF's with similar I_{mfc}'s. Thus, the voltage drop across the SPS and consequently its resistance at given minimum fusing current is higher as well. If the voltage drop between the load and the source in the car becomes more restricted in the future dual voltage automotive environment the SPS will present more trouble in meeting these new specifications than the CF

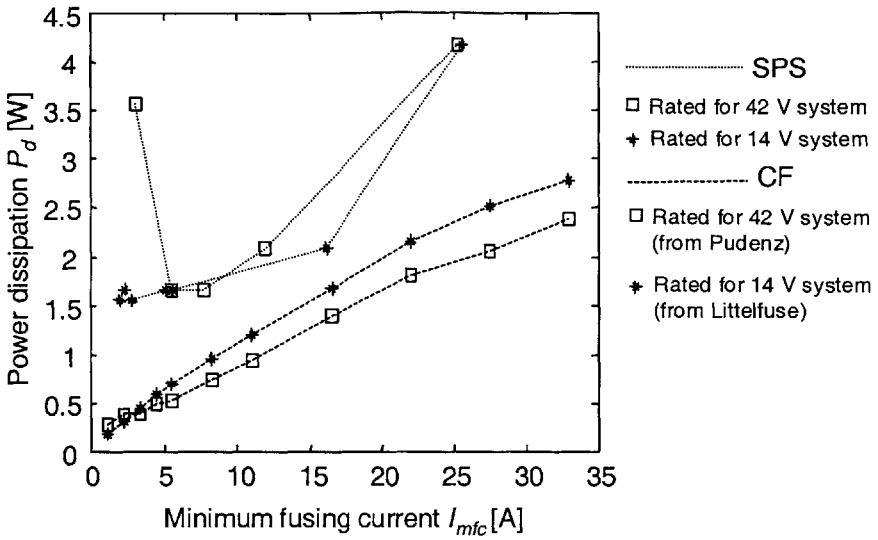

Figure 4.19 Comparison of minimum power dissipation as a function on I_{mfc} for SPS's produced by Infineon and conventional fuses. Parts rated to operate in both 42V and 14 V systems are shown

will. The on-state resistance of the SPS can be reduced by the use of the bigger MOSFET. Unfortunately, this even further increases already unfavorable cost of the SPS's.

As the system voltage is increased to 42 V, the power dissipation of a given SPS in normal mode of operation remains the same for the same I_{mfc}. Since a given SPS is capable of a given on-state resistance R_{DS}, the power dissipation will decrease if the same device is used for a 42 V load with the same power consumption as the 14 V load. Alternatively, a smaller MOSFET can be chosen for the 42 V loads. Thus, for a given power of the load the power dissipation of the protection SPS is reduced as the system voltage is increased from 14 V to 42 V as a result of reduced load current.

In order to theoretically predict the power dissipation of a PPTC, a good theoretical model is necessary. Due to nonexistence of this theoretical model and lack of comprehensive experimental data given by the manufacturer, simple experimental measurements were performed. The details of the experimental setup can be found in Appendix B . Since only a limited number of devices were tested the data represents power dissipation values for typical devices only and worst case and best case values cannot be extrapolated without more systematic testing that would cover the device performance variations due to manufacturing

process. As was explained in Chapter 2, after the PPTC trips its conducting-state resistance is substantially higher than the conducting-state resistance prior to tripping. This increased post-trip resistance causes higher dissipation in devices that have tripped.

Power dissipation was measured at published hold current for the device. This is the highest nominal current that can be systematically used in applications. Figure 4.20 plots the measured power dissipation of two PPTC types with different maximum voltage ratings as a function of hold current. The power dissipation of conventional fuses is also plotted for comparison. One can see that the devices rated to operate up to 60 V and suitable for the 42 V EDS have higher power dissipation than the devices rated for 14 V EDS. The power dissipation of devices rated for the 14 V EDS is comparable to the power dissipation of CF.

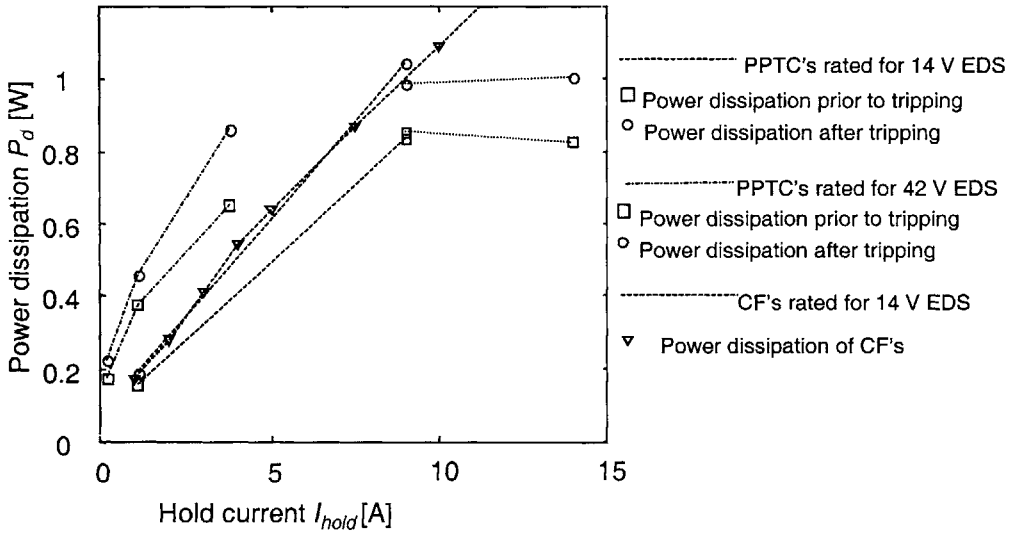

Figure 4.20 Experimentally determined power dissipation of PPTC prior to tripping and after at least one trip as a function of hold current. PPTC's rated for both 42 V and !4 V systems are shown. Power dissipation of fuses is plotted for comparison.

However, since the power dissipation of PPTC's is different for devices that have undergone a trip and the devices that have never been tripped before, two different data points were measured for each PPTC device tested. One data point represents the power dissipation of the device that has not tripped. The second data point represents the power dissipation in the PPTC one hour after the device was tripped and allowed to return to its low resistance state. The

experimental data verifies the increased power dissipation of devices that have just tripped and reset to their normal state. This is predicted by the increase of the post trip resistance explained in Chapter 2.

4.7. Post-trip current for resetable devices

Both, PPTC's and the auto resetable SPS's have post-trip current present after they have tripped. Since this current is delivering energy into the faulty circuit, the investigation of the magnitude of this current was performed to determine the possible impact of this current on the circuit.

Certain SPS's automatically restart after a fault. It is important to evaluate the post-trip RMS current of these devices. The post-trip current can be determined theoretically by averaging the circuit behavior.

An auto-resetable SPS operates by heating up to the critical temperature and then turning off. After it turns off it waits for the temperature of the SPS to fall 10°C under the critical temperature and turns back on. Figure 4.21 shows the

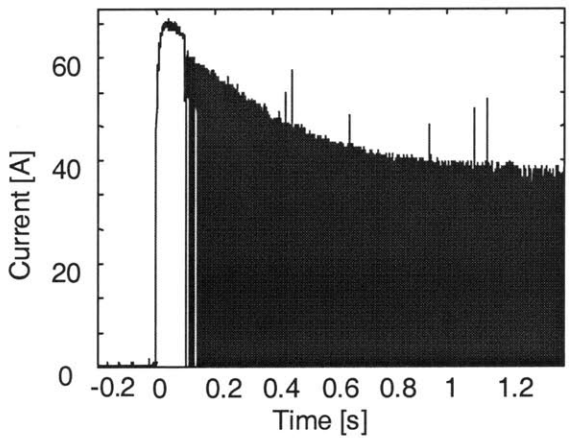

Figure 4.21. Experimentally recorded SPS current during the interruption of the fault current. Data shown is for BTS 640 S2 type SPS produced by Infineon.

actual value of the current as a function of time recorded using the experimental setup. Figure 4.22 is the blow up of a small portion of the waveform in Figure 4.22 after steady state is reached. Form these two figures one can see that there is the initial constant current regime which represents the heating up to initial

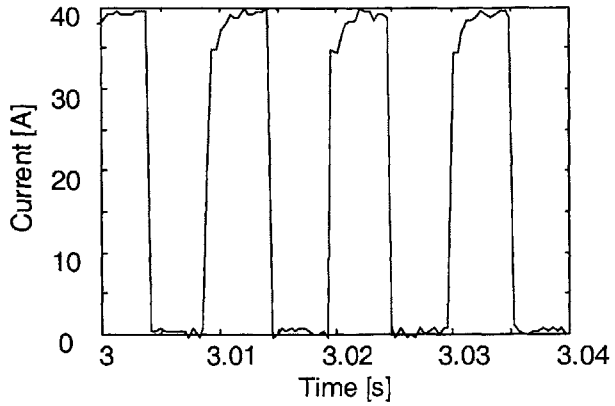

Figure 4.22. Blowup of the experimentally determined waveform shown in figure 4.21 after thermal steady state is reached.

turnoff and the regime where the device keeps turning off and on and the current is pulse width modulated (PWM) according to the thermal behavior of the SPS.

By averaging this PWM behavior a theoretical model can be obtained. In this average model the device is considered to be at constant temperature above ambient which is 5°C less than the T_{jmax}. By assuming that the device is at T_{jmax} the error introduced is minimal. In order to keep the device at T_{jmax} certain power needs to be delivered to the device. This power is just the power delivered to the device at I_{mfc} given by $I_{mfc}^{2*}R_{dev@T=150}$.

During the automatic turnoff, the same power needs to be delivered to the device in order to keep it at T_{jmax}. Thus the RMS value of the post-trip current is close to I_{mfc} of the device. Because the device is slightly cooler, the RMS value of post-trip current I_{post} is always less than I_{mfc}. However, as the device enters current limiting mode the power delivered to the device is the product of the voltage drop across the device and the limiting current. The voltage drop across the device is given by the following equation:

$$V_d = V_s - I_{scp@T=150} * R_c$$

The power required to keep the device at $T_{avg} = T_{jmax}$ is the same so the resulting I_{post} is given by:

$$I_{post}=I_{mfc}^{2*}R_{dev@T=150}{}^{*}V_d^{-1*}D^{1/2} \quad (4.6)$$

Where D is the duty ratio of the current. D is the percentage of the time the device is on during one period of the PWM behavior.

By combining these two relationships a plot of post-trip current as a function of prospective current I_p can be created. Figure 4.23 shows that as the prospective fault current gets large the steady state RMS value of post-trip current gets smaller. However, in case where the fault is an overload and the current limiting mode of the SPS is not reached the post-trip RMS current is to

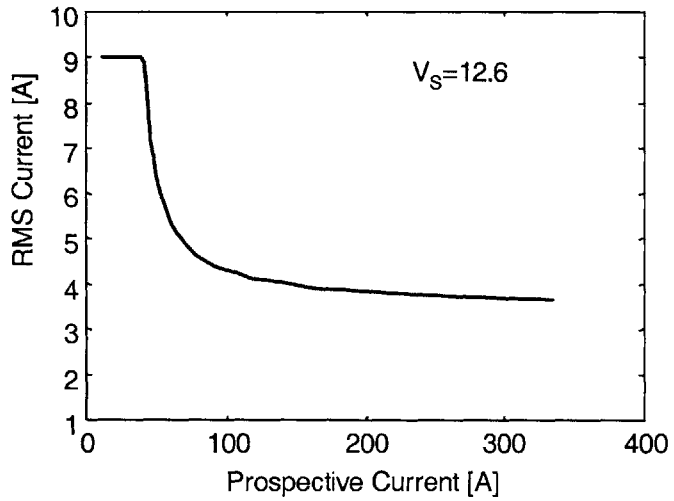

Figure 4.23. Computed theoretical steady state RMS value of post fault current for the BTS 640 S2 type SPS as a function of prospective current. Results computed assume the source voltage of 12.6 V..

first degree I_{mfc}. This is very important to notice since this current is delivering power to the fault. These are first order analysis and the prospective current might be lower. However the results do put a reasonable upper limit on the RMS value of post-trip current.

The reasons for the post-trip current to be lower are quite simple. Because the device is composed of a network of thermal resistors and capacitors the case might not have an average temperature of T_{jmax}. Thus the post-trip current is less than predicted by the model. The error in the model increases with increasing I_p.

The second effect is the effect of the inductance in the circuit. The inductance causes the average temperature of the device to be higher than 150 degrees. Thus the cooling of the device will take longer and the device will take longer to switch off. However the energy required to keep the device at this higher average temperature is the same since we need to heat the device only to 150°C degrees and the inductive turnoff causes the device to keep heating up. Thus the time that the device is on is increased by the time required for the inductive turnoff. On the other hand, the time that the device is off is proportional to the natural log of temperature difference that the device needs to cool down.

In order to verify the theoretical model an experimental investigation was performed on the data recorded in the circuit examples of which are shown in Figures 4.21 and 4.22. Figure 4.24 shows the experimentally determined values of the steady state post-trip current superimposed on the above presented theoretical model. Experimental data was obtained on the experimental setup described in Appendix B. Again results obtained represent only typical values. While it is apparent from Figure 4.24 that there is disagreement between experimental results and the above mentioned theory, The above mentioned theory is a good first order approximation of post-trip current. Furthermore the experimental verification validates the fact that I_{mfc} is never exceeded. Thus the

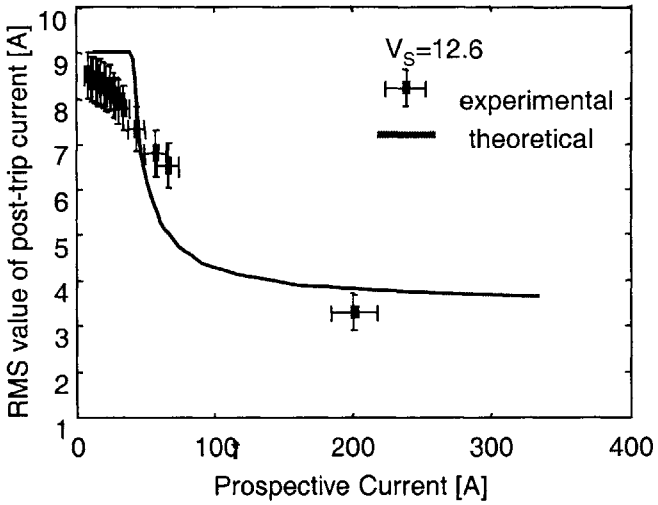

Figure 4.24. Experimentally determined values of the steady state RMS value of post-trip current superimposed with the theoretically predicted results shown in Figure 4.23. Device under test was the BTS 640 S2 type SPS.

upper limit of post trip current can be established as I_{mfc}. Such an upper limit would not depend on the source voltage. In reality, as the source voltage is increased from 14 V to 42 V the post-trip current is reduced by roughly a factor of 3 and as given by Equation 4.6 in the region where the SPS is in its current saturation region of operation. The post-trip current in the resistive region does not change.

Furthermore, having established that the post-trip current never exceeds the minimum fusing current, one is free to conclude that the steady state RMS value of the post-trip current does not present any problem to the circuit being protected. The circuit being protected must be capable of dealing with currents up to minimum fusing current during normal operation without negative effects on the circuit performance.

However, it is important to note that it takes some amount of time for the steady state RMS value of the post-trip current to be reached. Figure 4.25 shows the period by period computed RMS value of the post-trip current as a function of time. The time for the RMS value of the post-trip current to reach steady state can be orders of magnitude larger than the time for the initial trip. While it takes only tens of miliseconds for initial interruption, the time to reach the thermal steady state can be in excess of 5 seconds. The investigation of the impact of this transient on the circuit being protected falls outside the scope of this thesis.

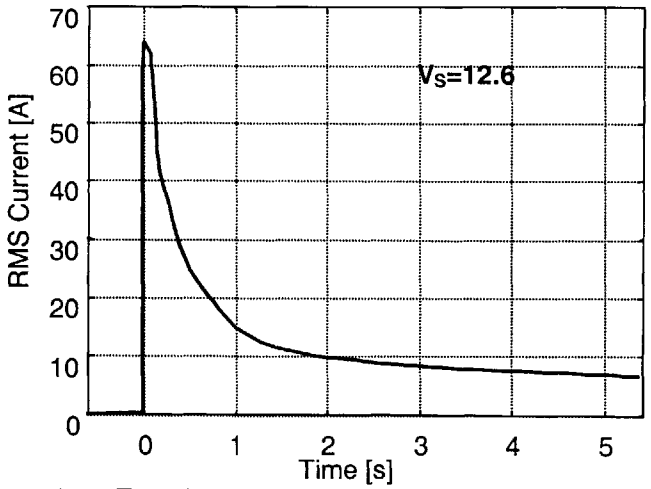

Figure 4.25. Transient behavior of the period by period RMS value of the post-trip current for the BTS 640 S2 type SPS.

Since the energy imparted on the circuit being protected exceeds the energy represented in SPS's *I-t* plots, damage to the circuit can happen. Therefore, it is important not to neglect this transient and further study of its impact on the *I-t* plots should be performed.

All PPTC's have steady state post-trip current present. This current insures that the device stays in its tripped state. When the prospective fault current is known, one can calculate the post current I_{post} flowing in the device after the device has tripped. The device becomes a constant power device in the tripped mode implying I^2R_{dev} is constant as explained in Chapter 2. The power dissipation in the tripped state is published in the data sheets for each individual device (19). Prospective current I_p gives the resistance present in the circuit. I_{post} is then calculated as follows:

$$I_{post} = \frac{V_S}{2R_C} - \sqrt{\frac{V_S^2}{4R_C^2} - \frac{P_d}{R_C}} \tag{4.7}$$

where P_d is the power dissipation necessary to maintain the device in high resistance state. Figure 4.26 shows I_{post} as a function of I_p for two supply voltages V_S. Thus by increasing the supply voltage the post-trip current is

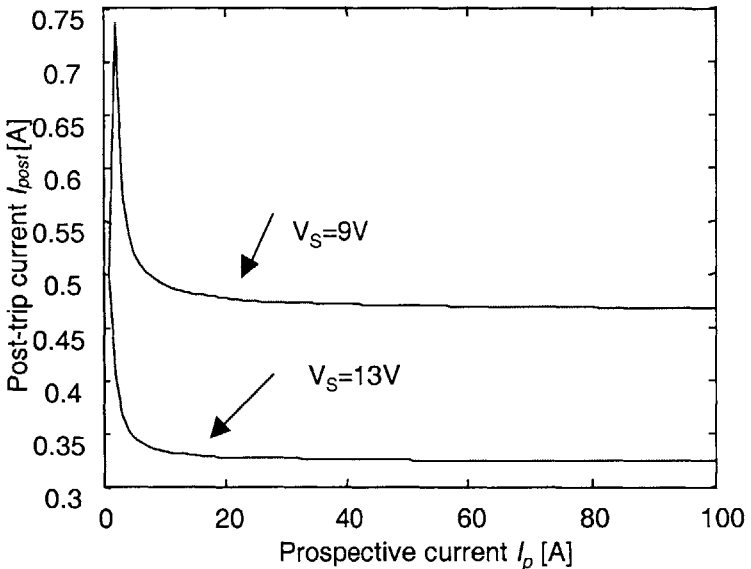

Figure 4.26 Theoretically computed post-trip current in the tripped state as a function of prospective current and two source voltages for a RUE900 type PPTC.

reduced. Figure 4.27 shows post-trip current as a function of supply voltage for fixed I_p. As the system voltage is increased from 14 V to 42 V the post-trip current is reduced roughly by a factor of 3 for the same prospective fault current. This is visible from Figure 4.27.

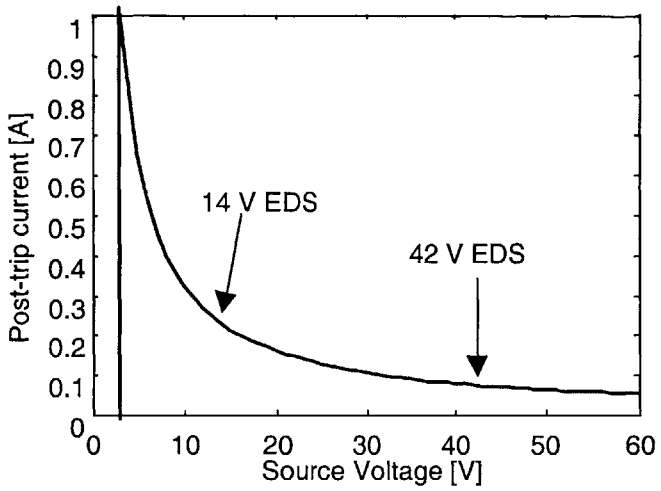

Figure 4.27 Post-trip current in the tripped state as a function of source voltage for I_p=30 A for a RXE375 type PPTC

In order to verify the above-presented model, an experimental investigation for the typical device was performed. The device tested was RUE900 type PPTC. The device was tripped into a high resistance state and allowed to reach a thermal steady state. After the value of the post-trip current

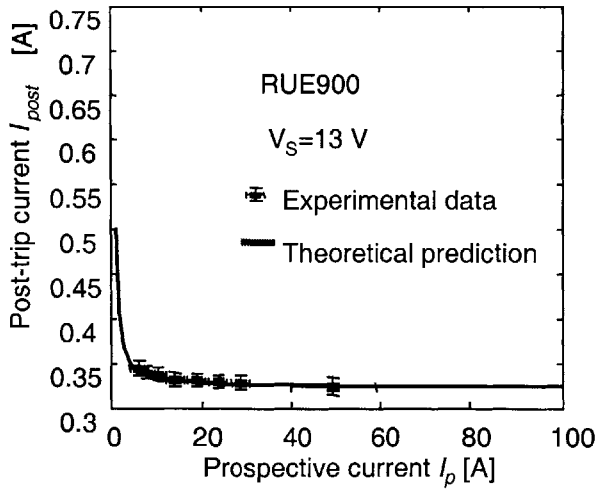

Figure 4.28. Experimentally determined steady state value of post-trip current superimposed with the theoretical predictions. The device under test was the RUE900 type PPTC.

was recorded the load was changed and the procedure was repeated for several values of post-trip current. Figure 4.28 shows the experimentally obtained data superimposed with results obtained with the above-presented theoretical model. The correlation of the two is extremely high and thus the prediction of the steady-state post-trip current for PPTC's is achievable.

The post-trip current of PPTC's is much lower than the post-trip current of SPS's. However, once the PPTC has tripped, the only way to reset it is to turn off the current. The SPS will reset to the normal mode of operation if the circuit returns to normal operating conditions. The PPTC needs to be turned off to be reset, as explained in Chapter 2. The same principle of operation applies to the latching SPS. However, latching SPS has no post-trip current present since it stays off after initial turnoff.

Chapter 5.

Circuit and system fusing and protection

5.1. Introduction

This chapter looks at several situations in which the protective device is used to protect elements of the circuit and is called to perform in a coordinated protection environment.

5.2. Protection of cables

In automotive environment the most important piece of equipment to be protected is the cable. In order to prevent cable damage the temperature of the cable should not exceed a certain temperature at which the cable insulation begins to deteriorate. Using Equation 2.1 we can find the *I-t* characteristic of the cable. However, now instead of the melting temperature for copper we use a melting or degradation temperature of the insulation (T_{ccable}). Cable *I-t* characteristics are shown in Figure 5.1. This cable characteristic has to be located to the right of the *I-t* characteristic of the associated protection device in

order to prevent cable damage. The exact equation for generating the cable *I-t* plots is given in Reference (6).

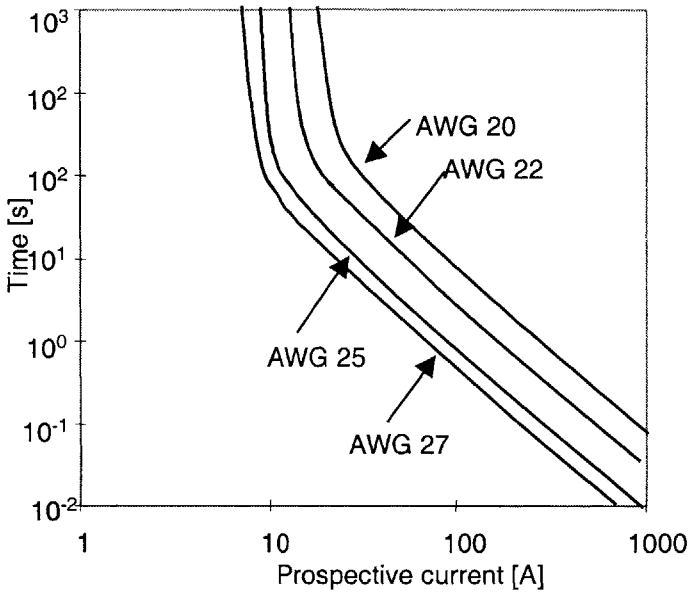

Figure 5.1 It characteristic for cables of different cross sectional area and PVC insulation

We can compare the performance of a CF, SPS, and a PPTC in protecting a cable. Two different analyses come into mind. The first one assumes that the cable and the protective device are at the same ambient temperature. The second analysis assumes that the cable and the protective device do not have the same ambient temperature.

5.2.1. Cable and Protection at same T_{amb}

The extent by which the cable *I-t* plot shifts as a result of ambient temperature changes is influenced primarily by the critical temperature of the insulation. If the critical temperature is far above the ambient temperature, the *I-t* curves shift only a little in response to small changes in ambient temperature. If the critical temperature is closer to the ambient temperature, the same small change in ambient temperature will produce a larger shift. A protection device that has a critical temperature close to the critical temperature of the insulation of

cables will have roughly the same shift in its *I-t* characteristic. This behavior can be called the tracking of the *I-t* plot for a cable by the *I-t* plot for a protective device.

Most of cables currently in use in the automotive environment have one of two types of insulation. The polyvinyl chloride (PVC) insulation is rated to operate between T_{amb} =-40°C to T_{amb} =85°C . The critical temperature of PVC insulation is 160°C (20). The cross linked polymer (XL) cable insulation is rated for operation between T_{amb}=-40°C to T_{amb}=125°C. The critical temperature T_{ccable} of this insulation is 250°C as given in Reference (20).

Thus we can see that the SPS will 'track' the cable characteristic best since its critical operating temperature T_{jmax} is close to both T_{ccable}'s. However, PPTC's will do almost just as well for the PVC insulation. Development of a PPTC with T_{trip}=150°C for the automotive environment is under way. Furthermore, CF that use diffusion pill technology will exhibit quite good tracking of the cable I-t characteristic in the regime where the exchange with the environment is substantial since the critical temperature in that regime is of the order of 200°C.

5.2.2. Cable and Protection at different T_{amb}

Here the cable can be at any ambient temperature T_{ambc} in its operating temperature range and the protective device can be at any other temperature T_{ambp} in its operating temperature range. The *I-t* characteristic for a cable will be fastest for T_{ambc} at the maximum allowed and the device characteristics will be slowest when T_{ambp} is at the lowest allowed operating temperature. To provide cable protection, the protection device *I-t* characteristic at T_{ambp}= $T_{ambpmin}$ must be to the left of the cable *I-t* characteristic at T_{ambc}= $T_{ambcmax}$. This can be achieved with all three device types.

However the maximum current allowed in this circuit is actually set by the I-t characteristic of the device when T_{ambp}= $T_{ambpmax}$. The device with highest critical temperature (T_{melt}, T_{jmax} or T_{trip} for CF, SPS or PPTC respectively) will be able to pass a highest nominal current through a particular cable under nominal

conditions (under the assumption of constant fusing factor f for all three devices) since it will have the smallest variation in its *I-t* characteristic between $T_{ambpmax}$ and $T_{ambpmin}$. Thus, one would conclude that CF without diffusion pill technology will perform the best in this application since they have the highest critical temperature and thus the smallest variation in performance as a result of ambient temperature changes as was shown in Chapter 4.

However, by noticing that the fusing factor of a SPS can be as low as 1 it becomes possible that the SPS might perform even better. An 9A ATO fuses has a I_{mfc}~10A however it has to be derated by another factor of .75 as given by the manufacturer and thermally derated to 85°C . This gives us a fuse that can safely pass 6A over the temperature operating range (-40°C to 85°C) and needs a cable that can pass 11A at its maximum allowed temperature. For the same cable, BTS 640S2 gives the maximum allowed current of 6.5A for the same fusing factor as a fuse.

This is a result of the fact that the fuse manufacturer suggests that a fuse should be derated by a factor of .75 from its nominal current to insure longer lifetime. Thus this causes the minimum effective fusing factor for a fuse to be 1.34. The limit of the fusing factor of the SPS is not clearly stated but it is reasonable to assume that the SPS will see some performance degradation if it is operated close to its I_{mfc}. However, this operation would occur only at T_{ambp}=-40°C and operation in this condition is unlikely to materially shorten device lifetime. The environmental conditions giving rise to this operating condition will occur only infrequently in the life of the vehicle (For most vehicles these environmental conditions will never occur). Further, should this condition occur, operation of the vehicle should soon increase the device ambient temperature.

It is therefore concluded that SPS's can provide the best degree of protection to the cable in both situations. They 'track' *I-t* characteristic of the cable most closely and also provide the best protection of the cable when their ambient temperature is different from the cable ambient temperature.

The full analysis involves comparing the *I-t* plots of the protective device and the cable. Depending on the situation, the fuse *I-t* plot might fit more closely

with the *I-t* plot of the cable and thus provide better protection. However, the converse is also true, the SPS's *I-t* plot might give better fit in other situations.

In almost all automotive applications, the lowest cost solution will be chosen. The degree of 'tracking' between device and cable characteristics is in these circumstances of value only if the SPS, if better, allows selection of a less expensive cable which offsets the price penalty of the SPS. Of course, if the SPS is serving an additional function, for example replacing a relay, economics of the decision is altered.

As the source voltage is changed to 42 V, the above analysis remains the same since the defining factor of the above analysis is the variation in performance as a function of ambient temperature changes. It was shown in Chapter 4 that the performance changes due to ambient temperature change stay the same as the source voltage is increased.

5.2.3. Self inductance of the cable

All cables have self-inductance, which can have influence on the operation of protective device. To calculate the self-inductance of the cable certain assumptions need to be made. It is easy to derive the self-inductance formula for a cable above a perfect conducting plane:

$$\frac{dL}{dl} = \frac{\mu_0}{2\pi} \ln\left(\frac{2h}{r}\right) \tag{5.1}$$

where L is the inductance of the cable, l is the length of the cable, h is the height of the cable above a perfect conducting plane, and r is the radius of the cable cross-section.

In the automotive environment the chassis of the car is used as a ground conductor and to first order can be treated as a perfect conducting plane. However, as the distance from this plane increases, the self inductance per unit length increases. Thus the exact calculation of the self inductance of the cable would involve performing the following line integral:

$$L(l) = \int_{L1} \frac{\mu_0}{2\pi} \ln\left(\frac{2h}{r}\right) dl \tag{5.2}$$

where line *L1* has to be parameterized in terms of some distance *x* and height *h*.

However the value of this integral will be largest if we assume a conductor of same length at a largest distance from the perfect conducting plane (car chassis). Approximately, this distance never exceeds half a meter in the car. Thus using the Equation 5.2 we can get the worst case self inductance of the cable by setting h to half a meter. All lower values of h result in lower self inductances.

To make the analysis complete we need the equivalent series resistance R_{ESR} of the source. This is important because the R_{ESR} of the automotive battery is of the order of the cable resistance and has strong influence on the circuit time constant.

Using the above equation for the self-inductance of the cable, the time constant τ (L_c/R_c) for the circuit as a function of cable length can be determined. This analysis applies for the short circuits. The cable is cut somewhere along its length and one must insure that the time constant of the resulting short circuit does not exceed the one allowed by the protection device. Figure 5.2 shows τ for

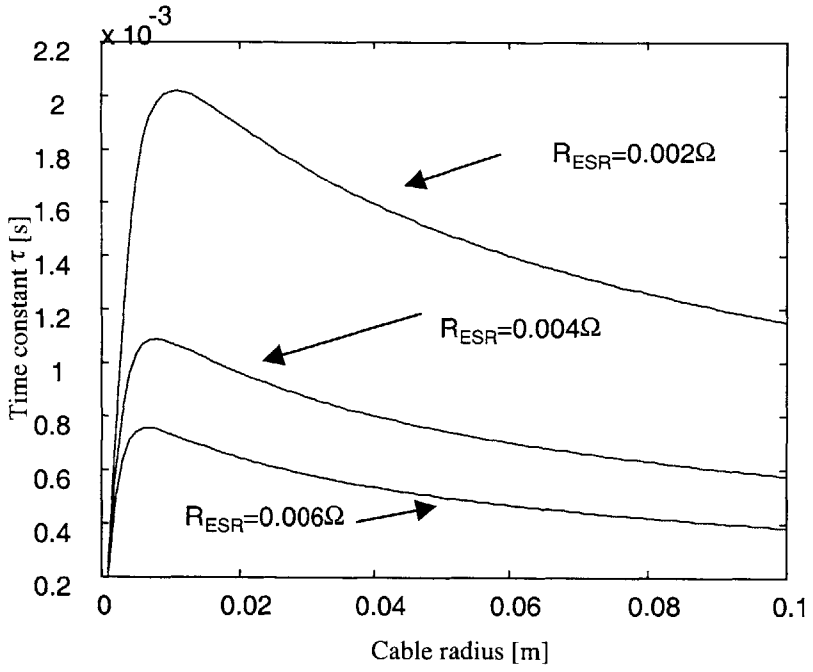

Figure 5.2 Dependence of the short circuit time (L_C/R_C) constant as a function of cable radius . Length of the cable is kept fixed at 5 m

the circuit as a function of cable diameter for a few values of R_{ESR} and a fixed cable length of 5 meters.

Figure 5.3 shows the circuit time constant as a function of prospective current for 20-gage cable protected by a ATO 10A type CF (the resistance of the fuse is used in the calculation of prospective current). Increasing prospective current represents shorter and shorter cable. The circuit time constant is largest for the lowest prospective fault current and consequently longest cable length. Thus the protection design engineer need only check that the time constant of the circuit shorted with full length of cable does not exceed the limitation specified by the protection device manufacturer.

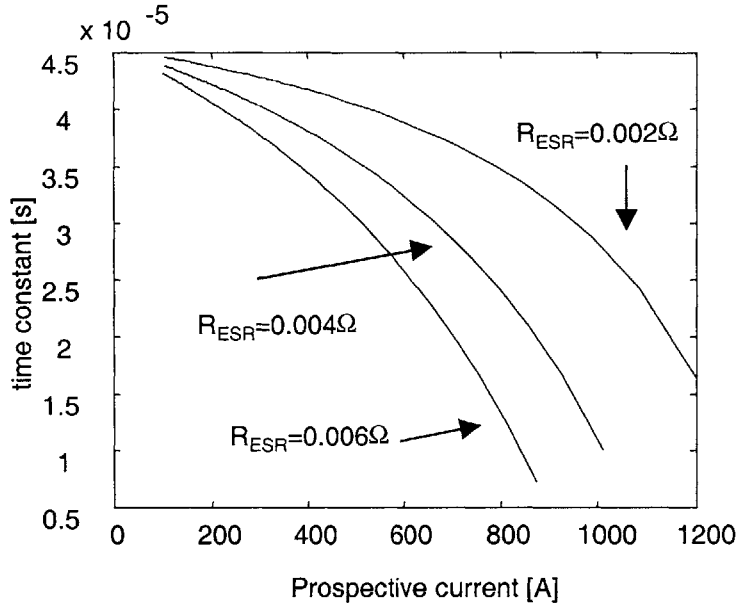

Figure 5.3 The time constant of the fault as a function of prospective current. The fault is considered to be generated by shorting of the cable

By examining Figure 5.3 it is concluded that the cable self inductance will not present problems to the protection devices. This is justified by the analysis in Chapter 4. The time constants due to cable presence are well below the allowed values for SPS's and CF's.

When there is additional inductance present in the circuit, analysis changes. If a fault occurs for which the current remains in its normal path through cables but the load is internally partially shorted, the inductance of the cable has to be added to the remaining load inductance when the time constant of the resulting

circuit is determined. The resulting time constant should not exceed the limits given in Chapter 4.

5.3. Parallel connection of protection devices

Sometimes it is hard to find the protection device with the appropriate I_{mfc}. One can then use two protection devices connected in parallel. However, it is not immediately clear what the maximum nominal current of this parallel connection is.

An analysis for a conventional fuse has shown that the maximum allowed current is by worst case analysis given by the sum of the nominal currents of the two individual devices (under the assumption of same fusible link material for both fuses). In reality the limit is actually higher since the fuses heat up to a different degree. However this current should again be derated by a factor of 0.75 (as given by the manufacturer for a single device). As an example we can consider two 10A ATO type fuses connected in parallel. The maximum allowed current passing through the parallel connection is 15A when the recommended derating is applied.

When the devices connected in parallel are PPTC's (only PPTC's of the same type and rating) the maximum allowed current is only forty percent more than the single PPTC's maximum allowed current I_{hold} (thus $1.4*I_{hold}$). This limitation is given by the manufacturer and can be found in (19).

It is not necessary to use SPS's in parallel since their I_{mfc} can be adjusted by changing the thermal resistance of the chip through addition of a heat sink. Thus a BTS 550 P can act as a protection device with I_{mfc} ranging from 17 A to 50+ A . Figure 5.4 at the end of this section shows the dependence of the *I-t* characteristic for the BTS 550 P type SPS on the thermal resistance R_{thja} of the device (11).

However, the general consensus is that the devices should not be connected in parallel since the maximum breaking capacity of one device can be exceeded more easily due to different speed of operation. In a 42 V system this will be even more likely if the 42 V side battery is optimized for high power

delivery (low equivalent series resistance). Furthermore, if the protection devices are used connected in parallel then the three device types should not be mixed in the same parallel connection. This case has not been analyzed due to its unappealing consequences. SPS's do not require a parallel connection thus the mixing would occur between PPTC's and CF's. However, even if the bound for the magnitude of the nominal current could be established one would in fact have a non-resetable device. Thus the advantage of the PPTC would disappear in the parallel connection.

It is interesting to note that in a situation where two fuses are connected in parallel one fuse always melts before the other one. The fuse that melts first

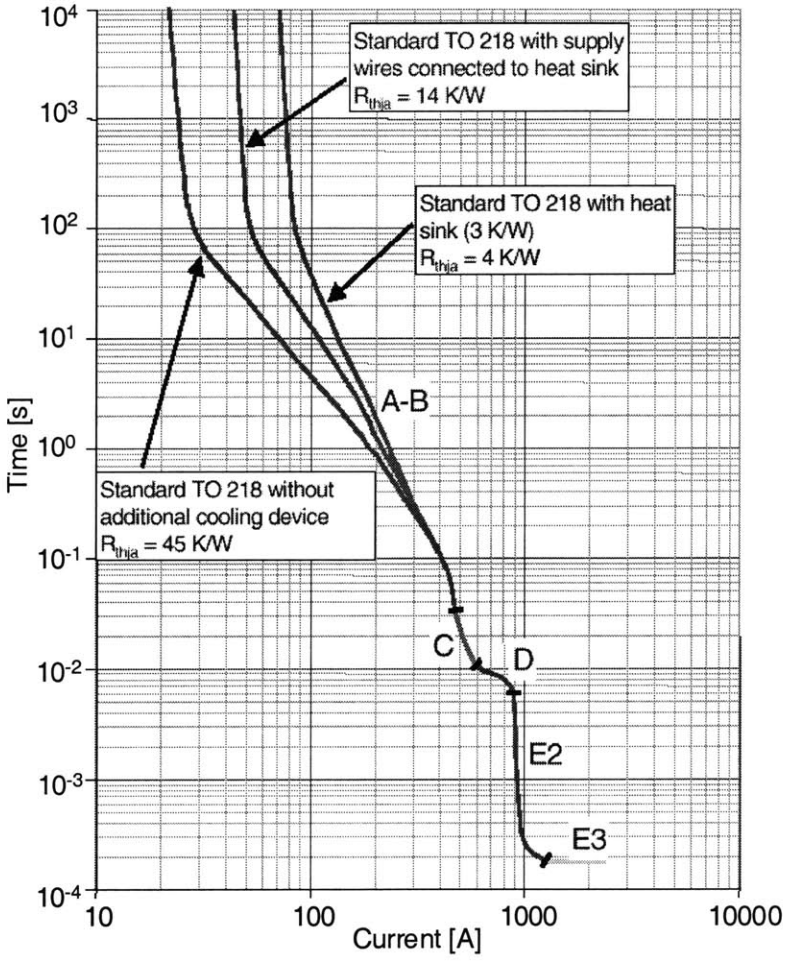

Figure 5.4 The effect of change in thermal resistance of the device on the BTS 550 P I-t characteristic.(Reprinted by permission of Infineon technologies)

does not commence arcing till the other fuse melts. This is a result of a low impedance path through the other fuse. However, the arc is established in both fuses as soon as the gap forms in the second fuse. The fuses arc together till the current is extinguished.

5.4. *Current-Limited Power Supply*

The present day automotive EDS has a battery connected to it. This battery can supply huge amounts of current at substantially high voltages. The first order model of the battery is a voltage source in series with the equivalent source resistance. This equivalent source resistance is as low as several mΩ. Thus the voltage drop across the battery terminals is rather low even for 400A of current. The battery can therefore supply high currents necessary to clear faults with low resistance such as short circuits.

If a current-limited power supply (CLPS) were to be used as the energy source in the automotive environment and the current limit was of the order of 100 A, then the situation in the case of short circuits is somewhat different than with the presence of the battery as an energy source.

In order to examine the behavior of the protective devices in such a system, the *I-V* characteristic of the CLPS is plotted along with load lines representing

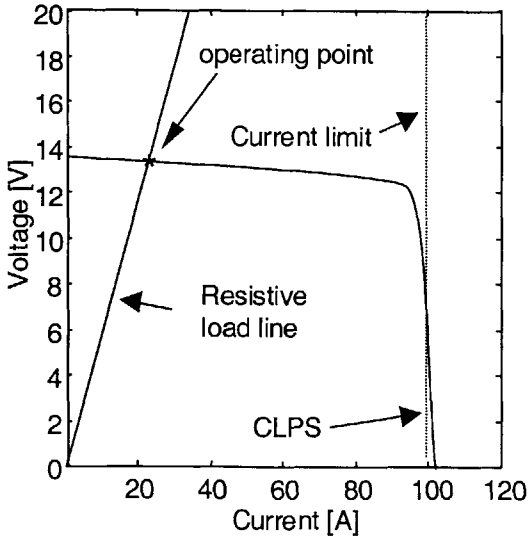

Figure 5.5 I-V Characteristic of a CLPS superimposed by a resistive load line. Current limit is roughly 100 A

normal and fault operating states. The example of this *I-V* plot with the load line of the series connected load resistance and the protection device is presented in Figure 5.5 for a resistive load and a conventional fuse.

Right away we can realize that if the protective device is ever to function, the minimum fusing current I_{mfc} of any single protection device connected to the CLPS has to be less than the current limit of the CPLS (I_{limit}). This brings us to realization that the usable current for the application in which one protection device protects the circuit is only I_{limit}/f (f is the fusing factor). Thus one comes to a conclusion that the full capacity of the CLPS can not be used in a protected system having only one protection device connected to the CLPS.

If there are multiple protection devices connected to the CLPS then under the assumption that only one fault happens at any given time we have the following restriction: The sum of the I_{mfc} for a protection device with greatest I_{mfc} and the load currents I_{load} of the remaining devices has to be less than I_{limit}. The I_{mfc} used in the calculation has to be the I_{mfc} of the device at its lowest operating temperature and I_{load}'s used have to be the maximum possible in any given combination of system parameters and operating conditions. This insures that the protection device will trip under all operating conditions when all the loads are on at the same time. The analysis just described assumes that the loads are resistive. If the loads are not resistive the situation somewhat changes. Covering all the possible outcomes of the combinations of loads is not covered in this thesis.

The above analysis suggests that from the theoretical point of view it would be most efficient to use as many protection devices as possible (as many as there are identifiable individual loads). Under those conditions the usable power from the CLPS at any given time will be maximized. However, in automotive industry this may not be an economically practical solution. The introduction of economics issues may cause the number of protection devices to be lower than the number of individual loads.

Continuing with the assumption that the loads are resistive, it is illuminating to discuss the performance of the three protection device types by using the

particular *I-V* characteristic for a CLPS given in Figure 5.5. Just to get the idea how the various devices compare, three devices with roughly the same nominal current I_{nom} were chosen. An ATO fuse with I_{nom}=10A, BTS 640 S2 SPS with I_{nom} =8.6 A and a RGE900 with I_{hold}=9A are the devices used.

Consider a short circuit in which the only remaining resistance in the circuit is the resistance of the protection device. In this case, notice that the BTS 640 S2 does not cause the CLPS to reach its current limit. However, both the CF and the PPTC do cause the current limit to be reached and the system voltage is pulled down. Figure 5.6 shows the load lines of the 3 devices and their intersection with the load line of the CLPS.

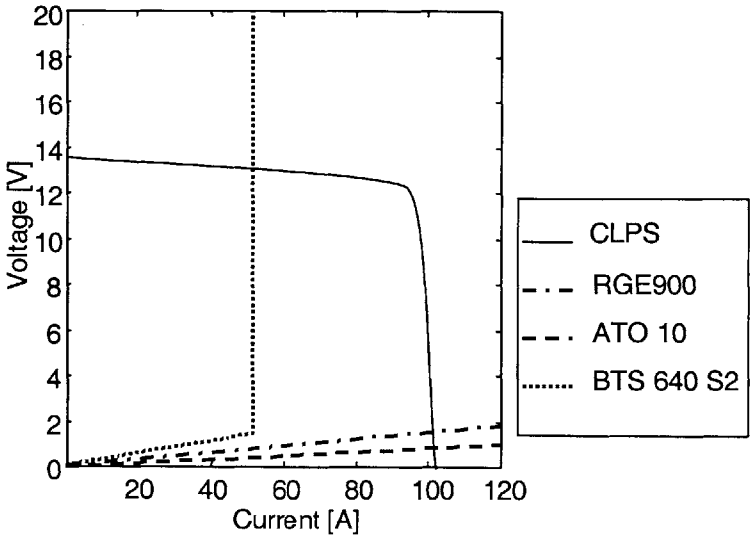

Figure 5.6 Load lines of three device types superimposed onto the I-V characteristic of a CLPS

In situations where circuit resistance Rc is present during a fault, the load lines of the PPTC and the SPS behave as resistive load lines. The load line of the BTS 640 S2 behaves differently. The current limit I_{scp} of the SPS can not be exceeded. The behavior of the load line under different circuit resistance of the fault is depicted in Figure 5.7.

More than one load might be turned on when a fault happens. This only makes the case for a fuse and the PPTC even worse. The other loads lose their nominal current and all current flows in the fault, if the impedance of the fault is low enough. The exact behavior for different values of fault resistance is

described by the equation for parallel impedances. A single resistor can represent all the loads that are operating under nominal (faultless) conditions. This resistor is in parallel with a fault.

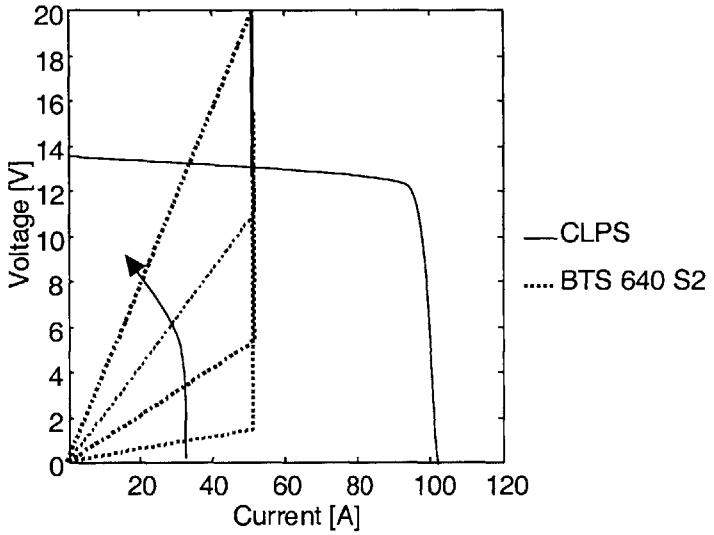

Figure 5.7 I-V characteristic of the CLPS and a BTS 640 S2 as the fault resistance changes (increasing values of R_c are indicated by the direction of the arrow)

The SPS does not cause the current limit of 100 A to be reached as long as the sum of nominal currents in the other loads does not exceed the difference between the limiting current of the CLPS I_{limit} and the maximum allowable current through an SPS I_{scp}. For the BTS 640 S2 this leaves us 50 A of current that can flow in the other loads without the voltage of the source dropping. However just as well a situation could happen where 90 A of nominal load current exists in other loads causing all three device types to reach the current limit and cause the system voltage to go down (for a low impedance fault). Under the assumptions that all loads combined total 100 A of current and that unaffected loads (no fault associated with them) are not permanently on but have a ½ probability of being on or off at any given time, then the probability of an SPS causing the system voltage to go down is also ½.

The analysis above reveals that, if cost is not a consideration, an SPS is the best choice of a protection device in a system with a current limited power supply. However this choice is justified only if the limiting current of the SPS does not exceed I_{limit}.

One of the proposed architectures for the future 42-14 V electrical power distribution system has the alternator on the 42 V side and delivers power to the 14 V side through a DC-DC converter. This DC-DC converter is a current-limited power supply and the above analysis applies. However, while the steady state characteristic is equivalent to the characteristic of the CPLS presented in this chapter, the transient behavior may be significantly different. As the power demand on a DC-DC converter is increased (due to the occurrence of a fault) the operating point of the circuit follows a certain line in the *I-V* space. Eventually it reaches the steady state and the operating point lies on the steady state characteristic at the same location that it would for the CLPS presented at the beginning of this section. This thesis does not investigate this transient behavior. However, this transient behavior does theoretically imply that the system voltage might transiently drop to a value less than predicted by the steady state

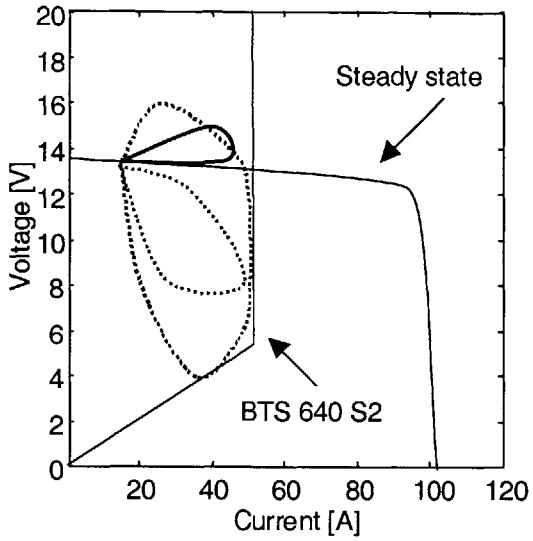

Figure 5.8 Trajectories of the operating point in I-V space during a fault protected by a SPS for a CLPS with the indicated steady state characteristic

characteristic even in the case of SPS's. Several probable trajectories of the operating point through *I-V* space are depicted in Figure 5.8. The trajectories that would cause the system voltage to be reduced are shown as dotted lines.

The second proposed architecture has an added 12V battery connected to the DC-DC converter, which then augments the current limit of the power supply.

However, in a situation where this battery is in a low state of charge, its terminal voltage is low and the equivalent series resistance is high. Using the battery model explained by H. L. N. Wiegman and R. D. Lorentz (21), the equivalent series resistance R_{ESR} (at T_{amb} =25°C) of the battery as a function of state of charge during discharging is given by:

$$R_{ESR} = 0.04 * R_n * \sqrt{\frac{1}{Q_n + 0.2}} \tag{5.3}$$

where Q_n is the normalized state of charge ($0 < Q_n < 1$) and R_n is a parameter determined by dividing the nominal voltage V_n by the current (I_n) necessary to drain the battery from the state of charge equal to one to the state of charge equal to zero in one hour. Furthermore, the voltage across the battery in the above mentioned model is given by:

$$V = Q_n * (V_n - V_0) + V_0 \tag{5.4}$$

where V_0 is the voltage of the battery at which the state of charge is zero. Figure 5.9 shows the R_{ESR} as a function of state of charge for an automotive battery with V_n=13 V, V_0=8 V and I_n=20A.

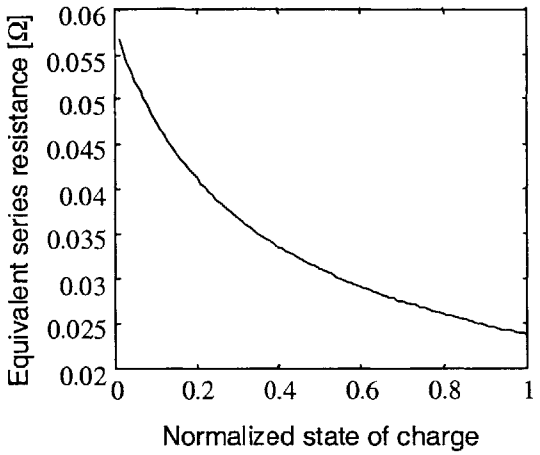

Figure 5.9 Equivalent series resistance of the 13 V automotive battery as a function of state of charge

If the state of charge of the battery is low, the resulting steady state *I-V* characteristic representing the parallel combination of the generator (modeled as

a CLPS of 100A capacity) and the discharged battery is given in Figure 5.10. This curve has strong qualitative similarity to that of the CLPS alone. Thus, the analysis presented in this chapter is important in all situations where the alternator is not present.

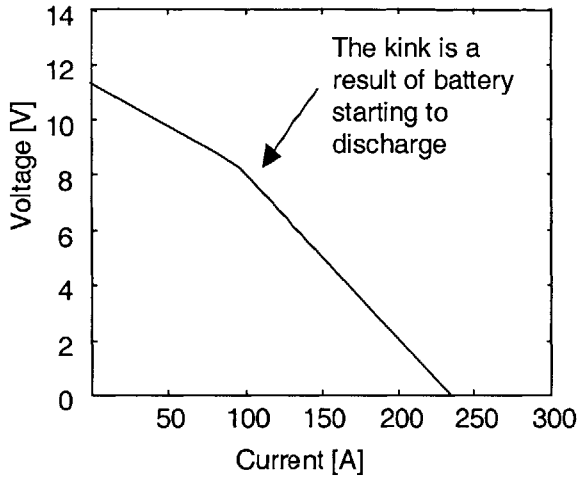

Figure 5.10 Steady state I-V characteristic of the current limited power supply together with the battery of low state of charge

In the present day automotive electrical distribution system, the alternator may be able to supply 200 A of current. To a coarse approximation, the alternator *I-V* characteristics is that of the CLPS. Most of the faults not associated with short-circuiting of the cable do not exceed the above-mentioned current limit (~200A). As presented in Chapter 2, the interruption of current at twice the prospective fault current is 4 times faster for a fuse (assuming it is operating in the regime of operation where exchange of heat with the environment is negligible).

A dual voltage power distribution system with a DC-DC converter linking the two voltages (14 V and 42 V) and power generation on 42 volt side might or might not have a battery connected to it. If it does not have the battery, the CLPS analysis described first applies. If it does have a battery and that battery is in a low state of charge, the effective current limit is still present as visible in Figure 5.10. Thus, for the above-mentioned battery and a CLPS with a current limit of 100 A the time to melt a fuse during a low impedance fault on the 14 V side

(current limit reached) would be 2 times longer than for 14 V systems with a 200 A alternator and the same low state of charge battery. However, the time to interrupt the fault for a BTS 640 S2 would to first order be the same (operating region E1 described in Chapter 2).

5.5. Protection Coordination

Protection coordination is the coordination of the operating characteristic of two or more protection devices in such a way that under fault conditions the device intended to operate does so while the remaining devices remain unaffected. This implies that there is more than one protection device between the load and the power source.

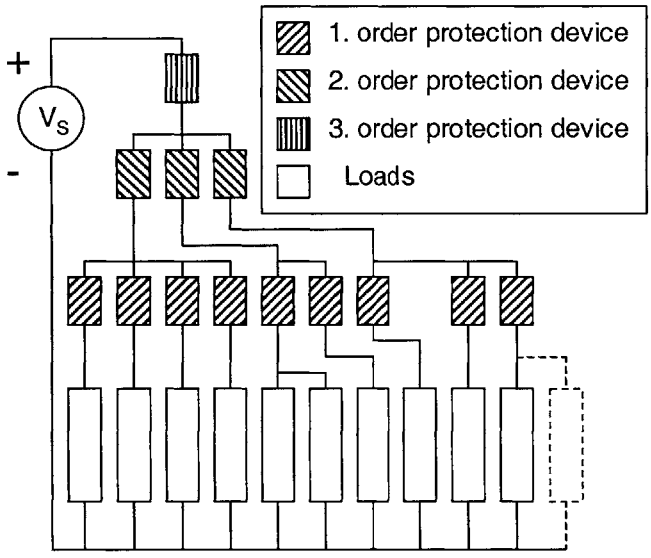

Figure 5.11 Tree structure of the coordinated automotive protection systems. The order of protection devices is shown

In the automotive environment the protection devices are organized in a tree structure depicted in Figure 5.11. In discussing the coordination of protection devices it is helpful to introduce the concept of orders assigning the first order to the protection devices connected right to the load. Then, the order of any protection device is the number of protection devices present (including the device whose order is being determined) between the load and the protection device along the path towards positive terminal of the voltage source. Figure 5.11 also shows the device orders.

The purpose of designing a coordinated protection environment is to ensure that the maximum amount of the system is left operational after the fault is cleared. This can be achieved with just one order of coordination. However then the cables that transfer the power to the load have to be pulled individually for each load. The result of one order of protection is multiple cables that follow the same physical path in a vehicle. The tree structure depicted in Figure 5.11 allows the power to be delivered to multiple loads over the same cable if the loads are located in the same physical neighborhood. For example, all the power required for loads in the passenger compartment can be delivered on the single wire protected by a second order fuse. After the power reaches the passenger compartment the individual wires associated with each load are protected by their own first order fuse.

It is common practice in the automotive industry to have several loads protected by one fuse. Having an individual fuse for each load would involve having more than 100 fuses. Economics of the automotive industry could not afford the cost associated with so many fuses. As a result, critical loads are more likely to have their own fuse while less critical loads are more likely to share a fuse with other devices.

Furthermore, the number of orders of protection devices should also be as low as possible for any particular load to insure the minimum voltage drop from the source to the load. Thus some loads might have more than one protection device associated with them while others might have only one. This further requires that the order of the protective device be defined as relative to a particular load (a fault can be considered a load as well!). A protection device might have one order with respect to one load and another order with respect to another load. When two loads of different criticality are connected to a protection device, and the order of the protective device relative to a more critical load is 2 then the order of the less critical device has to be at least 2. This insures that a fault on a less critical device does not interrupt the normal operation of the more critical device. Figure 5.12 shows this dependency

To achieve successful coordination, a protection device of order 1 relative to a fault (consider the fault as a low impedance load) should clear the fault and

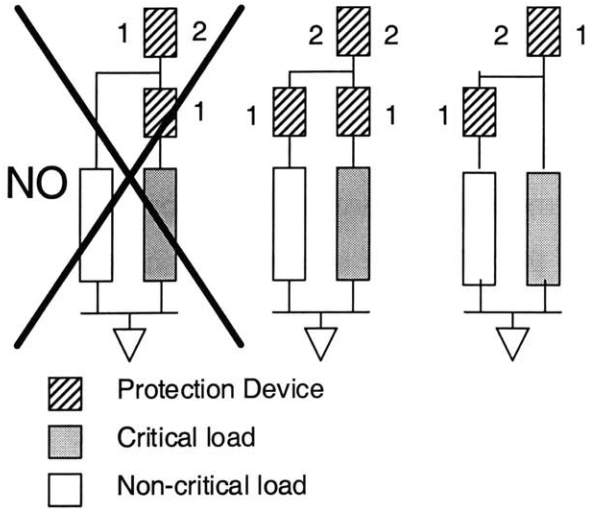

Figure 5.12 Protection coordination of two loads with different criticality.

leave the remaining devices of higher order unaffected. For this to happen under all circumstances *I-t* curves need to be coordinated in a certain way.

5.5.1. Coordination of the I-t curves

When a fault occurs and more than one order of protection devices exists the first order devices relative to the fault is required to clear a fault. This principle insures that the smallest possible portion of the system loses its functionality due to the fault.

This section investigates the method of protection coordination that insures adherence to this principle for two orders of protection devices. Generalizing to more than 2 orders involves insuring the principle holds for any pair of devices. Thus if we have three orders of protection devices relative to a fault we need to insure that the first order protection device clears a fault before second order does or the third order does.

In order to achieve this principle in practice one needs to know the fastest *I-t* curve for the higher order protection device and the slowest *I-t* curve for the first order protection device. Thus, if the first order protection device is a fuse we

need to have its clearing (melting +arcing) *I-t* curve at lowest ambient temperature for this device's temperature operating range. For an SPS and a PPTC we need to have the *I-t* curve that includes the inductive turnoff at their lowest operating temperatures. The lowest operating temperature is usually – 40°C. For the higher order device we need to insure that the device does not start turning off current at its highest ambient operating temperature. For the fuse that requires having the melting *I-t* curve at 85°C or 125°C (depending on the location of the fuse). For the SPS this requires having a initial turnoff *I-t* plot at 85°C or 125°C that does not include the inductive turnoff times. PPTC's unfortunately do not have published *I-t* curves representing the time to the beginning of turnoff. Without this information the PPTC devices cannot be coordinated. Therefore, they should not be used as higher order protection devices. Since their nominal current carrying capacity is not huge they are usually used as first order protection devices only.

The conditions outlined in previous paragraphs are conservative; if they are followed, the system will be coordinated. In some circumstances proximity of lower order and higher order devices may cause the temperature assumptions to be unrealistic. For example, both protection devices could be sitting in the same ambient temperature. In these alternate cases, the most unfavorable credible set of temperatures should be used.

Protection coordination of two fuses is explained in the literature (4) but the method described in this thesis makes the achievement of coordination more obvious and visually easier. The fuse characteristics are plotted on the same *I-t* plot for both order fuses. The characteristic of the high order fuse must lie to the right of the low order fuse.

If the high order fuse has additional loads connected to it, its *I-t* characteristic is then shifted along the *I* axis by the maximum possible instantaneous current I_{max} in those high order loads. This means that the high order fuse characteristic is plotted with respect to (I- I_{max}) while the low order characteristic is plotted with respect to I . If the high order melting *I-t* plot still lies to the right of the first order clearing *I-t* plot the coordination is achieved. In principle this insures that the high

order fuse does not begin to melt in the time required for the first order fuse to clear a fault.

However, when the first order device is an SPS and a high order device is a fuse, the SPS limits the current at I_{scp}. Thus the largest prospective current that the high order fuse sees is (I_{scp} + I_{max}). The high order fuse's *I-t* characteristic need not be considered beyond the above-mentioned current. This statement assumes that the lower order device functions. Figure 5.13 illustrates this

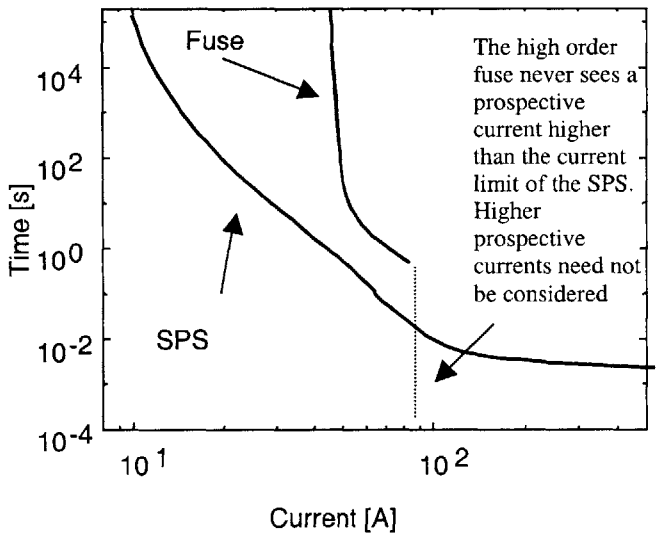

Figure 5.13 Coordination of the first order SPS and a fuse demonstrating the constant time perceived by the high order fuse

situation on the *I-t* plot. Thus, coordination of the first order SPS and a higher order fuse is somewhat easier to achieve.

When a first order PPTC needs to be coordinated with a high order fuse the procedure is the same as for the case of two fuses.

The situation is quite different if the high order protection device is an SPS. When a first order SPS is connected to a high order SPS, the coordination is the same as in the case of a first order SPS and a high order fuse. However if a first order fuse is connected to a high order SPS, problems might arise. During a fault the system resembles the current limited power supply system from the point of view of the low order fuse. Thus the time to melt becomes a constant when the current limit of the SPS is reached and coordination might not be achievable.

However, up to this point, this author has not indentified a single case where the coordination was not achievable when the characteristic of the first order fuse entirely lies to the left of the high order SPS. The possibility of the situation should however be noted and the hypothetical *I-t* graphs corresponding to that

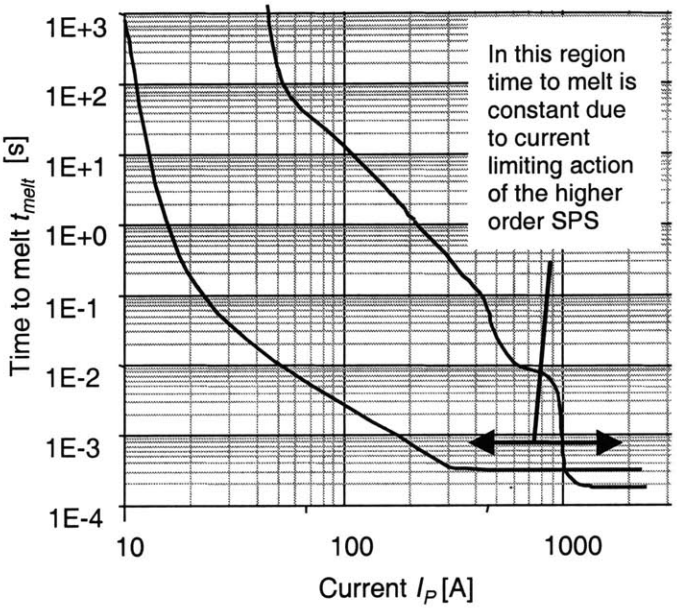

Figure 5.14 Hypothetical situation in which an SPS fails to coordinate with a low order fuse in the occurrence of the fault

situation are depicted in Figure 5.14.

In the case of the first order PPTC and the higher order SPS, the same situation applies as in the case of a fuse. Again the coordination was achievable as long as the SPS characteristic lies to the right of the PPTC characteristic

Thus we can see that the coordination of protection devices of different types can be achieved. The intermixing of the devices is thus permitted. This allows us to use SPS's as high order protection devices. The benefit of doing this becomes apparent when one considers a fault relative to which an SPS is a first order device. If this fault is removed by some reason after the SPS clears it, the SPS can be restarted and the functionality of all the devices that saw the SPS as a higher order device is restored. A fuse in the same circumstances would need to be replaced, and this would be nuisance to the user.

Furthermore, if the lowest order of protection of the SPS is equal or higher than 2, the inductance that the SPS has to be capable of turning off is the inductance associated with the cable that carries power to the lower order devices. By removing the stringent restriction of turning off high inductance loads in nominal operation and overload conditions (stalled motor), the SPS performance is more superior at both 14 V and 42 V. The behavior of high order protection devices is most important at high currents since the faults they are required to clear are associated with short circuiting of the cables. In a 42 volt system the time to initial turnoff of an SPS for a given resistance of the shorted cable is 3 times faster than the time at 14 V and the same resistance. This is a result of the operating regime E1 explained in Chapters 2 and 4.

Chapter 6.

Conclusion

6.1. Conclusions

After performing the analysis of operation of three types of protection devices, we conclude that all three of them can be used as protection devices in the future automotive electrical environment. Furthermore, we come to a conclusion that conventional fuses still have the best mode of failure (always as a open circuit), and can deal with highest amounts of inductance present in the fault. The new 42 V system might be more problematic than the current 12 V EDS from the fault inductance point of view. If one considers the fact that some of the proposed future loads are electromagnetic (fully flexible independent valve drive and electromagnetic suspension) and that their energy storage requirement and consequently inductance is substantial, it is justified to expect that there will be more inductance related problems in the 42V EDS.

SPS's closely follow the CF in their performance in all aspects excluding the turnoff of inductive faults. PPTC's are more limited in their usefulness due to largest variability of performance for a given part type, post and pre-trip

performance and ambient temperature sensitivity. Furthermore the PPTC's have not been correctly characterized using the means of characterization presented in Chapter 3. Their *I-t* curves do not depict virtual time but average times. Furthermore, the *I-t* plot of virtual time to beginning of the turnoff is necessary in order to facilitate the protection coordination of PPTC's with other protection devices. Comprehensive experimental or theoretical investigation of PPTC performance during turnoff of inductive faults should be made by the manufacturer in order to facilitate a more systematic use of PPTC in automotive highly inductive environments. However, the SPS's and PPTC's offer added functionality including resetability and are in that respect superior to CF.

Neglecting economical considerations which render CF superior to other technologies, smart power switches are the best performing protection device evaluated in this thesis (for use in the 42 V EDS). However, limitation on the amount of load inductance of smart power switches during normal operation makes it hard to use them for turning on and off high inductance loads under nominal current conditions and for turnoff of faults with substantial amount of inductance (such as stalled motors). If the limits on inductance of the polymeric positive temperature devices (PPTC's) could be established PPTC might prove to be a good replacement for high inductance applications that require resetability. In specific applications where feedback of the status of the load or of amount of current is necessary SPS is an excellent option integrating the sense resistor function together with the electrically controllable switch and a protection function with resetability. Because of SPS's ability to perform all these functions and replace more than just a fuse in the EDS it might prove to be economically superior at 42 V. In the Current 12 V EDS, SPS's are already replacing the fuses and switches in automotive lighting circuits in some cars (e.g. BMW's).

While concerns have been raised about the power dissipation during normal operation for SPS's and PPTC's it was shown in this thesis that all three device types have relatively similar power dissipation. For the cases examined, the SPS had the highest normal operation power dissipation, by a small margin.

However, it should be noted that SPS's power dissipation was evaluated at their minimum fusing current and therefore, may be unrealistically high.

For the SPS's and PPTC's that are auto-resetable, the RMS value of the post-trip current of the PPTC's is much lower then the RMS value of the post-trip current for the SPS's with similar nominal current ratings. However, in order to reset a PPTC, the current must be turned off by the user. This makes the PPTC equivalent to the latching type SPS, whose post-trip current is zero. Therefore, SPS's are superior to PPTC's from the point of view of post-trip current and its magnitude.

Furthermore, in future dual voltage 14 V- 42 V system in which the power is supplied to the 14 V side through a DC-DC converter, the device with the best performance is the SPS, as long as its inductance limitation is not exceeded.

Conventional fuses still have the smallest resistance causing the smallest voltage drop on the 14 V side under nominal conditions.

Protection coordination of protection devices of different types can be achieved in the automotive environment. Different device types can be mixed together in order to obtain better functionality of the system. Unfortunately, PPTC's should not yet be used as high order protection devices because the minimum times to initiation of tripping are not known.

6.2. Recommendations for future studies

The first and most necessary future work needed is the determination of the limits on inductance present during a fault in a circuit protected by a PPTC. Whether the analysis is performed on purely experimental basis or both theoretical and experimental basis is irrelevant as long as some limitation is established. This analysis should be followed by the analysis of the inductance limitation for the new emerging automotive fuses rated to operate in the 42 V EDS.

Furthermore an analysis of protection on the current limited power supply system with constant power loads needs to be evaluated. These loads can take the current away from the fault and thus cause the interruption of the fault to be

impossible. They can cause their own fuse to blow as a result of system voltage drop even when there is nothing wrong with them.

As the new prospective power distribution system architectures for the dual voltage system are developed the protection should be analyzed for each architecture respectively.

References

(1) MIT/Industry Consortium on Advanced Automotive Electrical/Electronic Components and Systems, web site (http://auto.mit.edu/consortium/) containing details of the research.

(2) Barry Hollembeak. Automotive Electricity, Electronics & Computer Controls. Albany NY: Delmar Publishers, 1998.

(3) Eric Chowanietz. Automotive Electronics. Oxford, England: Butterworth-Heinemann Ltd., 1995.

(4) A. Wright and P. G. Newbery. Electric Fuses. New York, NY: Peter Peregrinus Ltd, 1982.

(5) J. G. Leach, P. G. Newbery and A. Wright. 'Analysis of high-rupturing-capacity fuselink pre-arcing phenomena by a finite-difference method'. *Proc. I.E.E.*, 120(9), pp.987-993, 1973.

(6) Littelfuse. Fuses for Automotive Applications. Utrecht, Netherlands: Littelfuse, 1996.

(7) Datasheets for Wickmann/Pudenz FKS 80V rated automotive fuses

(8) Datasheet for BTS 640 S2 type SPS by Infineon Technologies. Available through the web at Infineon smart power switch Profet family web site http://www.infineon.com/products/36/36336.htm

(9) Duncan A. Grant and John Gowar. Power MOSFETS: Theory and Applications. New York, NY: John Wiley & Sons, 1989.

(10) John G. Kassakian, Martin F. Schlecht and George C. Verghese. Principles of Power Electronics. Reading, MA: Addison-Wesley Publishing Company, 1992.

(11) Alfons Graf and Hannes Estl. 'Fuse Function with PROFET Highside Power Switches', Application note, Infineon (http://www.infineon.com/products/36/pdf/anps039e.pdf)

(12) Alfons Graf and Hannes Estl. 'Fuse Replacement with Smart Power Semiconductors', 8th Int. Conference Vehicle Electronics, October 8-9, 1998, Baden-Baden.

(13) Alfons Graf et al. 'Semiconductor Technologies and Switches for new Automotive Electrical Systems'. 18th Conference Vehicle Electronics, June 16-17, 1998 Munich. (http://www.infineon.com/products/36/pdf/anps038e.pdf)

(14) Hannes Estl. 'Sicherungsersatz mit Smart-Leistungsschaltern' thesis for Institut für Elektronik der Technischen Universität Graz, May 1998.

(15) Datasheet for BTS 660 P type SPS by Infineon Technologies. Available through the web at Infineon smart power switch Profet family web site http://www.infineon.com/products/36/36336.htm

(16) Data sheets for the Infineon Profet family of Smart Power Switches http://www.infineon.com/products/36/36336.htm

(17) R. D. Sherman, L. M. Middleman and S. M. Jacobs. 'Electron Transport Processes in Conductor-Filled Polymers'. *Polymer Engineering and Science,* Vol. 23, No. 1, pp. 36-46.

(18) Department of Physics, MIT. 'JOHNSON NOISE: Determination of the Boltzmann constant and the centigrade temperature of absolute zero'. Junior Physics Laboratory: Experiment #43. (http://web.mit.edu/8.13/JLExperiments/JLExp_43.pdf

(19) Raychem Corporation. Circuit Protection Databook: October 1998. Menlo Park, CA: Raychem Corporation 1998.

(20) πRade Koncar⊥ Electrical Industries and Engineering. Tehnical Handbook. Zagreb, Croatia: Ognjen Prica, 1984.

(21) H. L. N. Wiegman and R. D. Lorentz. 'Fundamental Analysis of a Battery State Regulation Technique Based on Terminal Voltage'. IEEE, SAE & AIAA, DASC-17, Seattle, WA, Nov. 1998.

Bibliography

BOOKS

Eric Chowanietz. Automotive Electronics. Oxford, England: Butterworth-Heinemann Ltd. , 1995.

C. H. Edwards, Jr. and David E. Penney. Multivariable Calculus with Analytic Geometry. Englewood Cliffs, NJ: Prentice-Hall, 1994 (Fourth edition).

Clifton G. Fonstad. Microelectronic Devices and Circuits. Hightstown, NJ: McGraw-Hill, 1994.

Duncan A. Grant and John Gowar. Power MOSFETS: theory and applications. New York, NY: John Wiley & Sons, 1989.

Barry Hollembeak. Automotive Electricity, Electronics & Computer Controls. Albany NY: Delmar Publishers, 1998.

Roger T. Howe and Charles G Sodini. Microelectronics: an integrated approach. Upper Saddle River, NJ: Prentice-Hall, 1997.

John G. Kassakian, Martin F. Schlecht and George C Verghese. Principles of Power Electronics. Reading, MA: Addison-Wesley Publishing Company, 1992.

Jan M. Rabaey. Digital Integrated Circuits: a design perspective. Upper Saddle River, NJ: Prentice-Hall, 1996.

Kenneth M. Ralls et al. Introduction to material science and engineering. New York, NY: John Wiley & Sons, 1976.

Herbert H. Woodson and James R. Melcher. ELECTROMECHANICAL DYNAMICS, Part II: Fields Forces and Motion. New York, NY: John Wiley & Sons, 1968.

A. Wright and P. G. Newbery. Electric Fuses. New York, NY: Peter Peregrinus Ltd, 1982.

HANDBOOKS

Robert Bosch GMBH. Automotive Handbook 3rd edition. Cambridge, MA: Robert Bentley, Publishers, 1993.

N. Bronstein and K. A. Semendjajev. Matematicki Prirucnik za inzinjere i studente. Zagreb, Croatia: Tehnicka knjiga, 1964.

πRade Koncar⊥ Electrical Industries and Engineering. Tehnical Handbook. Zagreb, Croatia: Ognjen Prica, 1984.

MicroSim Corporation. MicroSim® PSpice® A/D. Irvine, CA: MicroSim Corporation, 1996.

Ford Motor company. 1997 Taurus Sable: Electrical and vacuum troubleshooting manual. Detroit, MI: Helm Incorporated, 1996.

Littelfuse. Fuses for Automotive Applications. Utrecht, Netherlands: Littelfuse, 1996.

Raychem Corporation. Circuit Protection Databook: October 1998. Menlo Park, CA: Raychem Corporation 1998.

PUBLICATIONS, APPLICATION NOTES AND WEBSITES

Hannes Estl. 'Sicherungsersatz mit Smart-Leistungsschaltern' thesis for Institut für Elektronik der Technischen Universität Graz, May 1998.

Alfons Graf and Hannes Estl. 'Fuse Replacement with Smart Power Semiconductors', 8th Int. Conference Vehicle Electronics, October 8-9, 1998, Baden-Baden.

Alfons Graf et al. 'Semiconductor Technologies and Switches for new Automotive Electrical Systems'. 18th Conference Vehicle Electronics, June 16-17, 1998 Munich. (http://www.infineon.com/products/36/pdf/anps038e.pdf)

Alfons Graf and Hannes Estl. 'Fuse Function with PROFET Highside Power Switches', Application note, Infineon (http://www.infineon.com/products/36/pdf/anps039e.pdf)

J. G. Leach, P. G. Newbery and A. Wright. 'Analysis of high-rupturing-capacity fuselink prearcing phenomena by a finite- difference method'. *Proc. I.E.E.*, 120(9), pp.987-993, 1973.

R. D. Sherman, L. M. Middleman and S. M. Jacobs. 'Electron Transport Processes in Conductor-Filled Polymers'. *Polymer Engineering and Science,* Vol. 23, No. 1, pp. 36-46.

Department of Physics, MIT. 'JOHNSON NOISE: Determination of the Boltzmann constant and the centigrade temperature of absolute zero'. Junior Physics Laboratory: Experiment #43. (http://web.mit.edu/8.13/JLExperiments/JLExp_43.pdf)

Infineon Power Switches web site http://www.infineon.com/products/36/36.htm

Appendix A

Theoretical fuse composed of zinc

In order to solve Equation 2.1 for a fusible link many parameters of that fusible link need to be know. This appendix deals in more detail with Equation 2.1 and gives the exact values of the parameters used in order to obtain the results presented in Figure 2.1 and 2.2.

The theoretical treatment begins with Equation 2.1 and Equation 2.2:

$$mc_p\left(\frac{dT}{dt}\right) = I^2R - U(T - T_{amb}) \tag{2.1}$$

$$R = R_{amb}[1 + \alpha(T - T_{amb})] \tag{2.2}$$

If we choose to represent the fuse as a square piece of the metal as given in Figure A.1 then some of the parameters in Equation 2.1 and 2.2 can be further determined. The mass of the fusible link is given by:

$$m = A * L * \rho \tag{A.1}$$

where A is the cross sectional area, L is the length and ρ is the density of Zinc. The theoretical fuse in chapter 2 has the following parameters:

$A=10^{-5}\ m^2$

L=0.002 m

$\rho = 7140\ kg/m^2$

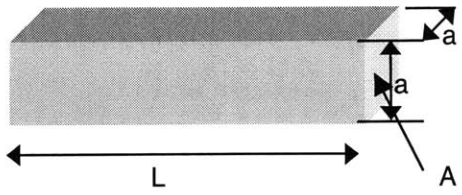

Figure A.1 Physical appearance of the fusible link

Furthermore, the resistance of the fusible link at room temperature is given by:

$$R_{amb} = \sigma \frac{L}{A} \tag{A.2}$$

Where σ is the conductivity of zinc and equals $0.06*10^{-6}$ Ω/m. The only remaining unknown is the coefficient of heat exchange with the environment and it is given by the following equation:

$$U = 2 * A * K * x^{-1} + C * L * k \tag{A.3}$$

where K is the thermal conductivity of zinc, x is the distance of the center of the fusible link to the fuse blades (Figure A.2), $C*L$ is the surface area of the fusible link exposed to air and k is the thermal conductance of the air to metal boundary. Figure A.2 shows the fusible link mounted onto the fuse clip contacts and defines x. Thus the exchange of heat with the environment is done through both heating of the air around the fusible link and heating of the contacts used to connect the fuse into a circuit.

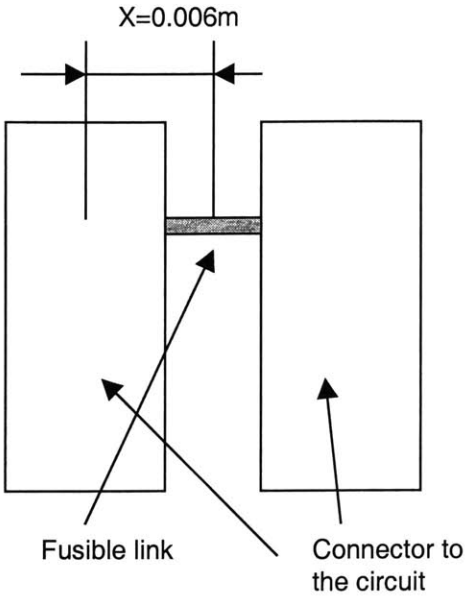

Figure A.2 Physical appearance of the fuse without housing

The value of *K* is 121.4 W / K m. The value of *k* on the other hand is only 13 W / K m^2. The circumference of the fusible link can be expressed as a function of *A* and the following result obtains:

$$U = 2 * (A * K * x^{-1} + \sqrt{A} * 2 * L * k \qquad \text{(A.4)}$$

Because k is so much smaller than K the second term can be neglected in the calculation. The ratio of the two terms for the hypothetical fuse here presented is 1230.

The major reason for variations in the fuse performance is the change in cross sectional area A. Both the length and the radius of the fusible link are altered as a result of the production process, However since they are altered by approximately the same absolute amount, the relative variation of the radius is much greater as a result of the fusible link being longer than its width. As the cross sectional area A changes, the energy necessary to melt the fuse changes with a linear dependence on A. The energy exchanged with the environment changes also as a linear dependence on A since the heat exchanged with the air is small compared to the heat exchanged with the fuse blades.

If time to melt is kept constant and the cross sectional area of the fuse is increased the current necessary to melt the fuse will increase. However the

energy necessary to melt the fuse will increase linearly with A and so will the energy exchanged with the environment. The ratio of the two energies for different values of cross sectional area A and constant value of time is kept constant.

Due to the fact that the energy used to melt the fusible link and the energy exchanged with the environment both vary in the same way with respect to changes in cross sectional area A. Equation 4.1 used in Chapter 4 is valid in the regime of operation where exchange of heat with the environment happens under assumption that variations in performance are a result of cross sectional area changes.

Appendix B

Description of the experimental setup

B.1 Introduction

During the course of the research, the normal mode of operation and fault interruption was tested for all three device types. The analysis which could contribute to the body of this thesis were included in the main part of the thesis. Experimental setups used to obtain experimental results of power dissipation and post-trip current levels presented in this thesis are explained in this Appendix.

B.2 Experimental setup for testing SPS's

Because of added functionality of SPS's over other protection devices the experimental setup used to test SPS's is somewhat different from the experimental setup of the other protection devices and will be presented separately. While the topology of the setup is indeed different the equipment used in the setup for testing SPS's and for testing other protection devices is the same.

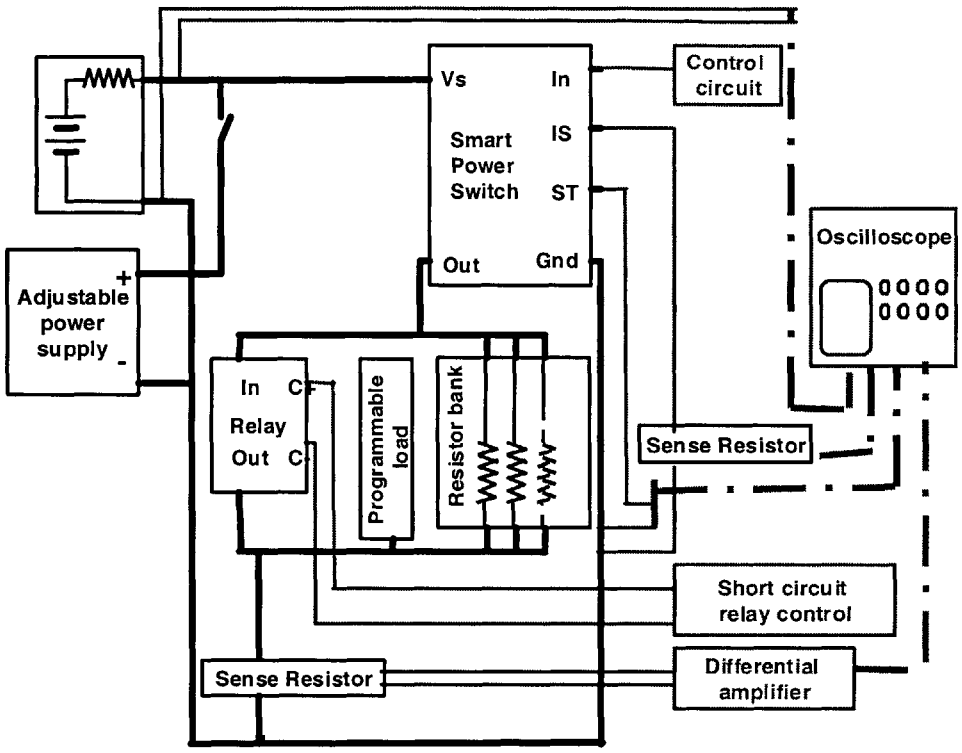

Figure B.1 The schematic of the experimental setup used to test SPS devices.

The diagram of the experimental setup is depicted in Figure B.1. The setup consists of three sections: the power stage, the control stage and the measurement stage.

The power stage consists of a power source which is either the automotive battery (ACDelco 65 Ah 1000A CA 850 CCA) or an adjustable power supply (HP 6012 0-60V 0-50A 1000W), SPS under test, programmable load (HP 300 W programmable load) and a load resistor bank (resistor bank consists of 300 W resistors with assorted resistance between 1 and 1.6 Ω connected in parallel). The load bank was connected in parallel with a high current low resistance relay which could simulate formation of hard shorts to ground. Furthermore, a high precision shunt resistor is included for determination of current (TiM Research Products F-2000-8 R=0.002455Ω 250W).

The control stage consists of several power supplies (not pictured in Figure B.1) used to control the relay and the smart power switch control circuitry (HP Harrison 6205 B Dual DC Power Supply). The control circuitry for the relay is

used to turn the relay on and off. SPS control circuitry makes the appropriate signal to turn the SPS on or off.

The measurement stage consists of a high bandwidth Tektronix digital oscilloscope which is used for data acquisition. To facilitate the data acquisition of current a differential amplifier was used. However, During normal mode of operation the currents through the SPS were too small to be easily detected by the shunt resistor and thus a LEM current probe (not pictured in Figure B.1) was used in that regime of operation (LEM Module LT 100-P up to 100A). The use of inductive current probes was avoided because they introduce stray inductance in the circuit.

B.3 Experimental setup for testing CF's and PPTC's

The experimental setup for testing CF's and PPTC's is somewhat different from the above setup due to the fact that they can not act as switches and do not provide status and current sense feedback. Figure B.2 shows the actual

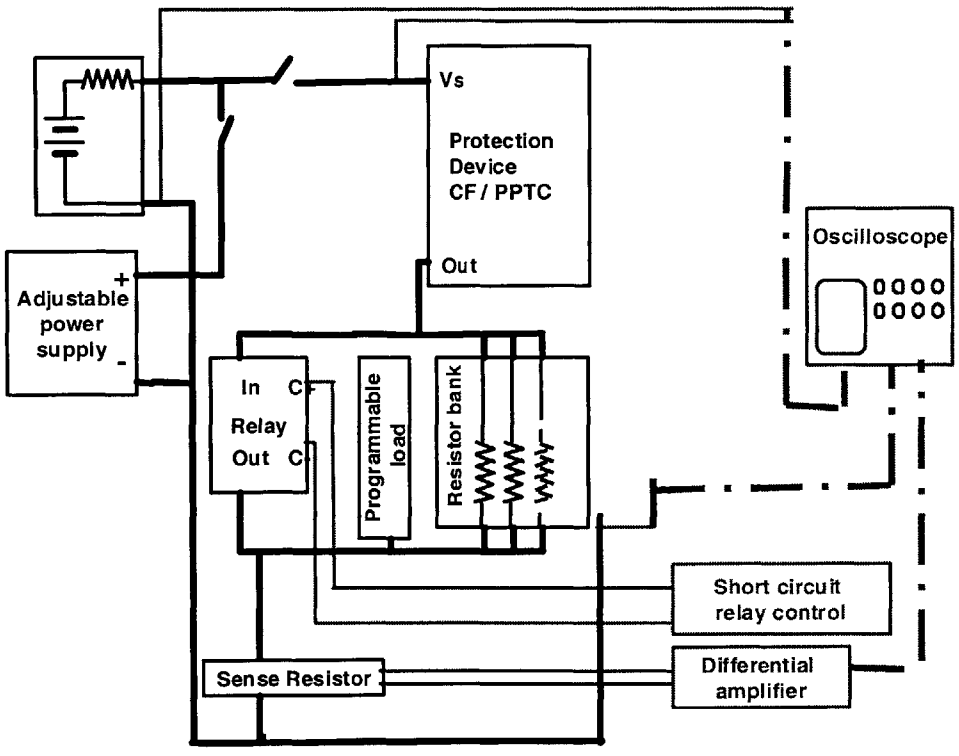

Figure B.2 The schematic of the experimental setup used to test CF's and PPTC's

differences introduced in the setup. All of the components were described in previous section. The only differences of consequence are the facts that there is no need to provide the ground connection to the protection device, and that there is no need (or possibility) to provide control commands to the protection device.